The 8th JUACEP Workshop at University of Michigan & UCLA

March 9 - 17, 2014

Japan-US Advanced Collaborative Education Program

Nagoya University

Published in November, 2014

Leaders of JUACEP
Professor Noritsugu Umehara
Professor Yang Ju

Japan-US Advanced Collaborative Education Program (JUACEP)
Graduate School of Engineering
Nagoya University
Furo-cho, Chikusa-ku, Nagoya, 464-8603, JAPAN
JUACEP@engg.nagoya-u.ac.jp
http://www.juacep.engg.nagoya-u.ac.jp

Table of Contents

<1> Participants from Nagoya University

Students

Name		Advisor
1. ARAKANE Shun	B3	Prof. S. Hata, Dept. Micro-Nano Systems Engineering
2. HAGIYAMA Yoshihiko	B4	Prof. N. Umehara, Dept. Mechanical Science and Engineering
3. HASEGAWA Takayuki	B4	Prof. F. Arai, Dept. Micro-Nano Systems Engineering
4. HIFUMI Kazuma	B4	Prof. Y. Ju, Dept. Mechanical Science and Engineering
5. HIRAYAMA Mikiro	B4	Prof. S. Nii, Dept. Chemical Engineering
6. HIROTA Akira	B4	Prof. T. Inoue, Dept. Mechanical Science and Engineering
7. ICHIKAWA Yoshiki	B4	Prof. T. Motohiro, Dept. Materials Science and Engineering
8. ICHIMURA Kazuyuki	B4	Prof. N. Umehara, Dept. Mechanical Science and Engineering
9. IMAEDA Kodai	B4	Prof. S. Hata, Dept. Micro-Nano Systems Engineering
10. KANO Hiroshi	B4	Prof. T. Inoue, Dept. Mechanical Science and Engineering
11. KAWASAKI Takayuki	B4	Prof. N. Umehara, Dept. Mechanical Science and Engineering
12. KIYOSAWA Yu	B4	Prof. Y. Uno, Dept. Mechanical Science and Engineering
13. KOJIMA Akihiro	B4	Prof. Y. Ju, Dept. Mechanical Science and Engineering
14. KUBOTA Naoki	B4	Prof. G. Obinata, Dept. Mechanical Science and Engineering
15. KUDO Naoki	B4	Prof. Y. Uno, Dept. Mechanical Science and Engineering
16. MAKANAE Yuki	B4	Prof. K. Yasuda, Dept. Chemical Engineering
17. MIYAMOTO Masashi	B4	Prof. S. Hata, Dept. Micro-Nano Systems Engineering
18. NAKAMURA Sho	B4	Prof. Y. Ju, Dept. Mechanical Science and Engineering
19. NAKATANI Eitaro	B4	Prof. N. Umehara, Dept. Mechanical Science and Engineering
20. NAKAYASU Fuminori	B4	Prof. N. Umehara, Dept. Mechanical Science and Engineering
21. NOTA Shuji	B4	Prof. Y. Ju, Dept. Mechanical Science and Engineering
22. OGASAWARA Masaru	B4	Prof. Y. Tsuji, Dept. Energy Engineering and Science
23. OKAJIMA Shotaro	B4	Prof. G. Obinata, Dept. Mechanical Science and Engineering
24. OMURA Kentaro	B4	Prof. G. Obinata, Dept. Mechanical Science and Engineering
25. SAITO Akira	M1	Prof. E. Shamoto, Dept. Mechanical Science and Engineering
26. SHIBASAWA Hotaka	B4	Prof. N. Umehara, Dept. Mechanical Science and Engineering
27. SUGIE Yoshimasa	B4	Prof. H. Kita, Dept. Chemical Engineering
28. SUZUKI Toru	M1	Prof. E. Shamoto, Dept. Mechanical Science and Engineering

29. TAKAHASHI Mamoru	B4	Prof. Y. Sakai, Dept. Mechanical Science and Engineering
30. TSUZUKI Akira	B4	Prof. S. Zhang, Dept. Computational Science and Engineering
31. WATANABE Shota	B4	Prof. T. Ujihara, Dept. Materials Science and Engineering
32. YAMAMORI Kenta	B4	Prof. H. Yamashita, Dept. Mechanical Science and Engineering
33. YAMANOUCHI Takuya	B4	Prof. E. Shamoto, Dept. Mechanical Science and Engineering
34. YAMASHITA Takahiro	B4	Prof. Y. Ju, Dept. Mechanical Science and Engineering
35. YOKOI Masataka	B4	Prof. Y. Sakai, Dept. Mechanical Science and Engineering

Faculty and staff

Name	
UMEHARA Noritsugu	Professor, Dept. Mechanical Science and Engineering
JU Yang	Professor, Dept. Mechanical Science and Engineering
MURASE Kohei	Associate Professor, Dept. Mechanical Science and Engineering
MORITA Yasuyuki	Associate Professor, Dept. Mechanical Science and Engineering
HARA Susumu	Associate Professor, Dept. Mechanical Science and Engineering
AOKI Hirofumi	Associate Professor, Dept. Mechanical Science and Engineering
ITO Yasumasa	Associate Professor, Dept. Mechanical Science and Engineering
YADA Chiharu	Administrative staff, JUACEP

Acknowledgment

We express our sincere appreciation to the faculty and staff members of the University of Michigan and UCLA and for their cooperation to accomplish this workshop and their warm welcome.

JUACEP

<2> Announcement leaflets

The 8th Nagoya U – U Michigan JUACEP Student Workshop on Engineering and Science

March 10, 11:50am-2:00pm

Duderstadt Hallway

- Poster presentations by graduate students in Engineering at Nagoya University
- Scholarship program for international student exchange

Complimentary lunch served

Organizers: Profs. N. Umehara and Y. Ju (Nagoya U)
Prof. K. Kurabayashi (U Michigan)

Japan-US Advanced Collaborative Education Program (JUACEP)
Graduate School of Engineering, Nagoya University
Web: http://www.juacep.engg.nagoya-u.ac.jp
Email: juacep-office@engg.nagoya-u.ac.jp

MICHIGAN

#	Title	Presenter
1	"Green" Separation of Metal Ions with Using Foam	Mikiro Hirayama
2	Dynamic Analysis of Multi-degree-of-freedom System from the viewpoint of Power Flow Theory	Akira Hirota
3	Non-linear Numerical Analysis of the Asynchronous Centrifugal Whirling Vibration in the Cylindrical Journal Bearing, Elastic Rotor System	Hiroshi Kano
4	Hydrogen Absorption Properties of Pd-doped Mesoporous Silica	Yoshiki Ichikawa
5	Synthesis of Magnesium Based Layered Hydroxide Particles and Investigations of the Chemical Heat Storage Properties	Yoshimasa Sugie
6	Control Strategy for Dexterous Handling Using Hemispheric Vision-Based Tactile Sensor	Naoki Kubota
7	Stabilization of Wheeled Personal Mobility for Handicapped People Against External Force	Shotaro Okajima
8	Objective Evaluation of the Passenger Perception in the Simulated Brake Motion by Reflex Eye Movements	Kentaro Omura
9	Suggestion of Recrystallization Solution Method by Highly Efficiently Nitrogen Supply and AlN Single Crystal Growth	Shota Watanabe
10	Forward-propagation Learning Systems with a Feedback Controller	Yu Kiyosawa
11	An Analysis of Whole Body Reaching Movement	Naoki Kudo
12	Effect of Hydrodynamic Cavitation on Escherichia Coli	Yuki Makanae
13	Experimental Study on Effect of Radical Quenching on between Wall and Methane-Air Premixed Flame	Kenta Yamomori
14	Investigation of Interatomic Force Under the Tip of Microwave-AFM Probe	Kazuma Hifumi
15	TEM Observation of Dislocation Motion Induced by Electric Current	Akihiro Kojima
16	Growth and Control of Aluminum Nanowires Based on Stress-induced Migration	Sho Nakamura
17	Development of Highly Ordered Silicon Nanowire Array	Shuji Nota
18	Study on Development of a Multi-inkjet Head for Building 3D Living Tissue	Takahiro Yamashita
19	Microneedle for Trans-dermal Drug Delivery Systems	Kodai Imaeda
20	Scheduling Sports Tournaments Using Local Search Heuristics	Akira Tsuzuki
21	Fabrication and Manipulation of 3D Hybrid Nanorobot for Single Cell Puncture	Takayuki Hasegawa
22	The Effect of Plasma-on Time on the Hardness of DLC Film Deposited with Microwave-assisted Plasma CVD	Yoshihiko Hagiyama
23	Suggestion of Super Low Friction Mechanism of CNx Coating against CNx under Oil	Kazuyuki Ichimura
24	Developments of Lubricant Sheet in Drilling Materials for Airplanes	Takayuki Kawasaki
25	Effect of Substrate Temperature on Deposition of Carbon Film Utilizing Molecular Structure of Adamantine	Eitaro Nakatani
26	Study of basic friction properties of Ta-CNx film	Fuminori Nakayasu
27	Study of Soot Separation Method of Diesel Engine Oil by Applying Electric Field	Hotaka Shibasawa
28	The Tribological Characteristics of DLC Film under High Temperature Vapor Environment	Takuya Yamanouchi
29	Analytical Prediction of Chatter Stability in Ball End Milling	Akira Saito
30	Cutting Force Model in Milling Operations with Self-propelled Rotary Tools Considering Bearing Friction	Toru Suzuki
31	Direct Reduction of Copper Oxide Nanoparticles Using Femtosecond Laser Pulses for Copper Micro Patterning	Shun Arakane
32	High Throughput Evaluation of Multi Cell Array for Searching Electrode Materials of Lithium-ion Battery	Masashi Miyamoto
33	Experimental Study of Heat Transfer Enhancement in Heat Pipe by Changing the Wetting Condition on the Wall	Masaru Ogasawara
34	A Research of Axisymmetric Jet Controlled by Vortex Generators	Mamoru Takahashi
35	Scale-up of a Test Facility for Realize Measurement of Liquid Axisymmetric Jet	Masataka Yokoi

Briefing Session on
Japan-US Advanced Collaborative Education Program (JUACEP)

March 10, 3:30am-4:00pm

2150 HH Dow

- Summer research experience!
- 3 credits transferrable to UM!
- Scholarship for graduate students!
- Experience Japanese culture!

Japan-US Advanced Collaborative Education Program (JUACEP)
Graduate School of Engineering, Nagoya University
Web: http://www.juacep.engg.nagoya-u.ac.jp
Email: juacep-office@engg.nagoya-u.ac.jp

The 8th Nagoya U – U Michigan JUACEP Student Workshop on Engineering and Science

March 10-11, 2014
Univ. Michigan, Ann Arbor, MI

Program

Monday, March 10, 2014

9:00am-9:30am	Welcome remark, Introduction of University of Michigan
10:00am-11:00am	North Campus tour
11:50am-2:00pm	Poster presentation
2:30pm-3:00pm	Introduction of College of Engineering
3:00pm-3:30pm	Talks by Japanese students studying at UM
3:30pm-4:00pm	Briefing session for UM students

Tuesday, March 11, 2014

9:30am-10:30am	UM 3D Lab tour
10:30am-11:30am	Wilson Student Team Project Center tour
1:00pm-3:00pm	Individual lab visits

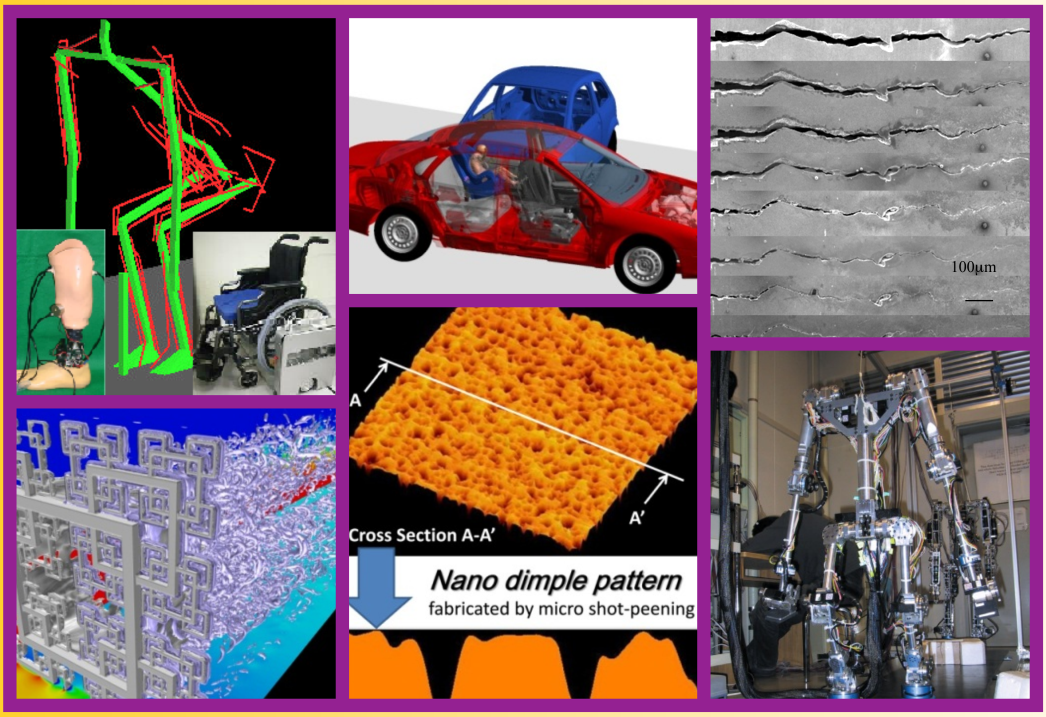

Organizers: Profs. N. Umehara, Y. Ju (Nagoya U)
Prof. K. Kurabayashi (U Michigan)

Japan-US Advanced Collaborative Education Program (JUACEP)
Graduate School of Engineering, Nagoya University
Furo-cho, Chikusa-ku, Nagoya, 464-8603, JAPAN
Phone: +81-52-789-3113 Fax: +81-52-789-3111
Email: yito@mech.nagoya-u.ac.jp, tokuda@esi.nagoya-u.ac.jp

The 8th Nagoya U – UCLA JUACEP Student Workshop on Engineering and Science

March 13, 12:00am-2:00pm
CNSI Lobby

- Poster presentations by graduate students in Engineering at Nagoya University
- Scholarship program for international student exchange

Organizers: Profs. N. Umehara and Y. Ju (Nagoya U)
Prof. J. M. Yang (UCLA)

Japan-US Advanced Collaborative Education Program (JUACEP)
Graduate School of Engineering, Nagoya University
Web: http://www.juacep.engg.nagoya-u.ac.jp
Email: juacep-office@engg.nagoya-u.ac.jp

UCLA

#	Title	Presenter
1	"Green" Separation of Metal Ions with Using Foam	Mikiro Hirayama
2	Dynamic Analysis of Multi-degree-of-freedom System from the viewpoint of Power Flow Theory	Akira Hirota
3	Non-linear Numerical Analysis of the Asynchronous Centrifugal Whirling Vibration in the Cylindrical Journal Bearing, Elastic Rotor System	Hiroshi Kano
4	Hydrogen Absorption Properties of Pd-doped Mesoporous Silica	Yoshiki Ichikawa
5	Synthesis of Magnesium Based Layered Hydroxide Particles and Investigations of the Chemical Heat Storage Properties	Yoshimasa Sugie
6	Control Strategy for Dexterous Handling Using Hemispheric Vision-Based Tactile Sensor	Naoki Kubota
7	Stabilization of Wheeled Personal Mobility for Handicapped People Against External Force	Shotaro Okajima
8	Objective Evaluation of the Passenger Perception in the Simulated Brake Motion by Reflex Eye Movements	Kentaro Omura
9	Suggestion of Recrystallization Solution Method by Highly Efficiently Nitrogen Supply and AlN Single Crystal Growth	Shota Watanabe
10	Forward-propagation Learning Systems with a Feedback Controller	Yu Kiyosawa
11	An Analysis of Whole Body Reaching Movement	Naoki Kudo
12	Effect of Hydrodynamic Cavitation on Escherichia Coli	Yuki Makanae
13	Experimental Study on Effect of Radical Quenching on between Wall and Methane-Air Premixed Flame	Kenta Yamomori
14	Investigation of Interatomic Force Under the Tip of Microwave-AFM Probe	Kazuma Hifumi
15	TEM Observation of Dislocation Motion Induced by Electric Current	Akihiro Kojima
16	Growth and Control of Aluminum Nanowires Based on Stress-induced Migration	Sho Nakamura
17	Development of Highly Ordered Silicon Nanowire Array	Shuji Nota
18	Study on Development of a Multi-inkjet Head for Building 3D Living Tissue	Takahiro Yamashita
19	Microneedle for Trans-dermal Drug Delivery Systems	Kodai Imaeda
20	Scheduling Sports Tournaments Using Local Search Heuristics	Akira Tsuzuki
21	Fabrication and Manipulation of 3D Hybrid Nanorobot for Single Cell Puncture	Takayuki Hasegawa
22	The Effect of Plasma-on Time on the Hardness of DLC Film Deposited with Microwave-assisted Plasma CVD	Yoshihiko Hagiyama
23	Suggestion of Super Low Friction Mechanism of CNx Coating against CNx under Oil	Kazuyuki Ichimura
24	Developments of Lubricant Sheet in Drilling Materials for Airplanes	Takayuki Kawasaki
25	Effect of Substrate Temperature on Deposition of Carbon Film Utilizing Molecular Structure of Adamantine	Eitaro Nakatani
26	Study of basic friction properties of Ta-CNx film	Fuminori Nakayasu
27	Study of Soot Separation Method of Diesel Engine Oil by Applying Electric Field	Hotaka Shibasawa
28	The Tribological Characteristics of DLC Film under High Temperature Vapor Environment	Takuya Yamanouchi
29	Analytical Prediction of Chatter Stability in Ball End Milling	Akira Saito
30	Cutting Force Model in Milling Operations with Self-propelled Rotary Tools Considering Bearing Friction	Toru Suzuki
31	Direct Reduction of Copper Oxide Nanoparticles Using Femtosecond Laser Pulses for Copper Micro Patterning	Shun Arakane
32	High Throughput Evaluation of Multi Cell Array for Searching Electrode Materials of Lithium-ion Battery	Masashi Miyamoto
33	Experimental Study of Heat Transfer Enhancement in Heat Pipe by Changing the Wetting Condition on the Wall	Masaru Ogasawara
34	A Research of Axisymmetric Jet Controlled by Vortex Generators	Mamoru Takahashi
35	Scale-up of a Test Facility for Realize Measurement of Liquid Axisymmetric Jet	Masataka Yokoi

Briefing Session on
Japan-US Advanced Collaborative Education Program (JUACEP)

March 13, 4:00pm-5:00pm

Room 3129, Engineering V

- Summer research experience!
- Scholarship for graduate students!
- Experience Japanese culture!

Japan-US Advanced Collaborative Education Program (JUACEP)
Graduate School of Engineering, Nagoya University
Web: http://www.juacep.engg.nagoya-u.ac.jp
Email: juacep-office@engg.nagoya-u.ac.jp

UCLA

The 8th Nagoya U – UCLA JUACEP Student Workshop on Engineering and Science

March 13-15, 2014
Univ. California, Los Angeles, LA

Program

<u>Thursday, March 13, 2014</u>

9:30am-10:30am	Welcome remark, Introduction of UCLA
10:30am-11:30am	Special lectures by UCLA professors
12:00am-2:00pm	Poster presentation
2:00pm-4:00pm	CNSI visit
4:00pm-5:00pm	Briefing session for UCLA students

<u>Friday, March 14, 2014</u>

9:00am-11:00am	Campus tour
11:00am-12:00am	Lab tour
1:30pm-4:00pm	Individual lab visits

<u>Friday, March 14, 2014</u>

all day	Individual lab visits

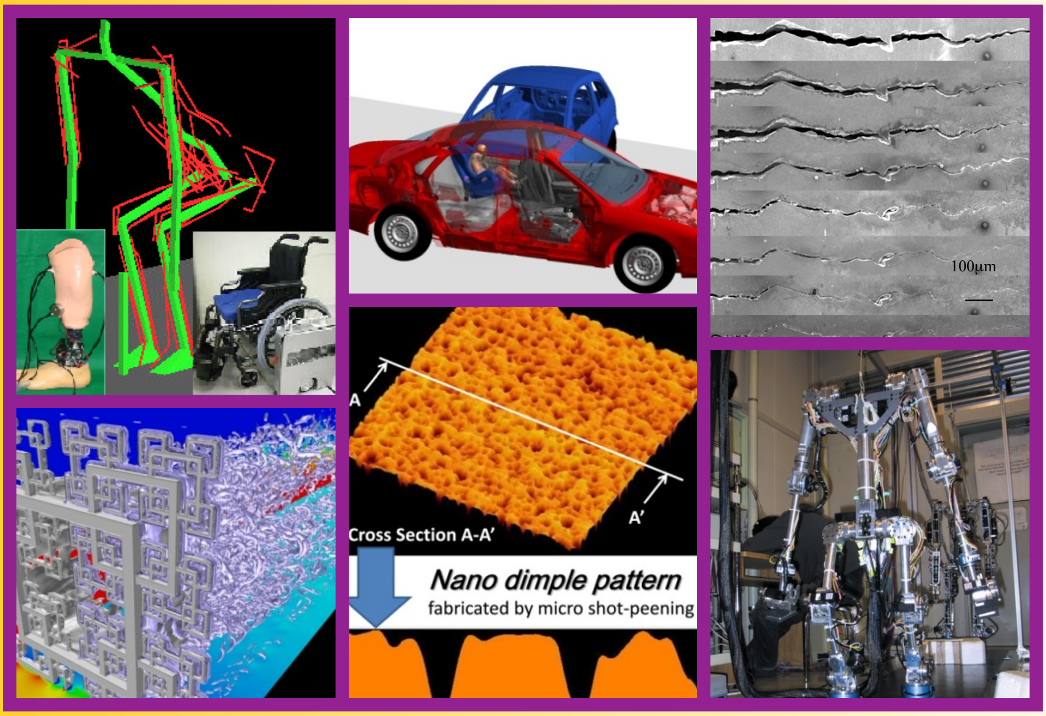

Organizers: Profs. N. Umehara, Y. Ju (Nagoya U)
Prof. J. M. Yang (UCLA)

Japan-US Advanced Collaborative Education Program (JUACEP)
Graduate School of Engineering, Nagoya University
Furo-cho, Chikusa-ku, Nagoya, 464-8603, JAPAN
Phone: +81-52-789-3113 Fax: +81-52-789-3111
Email: yito@mech.nagoya-u.ac.jp, tokuda@esi.nagoya-u.ac.jp

UCLA

<3> Presentation Posters

"Green" Separation of Metal Ions with Using Foam

Mikio Hirayama
Department of Chmical Engineering, Nagoya University, JAPAN

Background

Metal separation ····· Recycling valuable metals from industrial wastes

Wet processes
- •Solvent extraction
- •Ion exchange
- •Adsorption

Dry processes
- •Evaporation
- •Magnetic separation

Strong impact on environment
- •organic solvent
- •wastewater treatment

Strong demand for "Green" process!

Organic solvent free
Simple operation

Foam will adosorb target metals.
PONPE, the surfactant has strong affinity to Au and Ga.

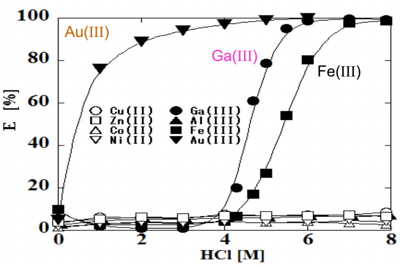

Extraction of various metal ions with PONPE

PolyOxyethylene NonylPhenylEther, PONPE

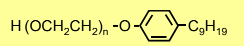

When PONPE was used to making foam, the foam would adosorb target metals.

"Green separation" of target metal

Our target is Ga····Why?

Ga

- •Japan requires more than 70% of world consumption of Ga.
- •It is wasted from industries of semiconductor, solar-cell, LED, etc.

Objectives

1. To achieve selective recovery of Ga from model solution containing metals
2. To separate Ga from industrial wastes

Ga recovery from GaAs substrate, a real waste

GaAs-substrate scrap

XRF analysis
composition [mass%]
Ga:48.2
As:49.6
Other metals were undetectable.

Leaching condition
- 6 M HCl : 100 cm^3
- ground solid : 10 g
- leaching time : 360 h

Leach liquor
Ga, As [ppm]
240 , 170

CCFS condition
- Feed : 20 ppm Ga (6 M HCl)
- Washing and Base sol. :
- 0.1 wt% PONPE20 (6 M HCl)

100 % Ga Recovery and Ga/As Sp 61

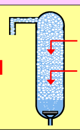

Counter Current Foam Separation (CCFS)

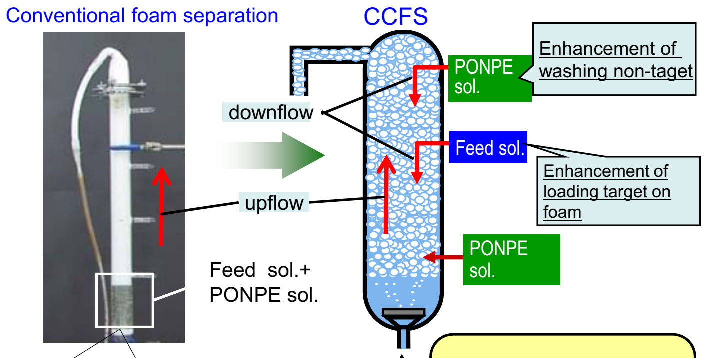

Target was enriched, but contamination with nontarget metals occurred.

Metal separation was improved by enhancing counter current.

Experimental

<Feed solution>
20 ppm Ga, Fe, Cu, Zn (6 M HCl)
<Base and Washing solution>
0.1 wt% PONPE20 (6 M HCl)
<Analysis>
ICP-AES

Separation degree, $$Sp\,[-] = \frac{(C_{Ga}/C_{Fe})_F}{(C_{Ga}/C_{Fe})_{In}}$$

Recovery percentage, $$R\,[\%] = \frac{(CV)_F}{(CV)_{In}} \times 100$$

C : conc. of metal V : flow rate
Subscripts F : Foam In : Feed

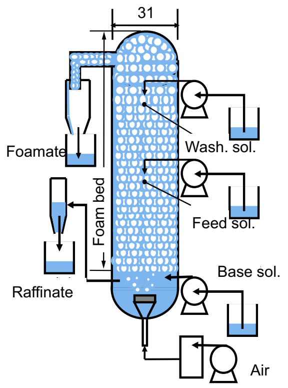

Searching for optimum operating conditions of Ga separation

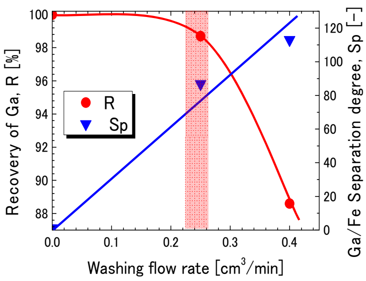

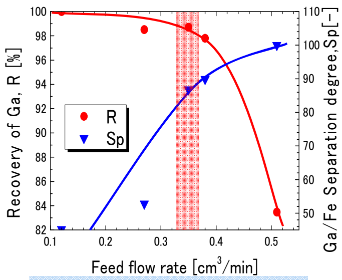

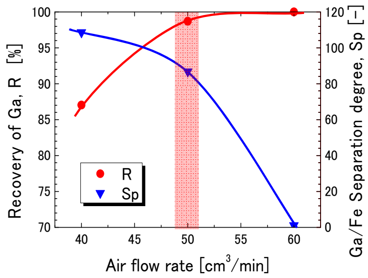

Optimum Condition

flow rate	[cm^3/min]
Air	50
Feed	0.35
Washing	0.25

Conclusion

1. Selective separation of Ga from model solution was achieved.
2. The optimum operation condition of CCFS was found for 100 % Ga recovery and high Ga separation degree.
3. Ga was successfully recoverd with CCFS from GaAs substrate.

Dynamic Analysis of Multi-degree-of-freedom System from the viewpoint of Power Flow Theory

○Akira HIROTA, Tsuyoshi INOUE

Introduction

Mechanical Design

- Realization of High Efficiency
- Satisfaction of comfortability and quietness

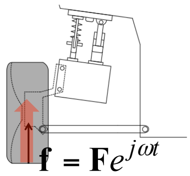

Need for reduction of adverse effect from the transmission of vibration to human body

Evaluation with Power

Rather than Amplitude or Acceleration

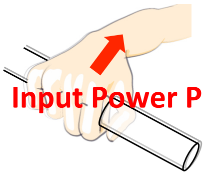

◆Research Objectives

- establishment of the method to evaluate vibration based on the viewpoint of Power
- Optimal design of dynamic damper utilizing the method above

Power Flow Theory

Motion Equation (Time domain)

$$\mathbf{M}\ddot{\mathbf{x}} + \mathbf{C}\dot{\mathbf{x}} + \mathbf{K}\mathbf{x} = \mathbf{f}$$

Fourier Tf. & $\frac{\mathbf{V}}{j\omega} = \mathbf{X}$

Motion Equation (Frequency domain)

$$\left(j\omega\mathbf{M} + \mathbf{C} + \frac{\mathbf{K}}{j\omega}\right)\mathbf{V} = \mathbf{F}$$

Modal transformation utilizing conventional Modal transformation matrix $\mathbf{\Phi}$ ($\mathbf{M}, \mathbf{K}$ are dominant)

$\mathbf{x} = \mathbf{\Phi}\boldsymbol{\xi}$ → $\mathbf{v} = \mathbf{\Phi}\dot{\boldsymbol{\xi}}$

Differenciate with respect to t

Power : $[\mathbf{f}^H, \mathbf{v}]$

- Time-averaged active power

$$P_{re} = \mathrm{Re}(\mathbf{F}^H\mathbf{V})$$

Deformation utilizing the motion of equation

$$P_{re} = \mathrm{Re}(\mathbf{V}^H\mathbf{C}\mathbf{V})$$ Quadratic form of velocity

Eigenvalue decomposition $\mathbf{C} = \mathbf{\Gamma}\mathbf{\Lambda}\mathbf{\Gamma}^T$

Modal transformation $\mathbf{V} = \mathbf{\Gamma}\mathbf{Q}$

$$P_{re} = \mathrm{Re}(\mathbf{Q}^H\mathbf{\Lambda}\mathbf{Q}) = \sum_i \lambda_i |Q_i|^2 = \boxed{\sum_i P_i}$$

Sum of all modal powers

Introduction of T

Relational expression between $\mathbf{q}$ and $\dot{\boldsymbol{\xi}}$

$$\mathbf{q} = \mathbf{T}\dot{\boldsymbol{\xi}}$$

What does $\mathbf{T}$ inform?

Model for analysis

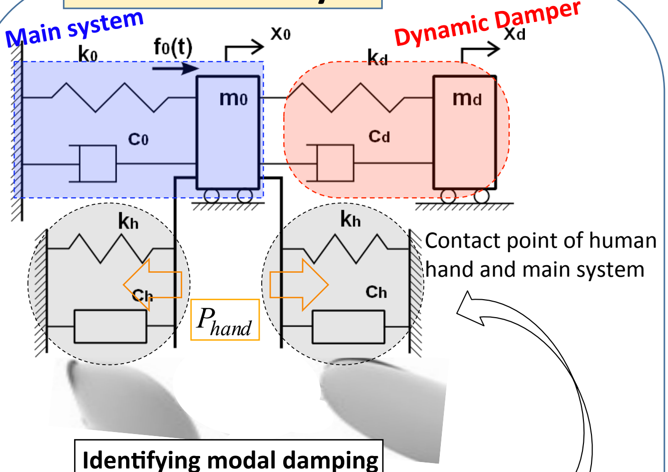

Identifying modal damping ratio of human hand

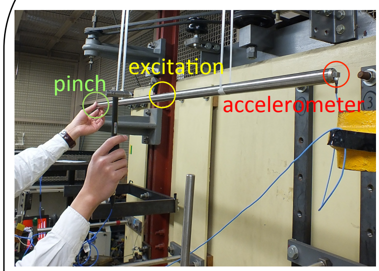

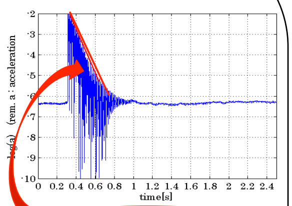

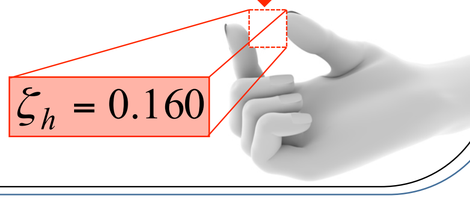

Optimal Design of Dynamic Damper with numerical method

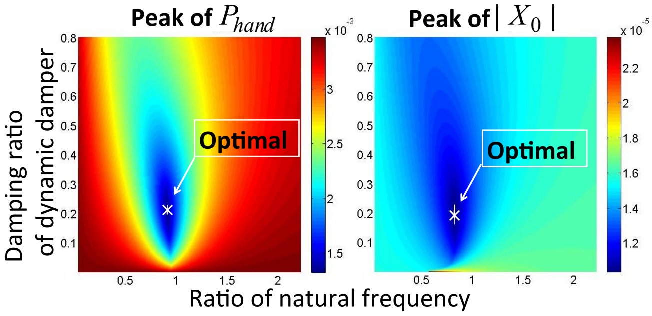

Characteristically Similar, however, a bit different

Summary

----Conclusions----

- Dynamic damper design by the way based on the viewpoint of **power** and **amplitude** are generally similar, however, strictly different.
- According to the fact demonstrated above, it is the best way to introduce a new evaluation function which is defined with optimum weight value for Power and Amplitude.

----Future Works----

- Consider non-linear factors such as non-linear damper which has hysteresis property.
- Time domain analysis
  (As one of the methods for dealing with non-linear system)

Non-linear Numerical Analysis of The Whirling Vibration (Oil-Whip) in The Full-circular Journal Bearing, Elastic Rotor System

○Hiroshi Kano, Tsuyoshi Inoue (Nagoya University)

Background

◆What is a journal bearing ?

- Oil Film Reaction Force support load
- A shaft and bearing rotate in a non-contact state
  ⇒ The life of a machine is semipermanent
- The Oil Film Reaction Force has nonlinearity
  ⇒ Analysis is difficult

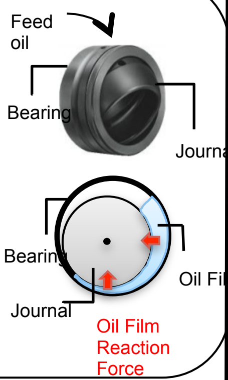

Whirling vibration (What is Oil-Whip?)

- Oil-Whip occured by the affection of Hydrodynamic
- Large amplitude of shaft with Oil Whip
  ⇒ Prevent the shaft from being operated safely
- ~~Frequency of whirling vibration always equals to natural frequency of shaft~~
- Oil-Whip occur at more than twice the natural frequency (UP)
- Oil-Whip stop at the twice the natural frequency on decrement Rotation speed (DOWN)
  ⇒ hysteresis phenomenon

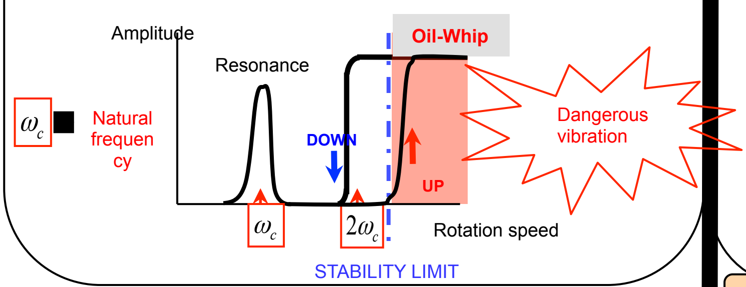

Equation of motion of rotor system

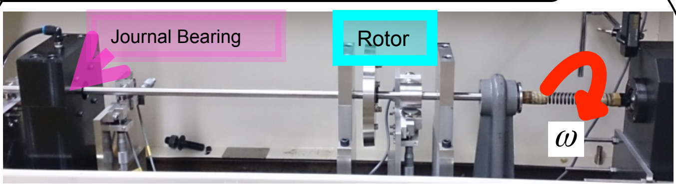

Four degree of freedom elastic rotor model

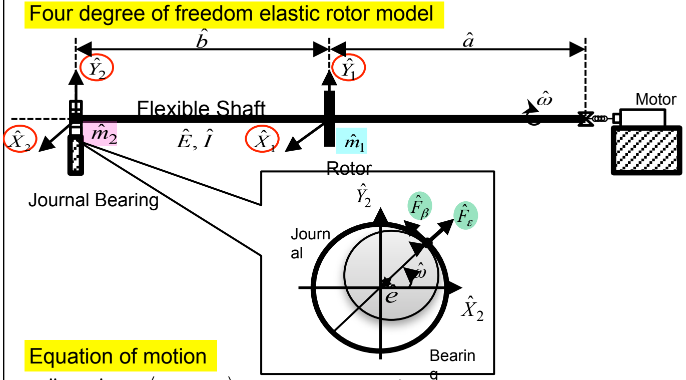

Equation of motion

$$
\begin{aligned}
&\hat{m}_1\ddot{\hat{X}}_1 + \hat{c}\dot{\hat{X}}_1 + \hat{k}_1(\hat{X}_1 - k\hat{X}_2) = \hat{U}\hat{\omega}^2\cos\hat{\omega}\hat{t},\\
&\hat{m}_1\ddot{\hat{Y}}_1 + \hat{c}\dot{\hat{Y}}_1 + \hat{k}_1(\hat{Y}_1 - k\hat{Y}_2) = \hat{U}\hat{\omega}^2\sin\hat{\omega}\hat{t} - \hat{m}_1\hat{g},\\
&\hat{m}_2\ddot{\hat{X}}_2 - \hat{k}_1(\hat{X}_1 - k\hat{X}_2) = \hat{F}_{JBx},\\
&\hat{m}_2\ddot{\hat{Y}}_2 - \hat{k}_1(\hat{Y}_1 - k\hat{Y}_2) = \hat{F}_{JBy} - \hat{m}_2\hat{g}
\end{aligned}
$$

Parameters equal to experimental device

$\hat{F}_\varepsilon, \hat{F}_\beta \Rightarrow \hat{F}_{JBx}, \hat{F}_{JBy}$

polar coordinates ⇒ rectangular coordinates

Analysis result

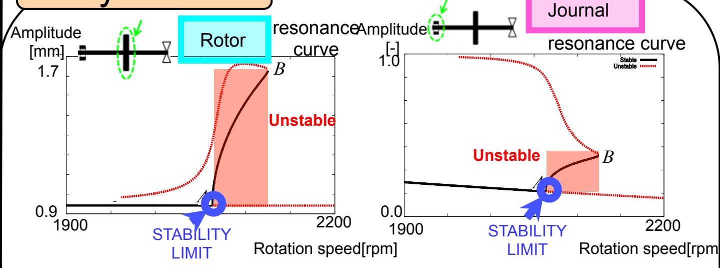

Frequency of whirling vibration

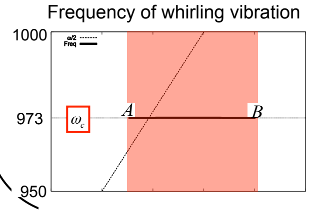

➢A→B (Unstable)
Large amplitude
Frequency of shaft = natural frequency ω_c
⇒Oil-Whip

Experimental results

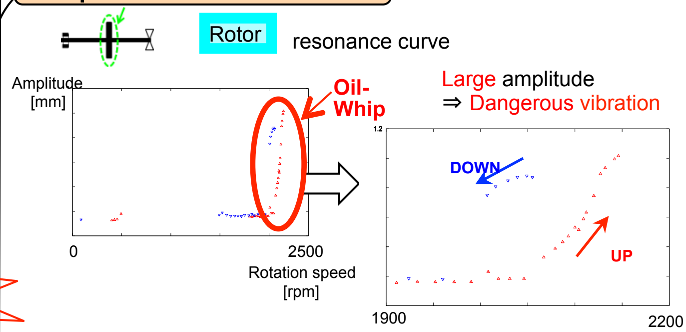

- A hysteresis phenomenon is caused
- Validity of equation of motion was confirmed by comparing the Analysis with the Experimental

Analysis result (parameter variation)

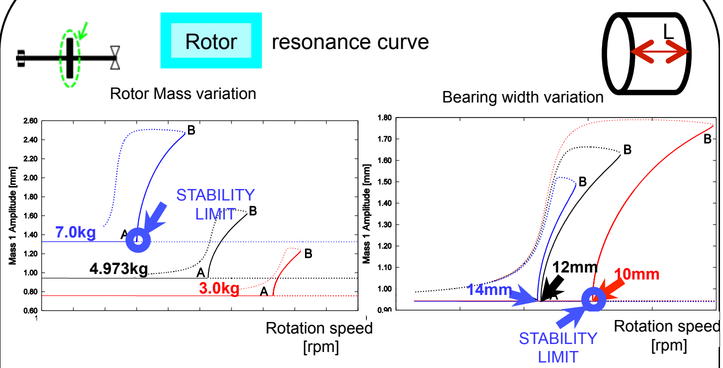

➢Rotor Mass → small Bearing width → short
⇒ STABILITY LIMIT (A) is improved
➢Frequency of shaft (A-B)= ω_c ⇒ Oil-Whip

Conclusions

- Validity of equation of motion was confirmed by comparing the numerical analytic result with the experimental result
- Phenomenon called Oil-Whip was confirmed by experiment

Future works

- Reserch of STABILITY LIMIT affected by key parameters variation of A governing equation
- Improvement of the experimental device

Hydrogen absorption properties of Pd-doped mesoporous silica

Yoshiki Ichikawa, ichikawa.yoshiki@d.mbox.nagoya-u.ac.jp Dept. of Mater. Sci. & Eng., Nagoya University, Furo-cho, Chikusa-ku, Nagoya, 464-8603, Japan

Introduction

Hydrogen absorption properties
in bulk materials ⇒ extensively studied.
in nano-sized materials ⇒**still unclear**
Some exotic “**nano-size effects** “ may improve storage capacity.

Approach

Experimentally evaluate hydrogen absorption properties of Pd nanoparticles in the absence of their size change by their agglomeration.
⇒Preparation of Pd nanoparticles of homogeneous sizes in pores of mesoporous silica.

Sample preparation

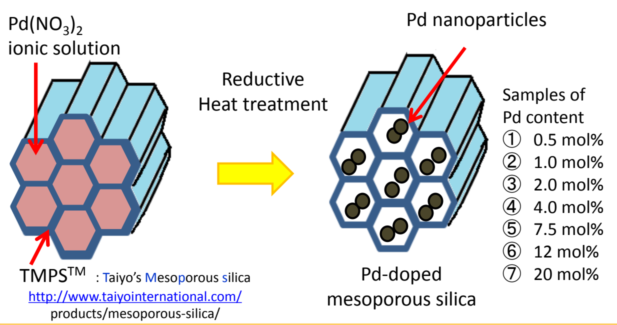

←Fig.1 Preperation of Pd-doped TMPS™

Fig.2→ Synthetic procedue of Pd-doped TMPS™

TMPS
↓ $+Pd(NO_3)_2$ aq
Evacuation for 1 h
↓
Stirring at room temp. for 24 h
↓
Drying in air at 130 ℃ for 6 h
↓
Heat treatment in air at 200 ℃ for 1 h
↓
H_2 Exposure at 0.2 MPa and room temp. for 10min

Sample characterization

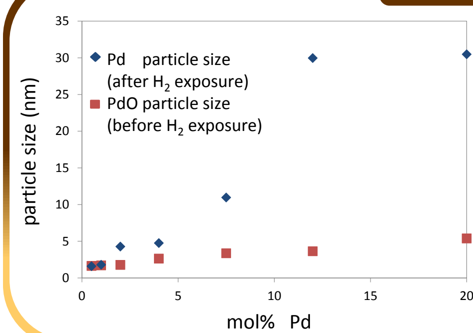

←Fig.3 Pd particle size vs mol% Pd (XRD peaks ⇒Scherrer’eq.)

Grain growth after H_2 exposure in the Samples of >7.5%Pd

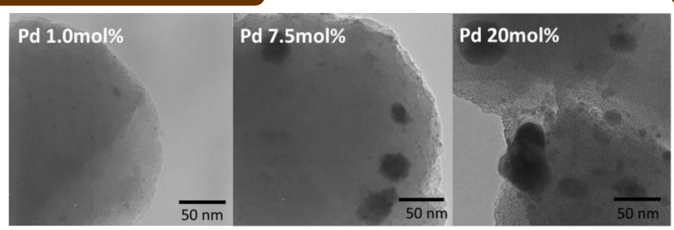

Fig.4 TEM images of samples ②,⑤,⑦

Pd>10nm in the samples of >7.5mol Pd locate outside of TMPS

H_2 absorption

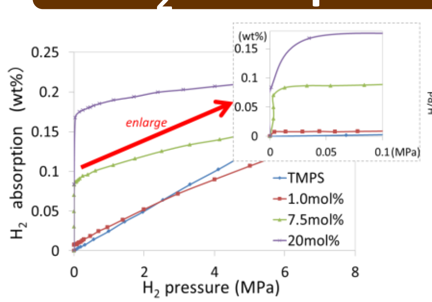

Fig.5 H_2 absorption vs H_2 pressure

At near 0 pressures, H_2 absorption due to Pd is observed

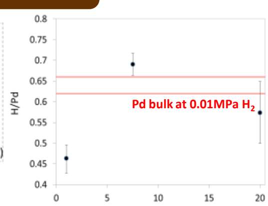

Fig.6 The calculated H/Pd at 0.01 MPa

The H/Pd of Pd nanoparticles is smaller than bulk.

Conclusion

① Pd nanoparticles in the low Pd concentration samples could be suppressed the grain growth by mesopores in TMPS.

② For larger than 7.5mol%, large particles agglomerated on the outside of surface TMPS were observed.

③ Pd nanoparticles in TMPS exhibited smaller hydrogen absorption capacity than Pd bulk.

This ongoing work is done with Dr. T. Hioki in Motohiro Lab. in Green Mobility Collaborative Research Center in Nagoya Univ. in collaboration with and partially supported by TOYOTA Central R&D Labs.,Inc.

GREMO

TOYOTA CENTRAL R&D LABS.,Inc.

Synthesis of Magnesium based layered hydroxide particles and investigations of the chemical heat storage properties

Nagoya University, Japan
○Y. Sugie, S. Yamashita, H. Kita

Introduction

Studies of thermal energy conversion and storage are vital for the improvement of energy utilization. In particular, the study of chemical heat-storage is important because of several advantages. Especially, it can store energy for long periods of time and its heat-storage density is higher than that of latent heat storage. Therefore, The chemical heat-storage technology of waste heat from industrial processes and co-generation systems will be contribute to "Energy Saving".

Fig. 1 Crystal structure of Mg(OH)$_2$*
*Gregorio Guadalupe Carbajal Arizaga, Kestur Gundappa Satyanarayana, Fernando Wypych, Solid State Ionics 178 (2007) 1143–1162

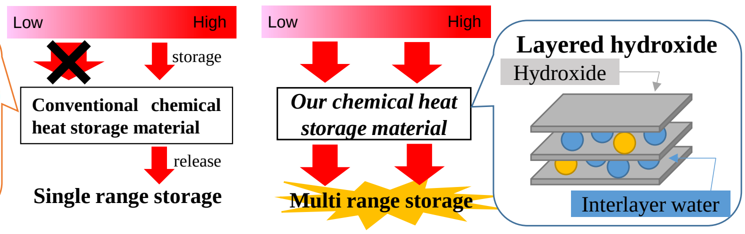

However, convectional materials such as Mg(OH)$_2$ have only single heat storage temperature range. Therefore, we focus on the layered hydroxide as a novel multistep heat-storage materials. They would be able to store heat by using the hydration-dehydration of interlayer water and hydroxide layer.

In this study, we investigate the effect of several experimental conditions on the synthesis of Mg based layered hydroxide by simple aqueous solution method. In addition, its multistep chemical heat storage properties was also investigated.

Experimental

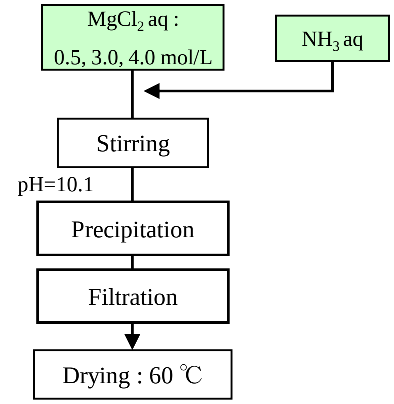

Characterization

SEM : Morphology

XRD : Crystal structure

TG/DTA : Thermal decomposition behavior

Results & Discussions

Morphology and crystal structure

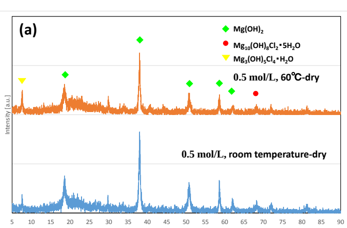

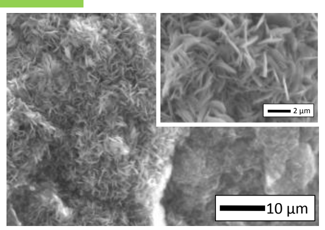

Fig. 2 SEM images of Mg based layered hydroxide particles

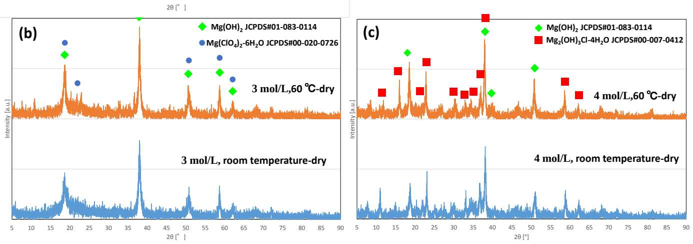

Fig. 3 XRD patterns of the sample with different initial MgCl$_2$ concentration: (a) 0.5 mol/L, (b)3.0 mol/L, (c)4.0 mol/L

0.5 mol/L
Mg(OH)$_5$Cl$_4$・H$_2$O
Mg$_{10}$(OH)$_{18}$Cl$_2$・5H$_2$O

3.0 mol/L
Mg(ClO$_4$)$_2$-6H$_2$O

4.0 mol/L
Mg$_2$(OH)$_3$Cl-4H$_2$O

The rate of Mg based layered hydroxide tend to increase as initial Mg concentration was higher.

but...

The concentration of Cl$^-$ tend to decrease.

Chemical heat storage property analysis

TG peak
At 70～180, 290～430℃ the weight loss (dehydration) was confirmed.

DTA peak
At 70～150, 290～430℃ Heat storage (dehydration) was confirmed.

Peak separation (reversed vertical axis)

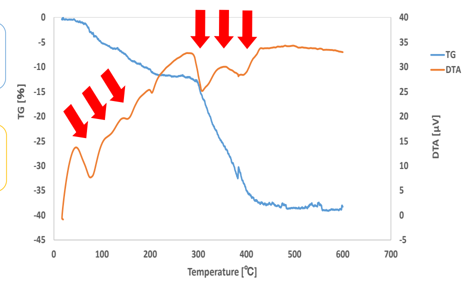
Fig. 3 TG-DTA of the obtained Mg based layered hydroxide (Fig. 2(c))

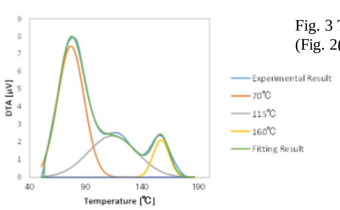

Fig.1 peak separation from 60 to150 ℃

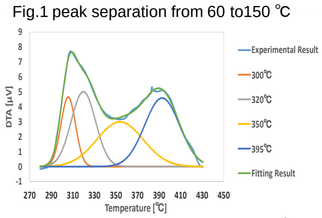

Fig.2 peak separation from 280 to 430 ℃

Table 1 The heat storage property between 60 and 150 ℃ of the sample with different initial concentration

concentration [mol/L]	heat of storage [μV・℃/g]
0.5	13.22
3.0	128.7
4.0	167.2

Table 2 The heat storage property between 280 and 430 ℃ of the sample with different initial concentration

Initial concentration / Peak position	0.5 mol/L	3.0 mol/L	4.0 mol/L
①300℃	—	78.88	90.19
②320℃	105.0	141.4	137.4
③Mg(OH)$_2$-350℃	1160	160.0	50.08
④395℃	103.0	183.7	385.7

The dehydration from hydroxide layer of Mg based layered hydroxide was changed to wide temperature range.

Conclusion

- Several Mg based layered hydroxide phases could be synthesized by changing initial Mg concentration and the amounts of layered hydroxide tend to increase with the increase of initial Mg concentration.
- It is found that Mg based layered hydroxide have a large heat storage capacity as compared with conventional Mg(OH)$_2$ using dehydration of interlayer water and magnesium hydroxide layer.
- Mg based layered hydroxide particles were expected to apply for the multistep heat-storage materials.

Control Strategy for Dexterous Handling Using Hemispheric Vision-Based Tactile Sensor

Naoki Kubota[1] , Goro Obinata[2]
[1]School of Engineering, Nagoya University [2]EcoTopia Science Institute, Nagoya University

The goal of this work is designing a control strategy for griping and lifting an object using tactile sensors and verifying this strategy experimentally. We can handle the object of which we do not know the shape, mass and friction properties in advance beginning handling.

1. Purpose

- To develop a robot hand with tactile sensors for dexterous handling of the unknown object.
- To improve tactile sensors for the robot hand.

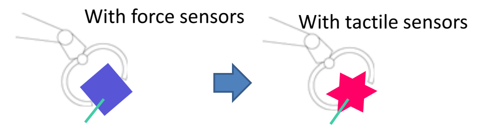

2. Vision-based tactile sensor

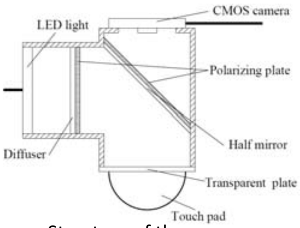

Structure of the sensor

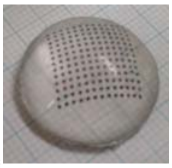

Touch pad with dots

3. Slip estimation method

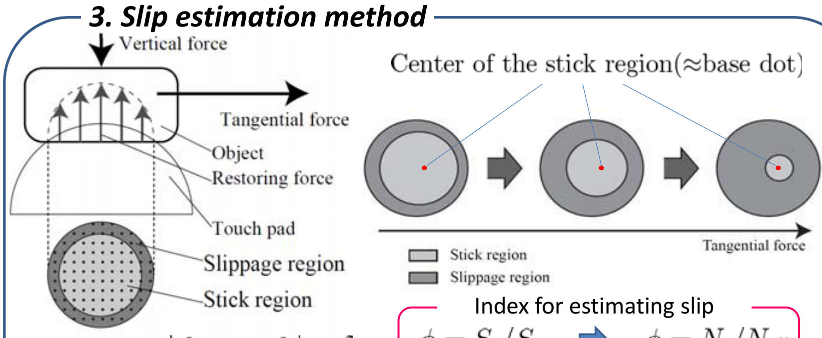

$|d_{\mathrm{base}} - d_i| < \delta$

Stick dot (dot in stick region)

Index for estimating slip

$\phi = S_s / S_t$ → $\phi = N_s / N_{\mathrm{all}}$

Area → Number of dots

4. Apparatus

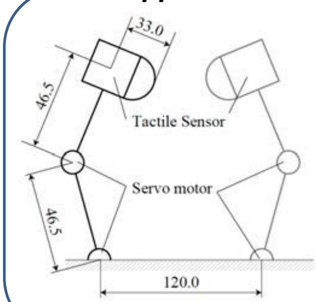

Robot hand

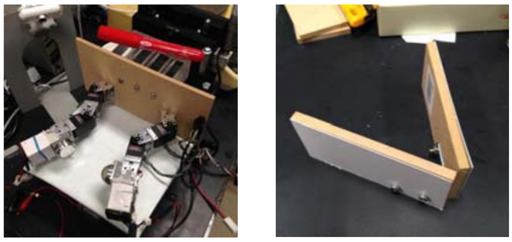

Handled object

5. Control Strategy for handling

5.1. Shape estimation

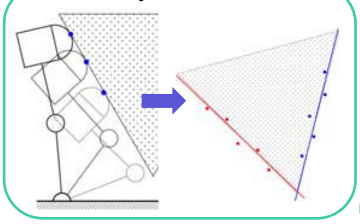

5.2. Analyzing the force vectors

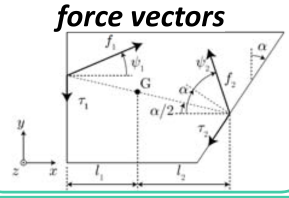

5.3. Lift the object by stick degree feed back

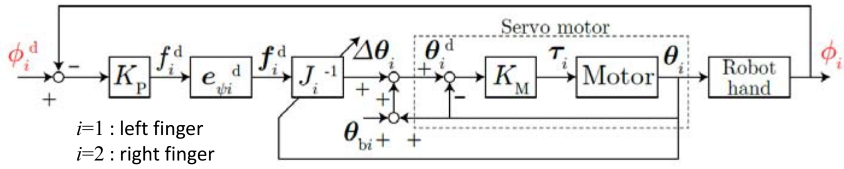

i=1 : left finger
i=2 : right finger

6. Experiment to grip and lift object

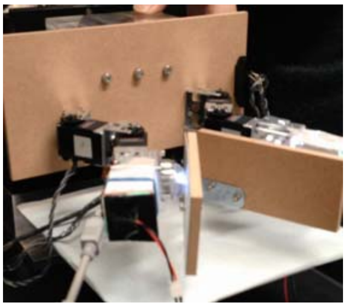

Prototype of the robot hand

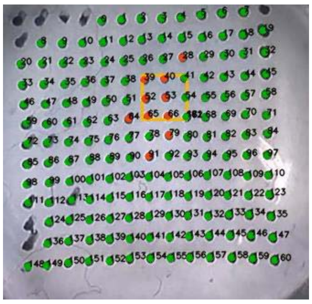

Image of the vision-based sensor

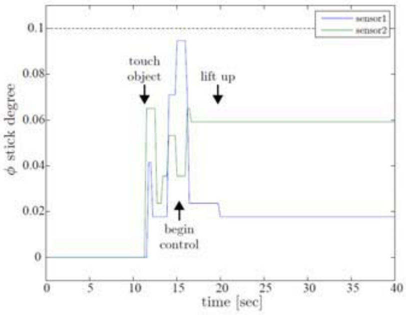

Stick degrees

7. Conclusion

- We designed the control strategy using the tactile sensors for handling.
- This control strategy feeds back stick degree to prevent slip
- The robot hand applied to this control strategy succeeded to grasp and lift the object stably.

8. Future works

We will apply our sensors to various handling tasks

The following tactile information
- force & moment
- friction, microscopic slip
- shape & attitude of a contacted object
- …etc.

Eg.

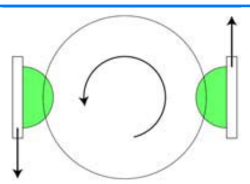

Rotating object

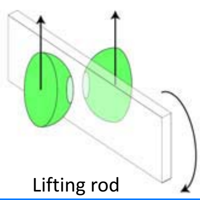

Lifting rod

Stabilization of Wheeled Personal Mobility for Handicapped People against External Force

Shotaro Okajima[1], Goro Obinata[2], Ko Yamamoto[2]
[1]School of Engineering, Nagoya University [2]Eco Topia Science Institute, Nagoya University

Introduction

The goal of this work is to stabilize the wheeled personal mobility for handicapped people when some external force is added to that one and to substitute this mobility for a wheelchair.

Concept of personal mobility

This personal mobility will be composed by a cart and a orthosis. The user can stand by using the orthosis and a steady handle. The wheeled-personal mobility is non-holonomic mobile robot, so the personal mobility has a weak point on just beside the mobile in being added a large amount of external force. In that condition, it is necessary for the user to turn a steering wheel. So, **we aim** to stabilize the personal mobility by using centrifugal force made by the trajectory tracking control in this research.

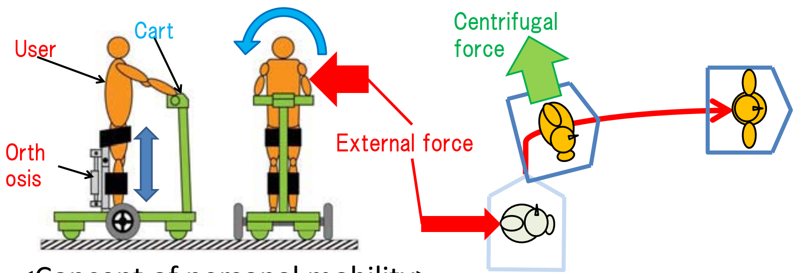

<Concept of personal mobility>

Modeling

To simulate, we regarded the user and the orthosis as a 2DOF inverted pendulum.

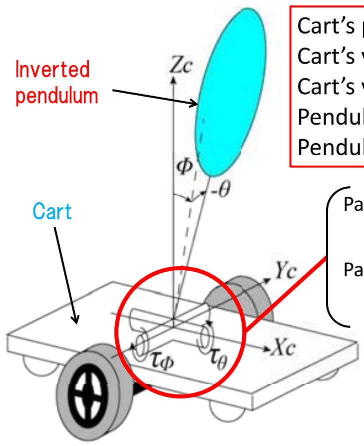

Cart's position: $\boldsymbol{x}_c = [\ x_c\ y_c\ ]^T$
Cart's yaw angle: ψ
Cart's velocity: v_c
Pendulum's pitch angle: ϕ
Pendulum's roll angle: θ

Passive torque of the pitch angle
$$\tau_\phi = k_2\phi + d_2\dot{\phi}$$
Passive torque of the roll angle
$$\tau_\theta = k_1\theta + d_1\dot{\theta}$$

<Wheel-driven mobile inverted pendulum>

Trajectory tracking control

Tracking control structure

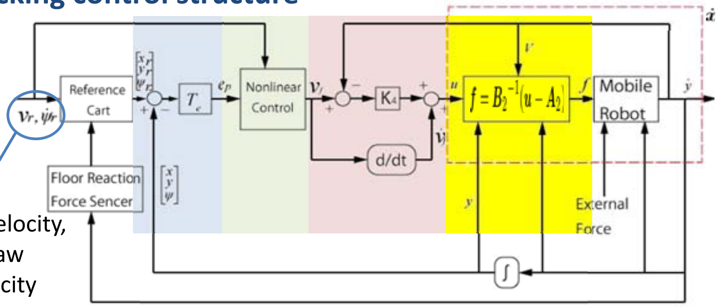

Reference velocity, Reference yaw angular velocity

$$\dot{\boldsymbol{x}} = \begin{pmatrix} A_1 \\ A_2 \end{pmatrix} + \begin{pmatrix} B_1 \\ B_2 \end{pmatrix} \boldsymbol{u}$$

: a difference vector $\boldsymbol{e}_p$ between reference position and real position.
: a nonlinear controller made with $\boldsymbol{e}_p$. It makes $\boldsymbol{e}_p$ zero as t → ∞.
: a PD control.
: a force controller made with $\boldsymbol{u}$ and $\boldsymbol{A}_2, \boldsymbol{B}_2$. $\boldsymbol{A}_2$, $\boldsymbol{B}_2$ are matrixes of cart's acceleration.

Simulation

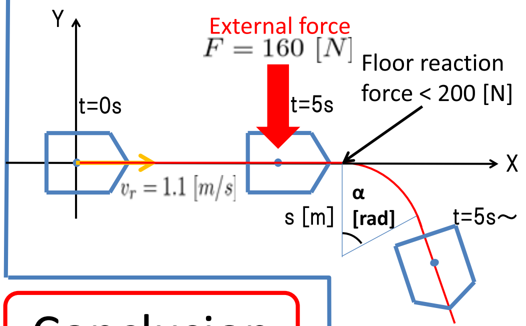

s=0.5 [m], α=-π/3 [rad], No shortening the pendulum size

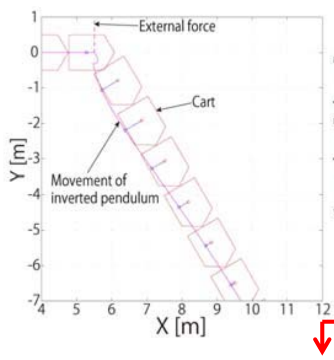

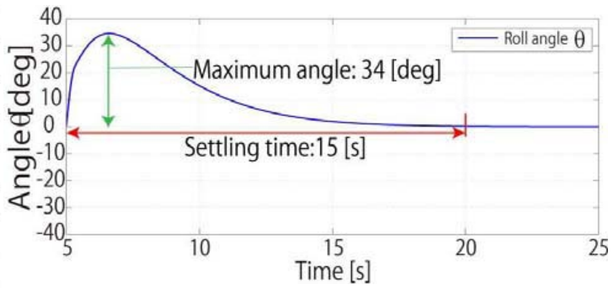

The idea for reducing the maximum roll angle and the settling time is to lower the COG.

s=0.5 [m], α=-π/3 [rad], Shortening the pendulum size

The normal pendulum size is 1 [m]. In this condition, we shorten the pendulum size from 1 [m] to 0.8 [m] in 0.1 [s]. To compare two figures of roll angle, maximum angle and settling time are reduced in shortening the pendulum size.

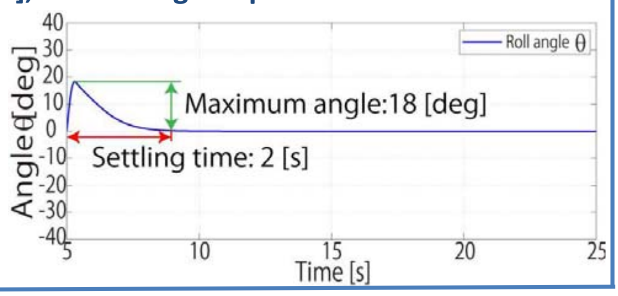

Conclusion

We confirmed the centrifugal force by trajectory tracking control made the inverted pendulum stabilized in this simulation condition.
In future works, we will change simulation conditions. For example, those are the external force's direction and magnitude. And, we will add feedback control to the trajectory tracking control.

Objective Evaluation of the Passenger Perception in the Simulated Brake Motion by Reflex Eye Movements

Kentaro Omura[1] , Hirofumi Aoki[2], Goro Obinata[3] , Ryoichi Kurasako[4], Kazufumi Toriya[5]

1) Department of Mechanical and Aerospace Engineering, Nagoya University
2) Institute of Innovation for Future Society, Nagoya University
3) EcoTopia Science Institute, Nagoya University 4)・5) Toyota Motor Corporation

1 INTRODUCTION

In the vehicle development process, it is important to evaluate the passenger comfort.

However, the evaluation of the passenger's perception during braking have been conducted subjectively so far.

➡ We propose a method to evaluate passenger perception

2 APPROACH

1.Motion Sickness

A typical reaction of the discomfort

Sensory Conflict Theory

Input → Sensory System (Vestibular, Visual, Somatosensor ...) → Actual Sensory Information → Mismatch ⇕ Discomfort

Input → Internal model (Build through the experience) → Model Output (= Predict Sensory Information) → Mismatch

2.VOR (Vestibulo-Ocular Reflex)

Attention as indicator of Sensory Conflict

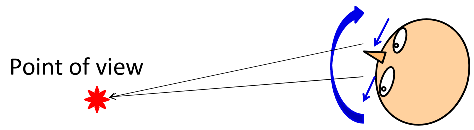

Reflex eye movements to stabilize the view
Based on the sensory information
from the vestibular organ

3.Model Based Approach

Ideal information processing of the VOR

Head Motion → Human → Actual VOR

Head Motion → VOR model → Model Output (= Ideal VOR) (−)
Head Motion → Human → Human Output (= Characteristic Changed VOR) (+)
Sensory Conflict → error

Hypothesis

Mismatch of the sensory information affect on the VOR characteristic

A method to measure the change of the VOR characteristic

3 EXPERIMENT

Subjects given simulated vehicle brake motions

Measuring Head Movements
by MAC3D motion capture system
Measuring Eye Movements
by limbus tracking method

Discuss the relationship between Subjects evaluation and VOR errors

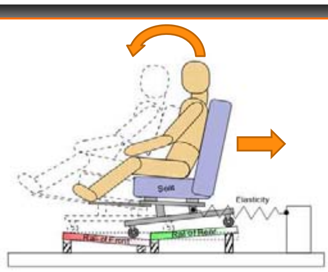

Condition #1
Deceleration + Pitch Down

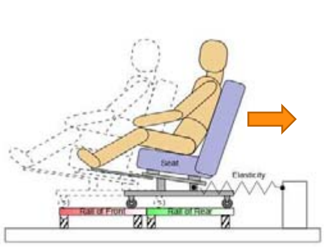

Condition #2
Only Deceleration

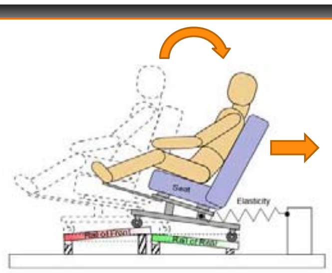

Condition #3
Deceleration + Pitch Up

Condition #1		Condition #2		Condition #3
Small	⬅	VOR error	➡	Large

$$NE = \frac{1}{Num}\cdot\frac{\sum_{i}^{Num}\left|\exp(i)-sim(i)\right|}{\sum_{i}^{Num} sim(i)}$$

Hypothesis

Small	⬅	VOR error (evaluation function)	➡	Large
Small	⬅	Sensory Conflict (Questionnaire)	➡	Large
Comfort	⬅	Subjective Evaluation	➡	Discomfort

Ask the ranking which is similar to vehicle brake motion

4 RESULTS AND CONCLUSION

1.Eye movement of the Subject

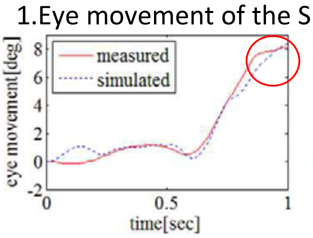

Condition #1

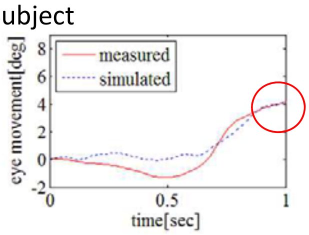

Condition #2

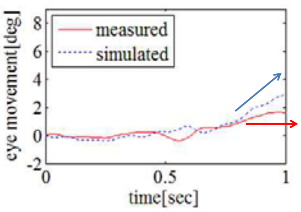

Condition #3

2.Relation between Evaluation Value and Subjective Evaluation

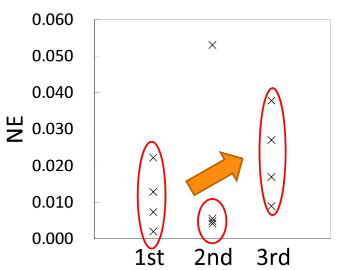

The ranking which is similar to vehicle brake motion

Subject Evaluation	Subjects felt the most comfortable with Condition #1 or #2 and the most uncomfortable with Condition #3
Evaluation function	Condition #1 and #2 are smaller than that of the Condition #3

➡ We confirm the correlation between the Evaluation value (VOR error) and the subjective evaluation

The 8th JUACEP Student Workshop at University of Michigan & UCLA Mar, 2014

Disinfection of Escherichia Coli by Hydrodynamic Cavitation

***Yuki Makanae* and Keiji Yasuda**

Department of Chemical Engineering, Nagoya University, Japan

Introduction

Problem of disinfection

Conventional technologies for disinfection have some problem. Chemical biocides are usually effective, but can generate dangerous or inconvenient organic by-product. On the other side physical methods tend to be more expensive.

Hydrodynamic cavitation

Hydrodynamic cavitation (HC) is expected to apply to the disinfection in wastewater. Costs of disinfection using HC will be much lower than these of conventional disinfection methods (chlorination, ozonization). And HC has some advantages such as safe operation, simple apparatus, and easy scale-up.

Purpose

In order to disinfect microbes effectively, operating conditions of hydrodynamic cavitation were investigated.

Mechanism of HC

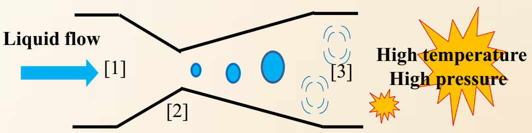

[1] Liquid flow rate accelerate through Venturi
[2] Pressure reduce in fluid and bubbles generation
[3] Bubbles collapse due to pressure recovery
Bubble collapse generates physical and chemical effects

Bernoulli's principle

$$\frac{1}{2}\rho v^2 + \rho g z + p = const \quad [Pa]$$

ρ [kg/m^3]	: Density	g [m/s^2]	: Gravity acceleration
v [m/s]	: Liquid velocity	z [m]	: Height
P [Pa]	: Pressure		

Condition of E. coli

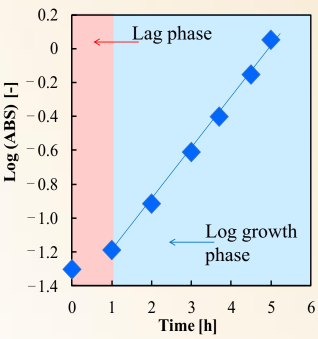

Lambert–Beer law

$ABS = kc$

k : Absorption coefficient
c : Molar concentration

[1] Lag phase
Restoration of cell
Maintenance of enzyme system
→No cell division

[2] Log growth phase
Start cell division
Generation time is cost.
→Be active

Comparison of Orifis and Venturi

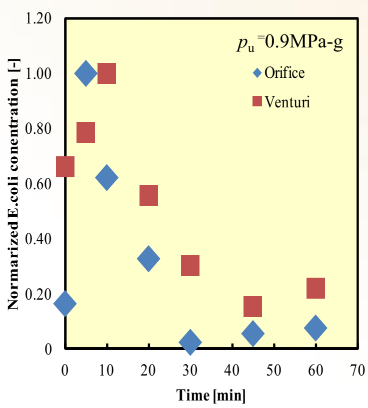

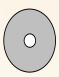

Φ = 2.7 mm

Disaggregation time

Orifise : 5 min
Venturi : 10 min

Orifice
∨
Venturi

Experiment

Apparatus

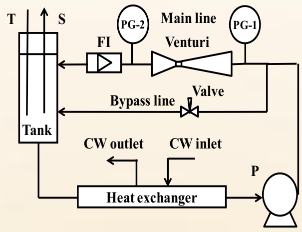

P	: Pump	PG	: Pressure gage
FI	: Flow indicator	T	: Thermometer
S	: Sampling point	CW	: Cooling water

Sample

E. coli suspension
(E. coli are diluted in 0.89 g/L of NaCl in deionized water)
Concentration : 1000 CFU/mL(colony forming unit per mL)

Operating condition

Sample volume	: 4.0 L
Temperature	: 25 ℃
Operation time	: 1 h
Upstream pressure	: 0.5~0.9 MPa-g
Inside diameter in pipe	: 7.5 mm
Power input	: 1.95 kW

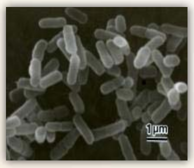

Result and Discussion

Effect of upstream pressure

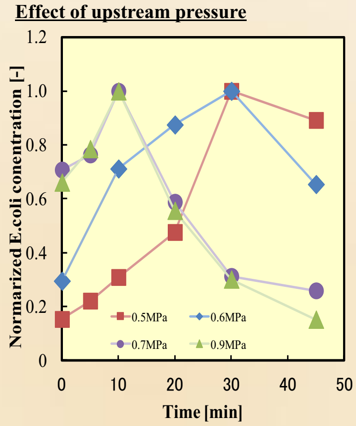

Upstream pressure ↑
⇒ Disaggregation time ↓

Reason

Liquid flow rate accelerate ↑
Number of bubbles ↑
Number of shock waves increases.

Death rate constant

$$\ln\frac{N}{N_0} = -k_d t$$

N [CFU/mL]	: Concentration
N_0 [CFU/mL]	: Max. concentration
k_d [1/min]	: Death rate constant
t [min]	: Time

As the death rate constant becomes higher, the effict of disinfection increases.

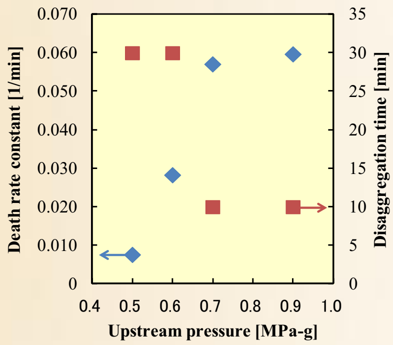

Disaggregation time ↓ ⇒ k_d ↑

Cavitation Number

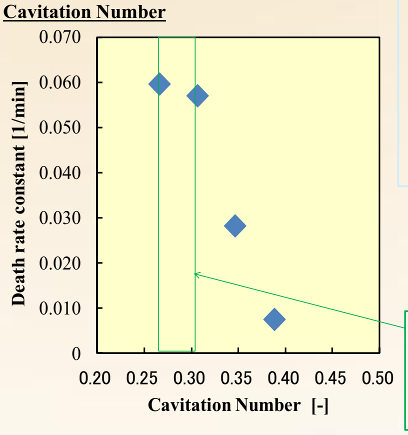

$$C_v = \frac{p_d - p_v}{p_u - p_d}$$

p_u [Pa]	: Upstream pressure
p_d [Pa]	: Downstream pressure
p_v [Pa]	: Vapor pressure of liquid

$C_v < 1$ Cavities are generated.
As the cavitation number becomes smaller, the number of cavity increases.

p_u ↑ ⇒ k_d ↑

but

Upstream pressure 0.7~0.9MPa-g
The number density of cavities ↑
These cavities start coalescing with each other
Increase of death rate constant decreases

Conclusion

(1) Upstream pressure is high, the effect of disaggregation is strong.
(2) The death rate constant increases with upstream pressure
(3) As the cavitation number becomes smaller, Death rate constant increases.
But if the number density of cavities increase, cavities start coalescing with each other. Increase of death rate constant tend to decreases.

Resources & Environment Lab., Chem. Eng., Nagoya Univ., Japan

Experimental Study on Effects of Radical Quenching by interaction between Wall and Methane-Air Premixed Flame

Kenta Yamamori Naoki Hayashi Hiroshi Yamashita
Kazuhiro Yamamoto （Nagoya University）

Introduction

Many combustors are surrounded by walls. Therefore, flames affected by them. The mechanisms of wall effects are as follows.

- Heat loss to the wall
- Radical quenching by surface reactions

Imperfect combustion and flame quenching occurs by them. As a result, generation of harmful matter and depression of combustion efficiency are caused.

Objectives

The interaction between CH_4-air premixed flame and wall is investigated.

When inlet velocities of premixed gas and surface materials of stagnation plate are changed,

- Inlet velocities at flame quenching
- Measurements of OH intensities by PLIF (Planar laser Induced Fluorescence)

Experiment apparatus

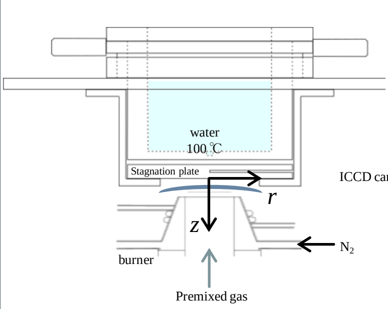

Combustor

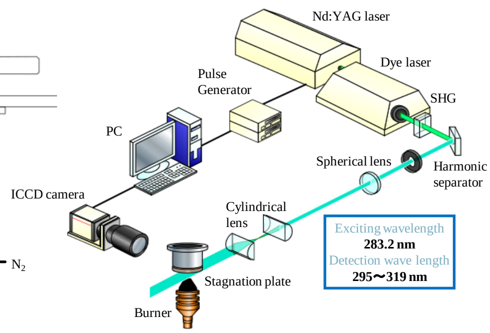

OH-PLIF system

Surface temperature calculation method

T: Temperature [K]
λ: Heat conductivity [W/(K•m)]
q: Heat flux [W/m^2]
l: Length [m]

$$q_{21} = \frac{1}{\frac{\ell_{steel}}{\lambda_{steel}} + \frac{\ell_{air}}{\lambda_{air}} + \frac{\ell_i/2}{\lambda_i}} \times (T_2 - T_1)$$

$$q_{32} = \frac{1}{\frac{\ell_i/2}{\lambda_i}} \times (T_{wall} - T_2)$$

from $q_{21} = q_{32}$ to $\boxed{T_{wall} = T_2 + \frac{\ell_i}{2\lambda_i} q_{21}}$

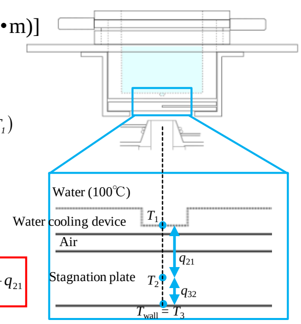

Experimental condition

Methane-air premixed gas combustion
Equivalence ratio: 0.75
Temperatures(T_{wall}): 700, 860, 900 K
Surface materials: Stainless steel, Copper, Ni metal
Inlet velocities: from 1.20 m/s to quenching

Quenching limits

Inlet velocities increase in each condition, until flames are quenching.

v [m/s]	T_{wall} [K]								
	Stainless steel			Copper		Ni metal			
Average	701.5	860.8	900.2	700.3	860.7	700.4	860.2	898.6
1.20	701.9	860.9	900.0	698.7	863.1	700.9	858.8	899.1
1.30	701.7	861.6	901.7	701.0	862.6	700.2	860.6	898.3
1.35	701.0	859.7	898.7	700.4	858.3	699.6	861.0	898.6
1.40	701.4	861.1	900.2	700.9	858.9	700.8	859.4	898.7
1.45	×	860.7	899.2	×	×	×	861.4	898.3
1.50	×	×	901.6	×	×	×	×	×
1.55	×	×	×	×	×	×	×	×

×…quenching

700 K: The quenching limit is the same with all the surface materials.
860 K: That for Copper is different from the others.
900 K: It is different between Stainless steel and Ni metal.

Distribution of I_{OH}

200 images are averaged.
I_{OH} is OH intensity in z-axis.

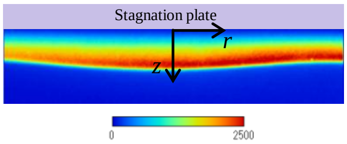

Surface material : Stainless steel
Surface temperature: 860 K
Inlet velocity : 1.40 m/s

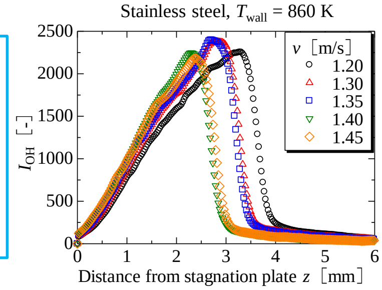

- The flame approaches to the wall with the increase in inlet velocity.

Comparison of $I_{OH,max}$

$I_{OH,max}$ is maximum of OH intensity in z-axis.

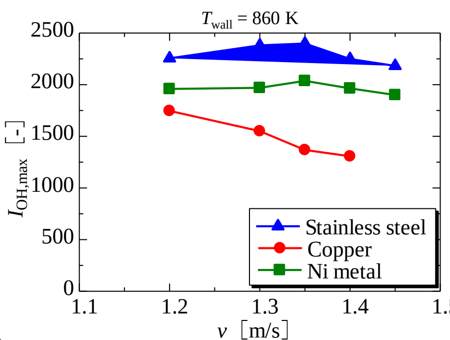

- $I_{OH,max}$ decreases in the order corresponding to Stainless steel, Ni metal, and Copper.
  - The reason is difference of surface reaction activity.
- OH intensity decreases with the increase in the inlet velocity.
  - The reason is influence of the walls because the flames approach to walls.

Conclusions

- The flames approach to the walls with the increase in inlet velocity.
- The inlet velocity at flame quenching is the same by surface materials at low temperature, but it increases in the order corresponding to Copper, Ni metal, Stainless steel at high temperature.
- Maximums of OH intensity decrease in the order corresponding to Stainless steel, Ni metal, and Copper.

Investigation of Interatomic Force Under the Tip of Microwave-AFM Probe

K. Hifumi, A. Hosoi, and Y. Ju
Department of Mechanical Science and Engineering, Nagoya University

Introduction

Recently, it has been reported that the effect of microwave gives an interatomic force in local area among materials. Therefore, it is thought that an identification of materials and an evaluation of electrical characteristics become possible by clarifying the relation between microwave and interatomic force. So, we investigated interatomic force under the tip of M-AFM probe by focusing on the force curve measurement method using M-AFM as the first step.

M-AFM

M-AFM is a kind of SPM, and it is a technique that combines microwave microscope technique and AFM. M-AFM can evaluate electrical properties by measuring microwave near-field signal and control the standoff distance by measuring the atomic force. M-AFM probe consists of AFM cantilever integrated with a parallel plate waveguide. To ensure effective transmission of microwave, gallium arsenide (GaAs) was used as the substrate.

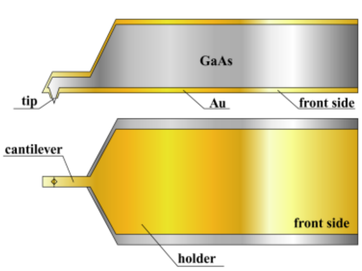

Schematic of M-AFM probe

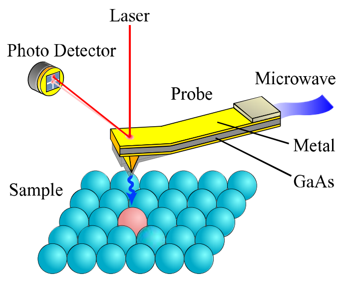

Conceptual diagram of M-AFM

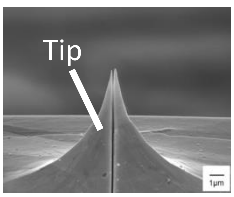

(a) SEM image of the tip

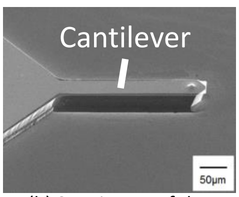

(b) SEM image of the cantilever

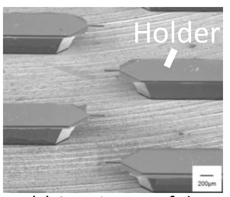

(c) SEM image of the M-AFM probe

M-AFM System

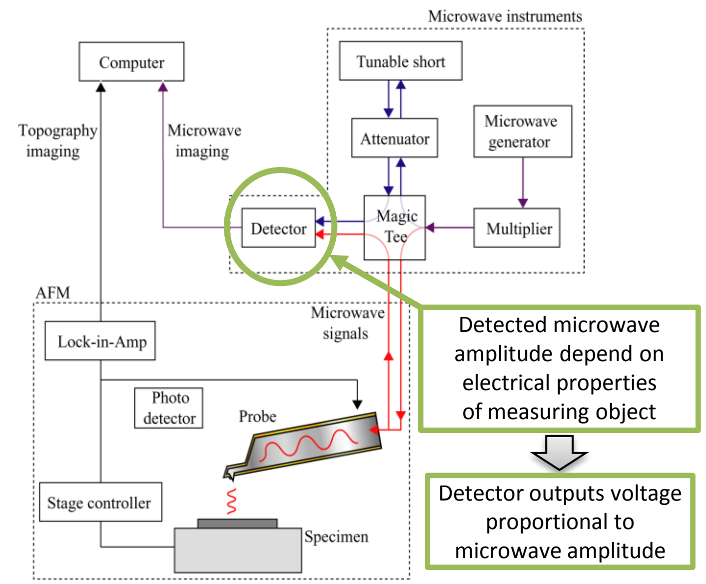

Diagram of the M-AFM system

Experimental Method

The force between a tip and a surface of samples is controlled constantly in AFM(NC-mode). Then a distance between the tip and the surface of samples is regarded as the standoff distance.
Force curve was determined when the probe was displaced from +22nm to -2nm as a basis of the standoff distance.

Condition of measurement
- NC-mode & M-AFM probe
- Frequency of microwave : 94GHz
- Amplitude of microwave : 0,5,10,15,20,25dBm
- Sample : Au, Si, Glass

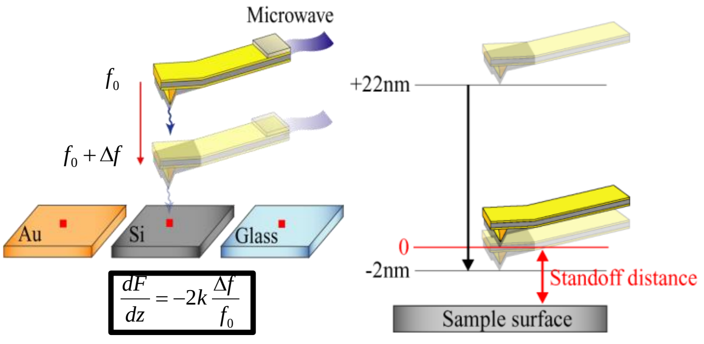

Measuring method of force curve

Experimental Results

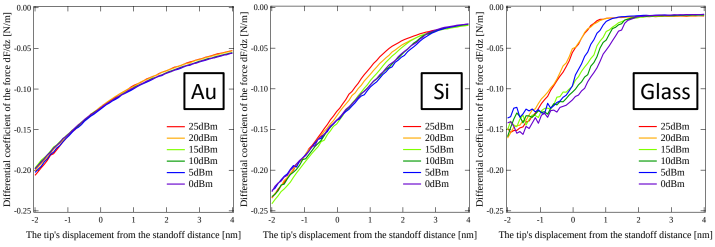

Results of experiment(Au, Si, Glass)

As results of the experiment, three things are observed. First, the graphic slope increases around the point of 0dBm(the standoff distance) as the amplitude of microwave increases. Second, the standoff distance increases as the amplitude of microwave increases. Finally, the amount of the graphic slope's change increases as the electric conductivity of a sample is smaller.

The standoff distance increases as the force between the tip and the surface of a sample increases by the principle of AFM. Therefore results of this experiment indicate that microwave works as a force that amplify the attractive force.

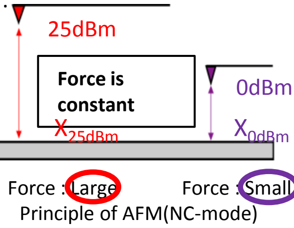

Principle of AFM(NC-mode)

Conclusions

Results of this experiment indicate actually that microwave works as a force that amplify the attractive force and the effect of microwave is different among samples which have different electric conductivities. Therefore, it is hoped that the evaluation of an electric conductivity become possible by interpreting such a force which amplify the attractive force under the tip of the probe.

TEM observation of dislocation motion induced by electric current

A.kojima, Y. Ju, and A. Hosoi
Department of Mechanical Science and Engineering, Nagoya University

INTRODUCTION

Fatigue is the main cause of failure accident in metallic structures. So various methods to heal a fatigue crack have been studied. Fatigue crack healing by controlling pulsed electric current is one of them. However, the mechanism of fatigue damage healing by electric current application is not clear. In this study, we focused on dislocations which have a close relationship with fatigue. We examine the change of dislocation induced by electric current and aim to elucidate the mechanism.

EXPERIMENTAL METHOD

Austenite stainless steel SUS316 was used as the experimental material. A CT specimen was employed as shown in Fig. 1. Fatigue tests were carried out with the CT specimen under the condition shown in Table1. After fatigue test, TEM sample was cut out from CT specimen as shown in Fig. 2. Samples were observed using TEM before current application and after each electric current application. Conditions of electric current application are shown in Table2. In the current application direction, the third application is the same as the first time and the second is from the opposite direction.

Table1. Conditions of fatigue test.

stress ratio R	0.05
applied force F	3 kN
frequency f	10 Hz
cycle number n	1.0×10^4

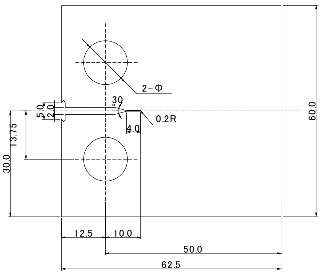

Fig. 1. Schematics of specimen.

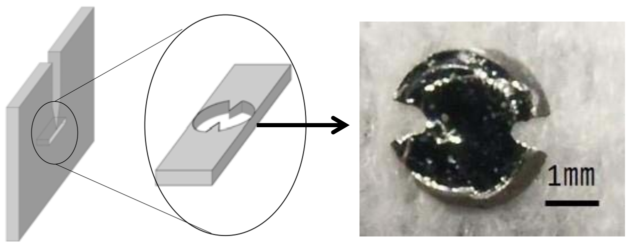

Fig.2. Conceptual diagram to prepare the TEM sample.

Table2. Conditions of current application.

	Application current [A]	Time [S]
first	1.0	60
second	Reverse 1.0	
third	1.0	

*All electric current applied is DC.

EXPERIMENTAL RESULTS

After the first current application, the number of dislocation increased in dislocation group X and dislocation Y occurred as shown fig.3-(b). In general, dislocation have a bulge in the direction receiving the external force. Therefore, it is considered from the shape of dislocations X and Y, that they received a force in the direction from lower left to upper right and moved in the same direction. After the second current application in the opposite direction of the first time, the number of dislocation X decreased and the shape of dislocations X and Y changed as shown in fig.3-(c). In addition, it is considered from the changes of the shape of dislocations X and Y, that they received a force in the direction from upper right to lower left and moved in the same direction. In the third current, there was no change in all dislocations.

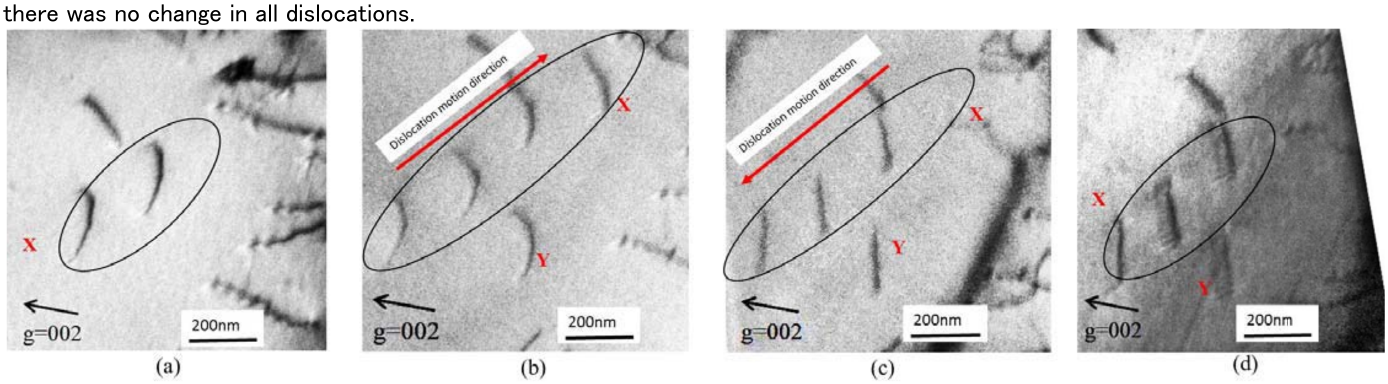

Fig. 3. TEM images of the dislocation
(a) before; (b) after first; (c) after second; (d) after third.

DISCUSSION

When the current application direction was opposite, the dislocation motion direction also became opposite. From the experimental phenomenon, it is considered that dislocation motion was caused by collision of electrons. In detail, metal atoms moved by collision of electrons. This is called electron migration. When the current application direction became opposite, collision electron direction became opposite. So, dislocation motion direction also became opposite.

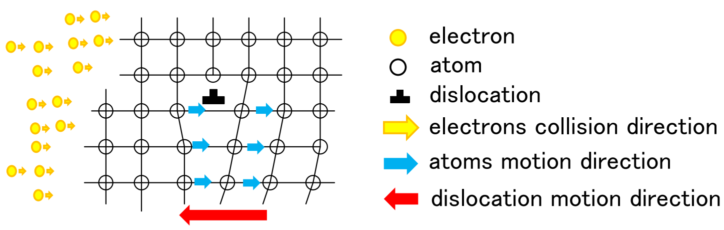

Fig.4. Conceptual diagram of dislocation motion .

CONCLUSIONS

Dislocations moved due to applying an electric current to metal materials. The reason is that electrons collided with metal atoms and metal atoms moved.

Growth and control of aluminum nanowires based on stress-induced migration

Sho NAKAMURA and Yang JU
Department of Mechanical Science and Engineering, Nagoya University
Furo-cho, Chikusa-ku, Nagoya 464-8603, Japan

Introduction

Metal nanowires may be used as a new functional element especially in MEMS, LSI and so on. In this study, we fabricate aluminum nanowires (AlNWs) by stress-induced migration which depended on hydrostatic stress gradient occurred in samples. Recent study shows that AlNWs have excellent electrical characteristics. To apply nanowires to nanometer-scale devices, revealing relationship between the dimensions of them and base film structure or heating conditions is needed. We report the fabrication of AlNWs through heating the samples in air and the influence of grain size, thickness of Al film, heating time, and heating temperature for the growth of AlNWs were studied.

Growth Principle of the Method

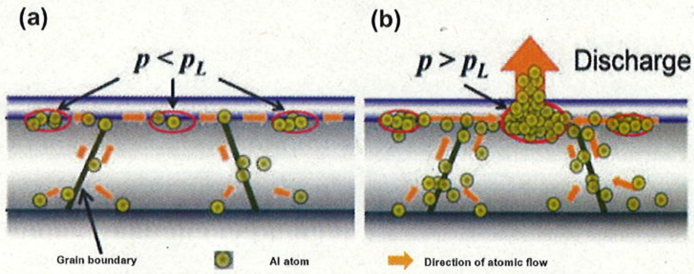

p : interfacial compressive stress p_L : compressive stress of lowest limit for nanowires formation

Stress migration is a phenomenon of atoms migration driven by the stress gradient. Atoms diffuse from a region of higher compressive stress toward that of lower one. When sample is heated, Al film is subjected to thermal stress because of the mismatch in thermal expansion coefficients between Al film and Si substrate. Al atoms diffused and migrated toward some site on the top face of Al film. If the accumulation of Al atoms at interface between the oxide layer and the Al film attains a critical value, Al atoms penetrated the oxide layer via any weak spot to form nanowires.

Experimental Details

First, Al film was deposited on the Si substrate by electron-beam deposition. Second, we measured the thickness and grain size of Al film by Kosaka Surfcorder ST-200 and Rigaku ATX-G respectively. Third, samples were heated in air by a ceramic heater. All samples were heated 3 hours at 523K. After heating, AlNWs were generated on samples. We measured the length and diameter of AlNWs and calculated the average values of 20 AlNWs. In this study, we heated 9 samples of Al films (Table.1). The thickness and deposition rate of each sample are different.

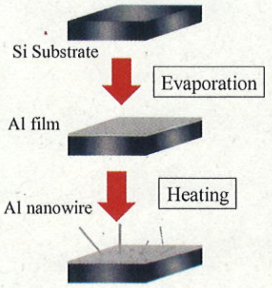

Fig.1 Schematics of AlNW growth

Table 1. Conditions of sample

Sample	Deposition rate [nm/sec]	Film Thickness [nm]
A		80 ± 5
B	0.02	100 ± 5
C		120 ± 5
D		80 ± 5
E	0.04	100 ± 5
F		120 ± 5
G		80 ± 5
H	0.08	100 ± 5
I		120 ± 5

Results and Discussion

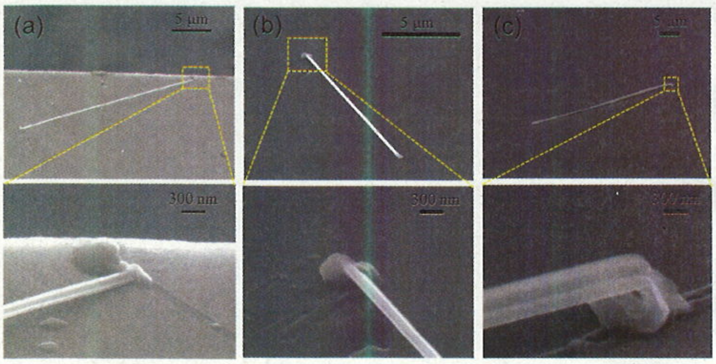

Fig.1. (a) SEM image of nanowire on sample B after heating, (b) SEM image of nanowire on sample E after heating, (c) SEM image of nanowire on sample H after heating.

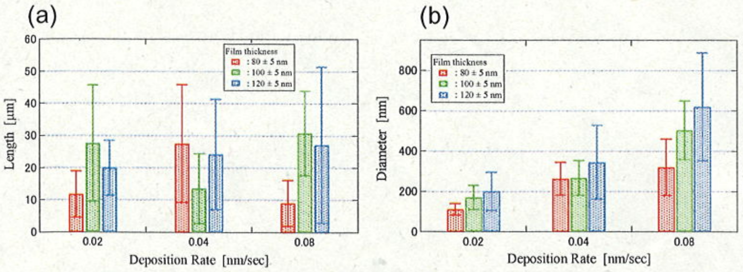

Fig.2. (a) Relationship between average length and deposition rate, for different film thicknesses
(b) Relationship between average diameter and deposition rate, for different film thicknesses

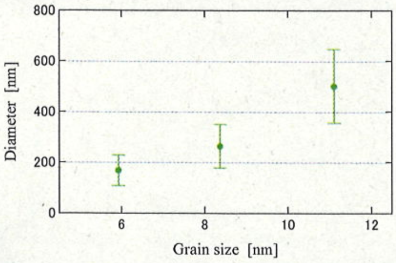

Table.2. Grain size of sample B, E, H

	Sample B	Sample E	Sample H
Grain size [nm]	5.92	8.36	11.1

Fig.4. Relationship between average diameter and grain size.

Fig.1 shows the result of after heating. AlNWs were generated on all samples. From Fig.2 (a), deposition rate and film thickness didn't affect the length of AlNWs. However, from fig.2 (b), as thickness is thin, the diameter is small. It is considered that driving force which generates AlNWs is due to stress gradient. So, we consider this is because driving force is small as the thickness of Al film is thin.

Fig.3 and Table.2 show the relationship between average diameter of AlNWs and deposition rate, grain size of Al film. These show that the diameter is small when grain size is small. We also observed the density of AlNWs is large when grain size is small. So we consider the decrease of driving force per one AlNW lead to size reduction of AlNWs diameter.

Conclusions

We generated AlNWs based on stress-induced migration and studied the condition of Al film to generate more thin AlNWs.

(1) Difference of deposition rate and film thickness does not affect the length of AlNW.

(2) As the grain size of Al film and film thickness are small and thin, the diameter of AlNW is small.

Development of highly ordered silicon nanowire array

Shuji Nota, Yang Ju
Department of Mechanical Science and Engineering, Nagoya University

Introduction

Electronic assembly relies on high-temperature processes such as reflow soldering or curing of adhesives. The high-temperature causes undesired thermal excursions and residual stress, which lead to reliability issues and restrict the application of temperature sensitive components. Therefore, there is an urgent need to attach electronic components on the circuit board with good mechanical and electrical properties at room temperature. So we've proposed Cu nanowire surface fastner (CuNSF) which has the bond strength and the electric conductivity. In this research, we made the highly ordered silicon nanowire (SiNW) array as the mold of the template to fabricate CuNSF.

Experimental Methods

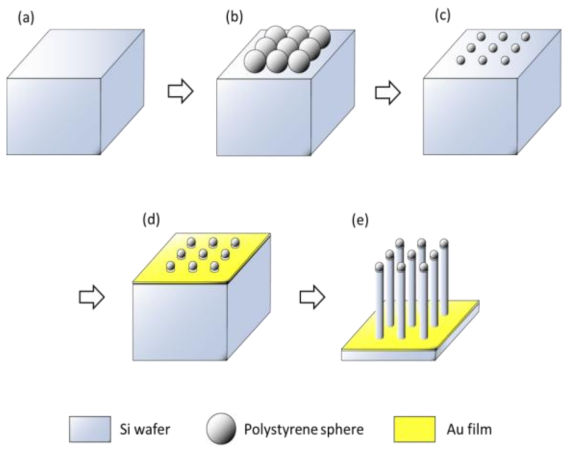

Figure.1 Schematics of SiNW array on the Si substrate.
(a) Cleaning and hydrophilization of the Si substrate
(b) Coating Polystyrene sphere (PS) on the Si substrate
(c) Etching of PS by Reactive-Ion Etching (RIE)
(d) Electron beam vapor deposition of Au
(e) Wet etching by HF/H_2O_2

Table.1 Condition of wet etching by HF/H_2O_2

Sample	Solution	RIE time [min]	HF/H_2O_2 wet etching time [min]	Original diameter of PS [μm]
A	4.6M HF + 0.44M H_2O_2	1	10	1.0
B		10	10	1.0
C		10	60	1.0
D		30	10	3.0

Experimental Results and Discussion

The PS monolayer on the Si substrate and that after RIE (10 min) are shown in Figure 2a, b. Then, the relationship between RIE time and diameter of etched PS was investigated (Figure 3). Additionally, the etched PS monolayer after deposition of Au is shown in Figure 2c.

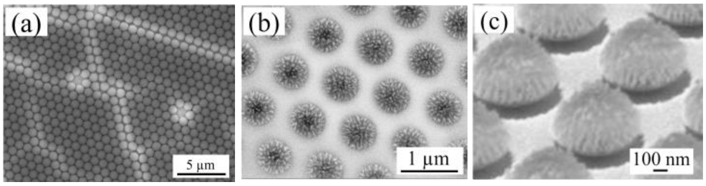

Figure.2 SEM images
(a) PS monolayer on the Si substrate; (b) after RIE 10 min; (c) after deposition of Au.

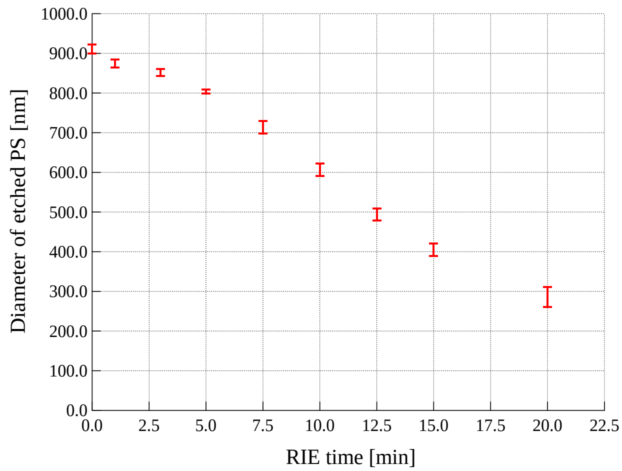

Figure.3 The relationship between RIE time and diameter of etched PS.

SiNW arrays on Si substrates are shown in Figure 4a-d.

(i) The RIE time was 1, 10 min for Sample A, B shown in Figure 4a, b. The diameter of SiNW array from 250 to 900 nm was obtained.
(ii) The wet etching time was 10, 60 min for Sample B, C shown in Figure 4b, c. The length of SiNW array from 0 to 12 μm was obtained.
(iii) The original diameter of PS was 1.0, 3.0 μm for Sample B, D shown in Figure 4b, d. The density of SiNW array from 1.1×10^7 to 1.0×10^8 NWs/cm^2 was obtained.

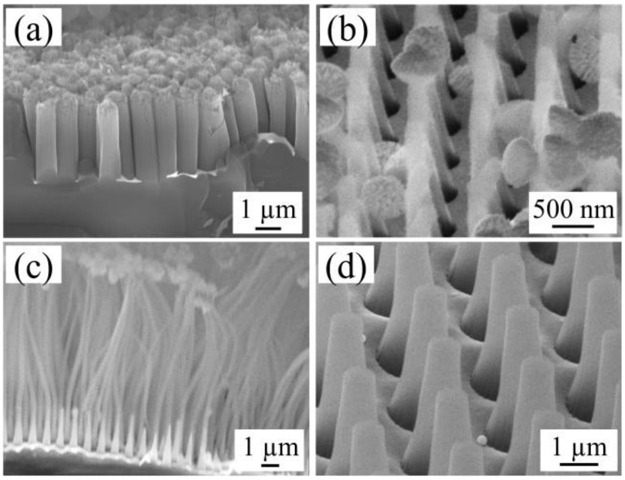

Figure.4 SEM images of SiNW arrays
(a) Sample A; (b) Sample B; (c) Sample C; (d) Sample D.

First, especially in the case of the high aspect SiNW array (Figure 4c), tens of SiNWs as a bundle are observed. One reason is the mass of the PS on the top of the SiNW. Another reason is H_2 gas generated through Si etching.

Finally, the diameter of SiNW is smaller than that of etched PS. This reason is the HF/H_2O_2 etching solution which isotropically etch Si.

Conclusions

Highly ordered SiNW arrays are obtained.

(1) Length of SiNW array: up to 12 μm
(2) Diameter of SiNW array: from 250 to 900 nm
(3) Density of SiNW array: from 1.1×10^7 to 1.0×10^8 NWs/cm^2

Study on development of a multi-inkjet head for building 3D living tissue

Takahiro Yamashita, Yasuyuki Morita, Yang Ju
Department of Mechanical Science and Engineering, Nagoya University

Introduction

Recently, research field called tissue engineering has attracted attention. Tissue engineering is a field of research that manufacture tissue artificially. 3D bioprinter is one of the manufacturing method of tissue has been attracting attention. 3D bioprinter is that how to construct a tissue by placing cells in three dimensions using inkjet technology. However, there is a problem that it takes time to manufacture tissue. One of the solutions for the problem is to use ink jet nozzles of the electrostatic actuator method. This method is capable of high speed by driving multi-nozzle simultaneously. However, there is no inkjet nozzle of the electrostatic actuator method suitable for cells. Therefore, in this study, development of multi-jet nozzle of the electrostatic actuator method suitable for cells was attempted.

Experiment process

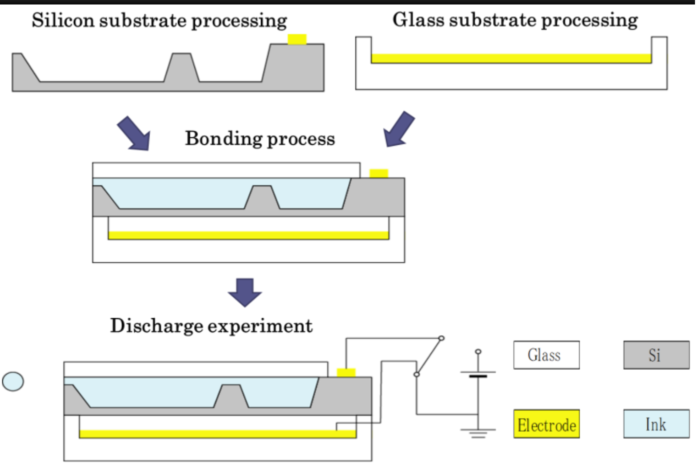

Inkjet Nozzle Fabrication by Wet Etching

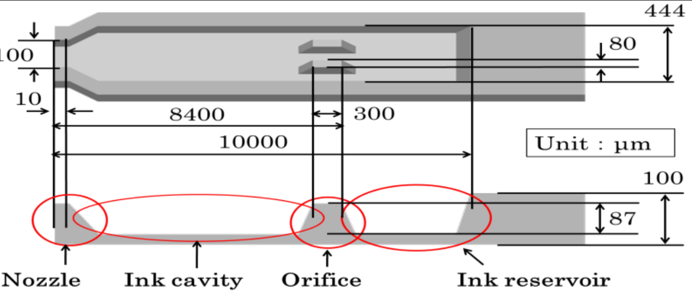

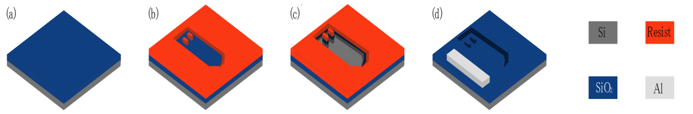

(a) Coating the oxide film on the surface for etching mask
(b) Patterning of the etching mask for the inkjet nozzle fabrication
(c) Forming the inkjet nozzle by wet etching
(d) Forming the electrode by electron beam evaporation method

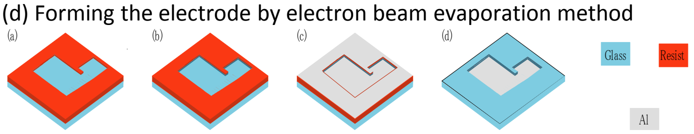

(a) Patterning of the etching mask for the electrode pattern
(b) Forming the electrode pattern by wet etching
(c) Depositing the metal
(d) Forming the electrode pattern by lift-off process

Electrostatic actuator method

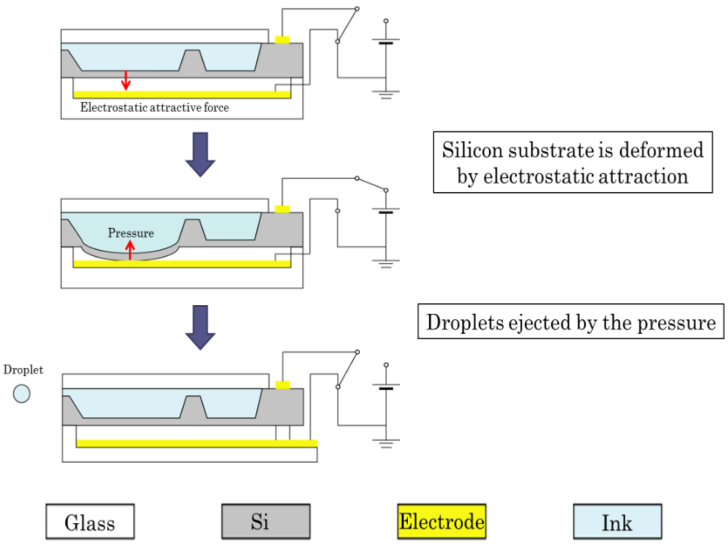

Experimental Results and Discussion

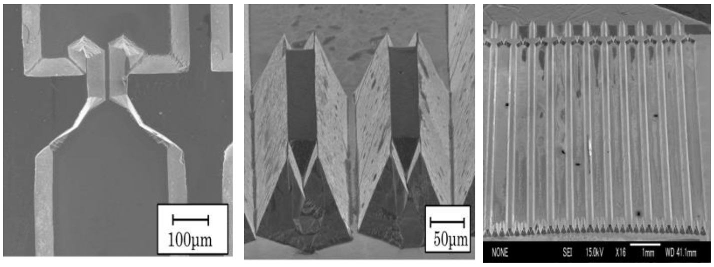

(a) SEM image of the nozzle
(b) SEM image of the orifice
(c) SEM image of the overall view

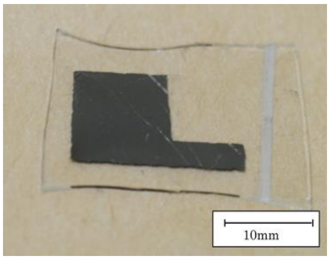

Photo of the glass substrate

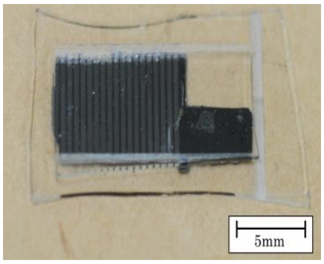

Photo of the inkjet nozzle were produced

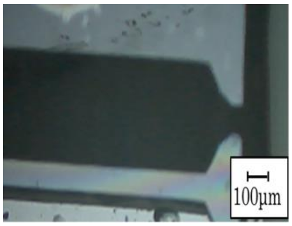

Discharge experiment

Discharge experiment was performed using inkjet nozzle were produced, but droplets were not observed. This is because the ink had penetrated into the nozzle tip by capillary. The design and fabrication process was reviewed in order to solve this problem.

Conclusions

(1) Multi-jet nozzles were designed and developed.

(2) The discharge was not observed, but the improvement plan was proposed.

FABRICATION OF ROUNDED KNIFE-EDGED STRUCTURE FOR TRANS-DERMAL DRUG DELIVERY SYSTEM

Kodai Imaeda[1], Katsuhiko Bessho[2], Mitsuhiro Shikida[3]
[1] Dept. of Mechanical and Aerospace Eng., Nagoya University, Nagoya, Japan
[2] Dept. of Mechanical Engineering, Nagoya University, Nagoya, Japan
[3] Center for Micro-Nano Mechatronics, Nagoya University, Nagoya, Japan

ABSTRACT

Either a pyramid or a circular corn is generally used as a shape for the micro-needles, which are applied in trans-dermal drug delivery system (DDS) . In this paper, we newly proposed a round-edged knife structure having a large surface area to increase a dosage amount in the trans-dermal DDS. We developed the process for producing a biodegradable round-edged knife by applying TMAH wet etching and PDMS molding. The penetration of the fabricated round-edged knife into a mouse skin was also experimentally confirmed.

TRANS-DERMAL DRUG DELIVERY SYSTEM

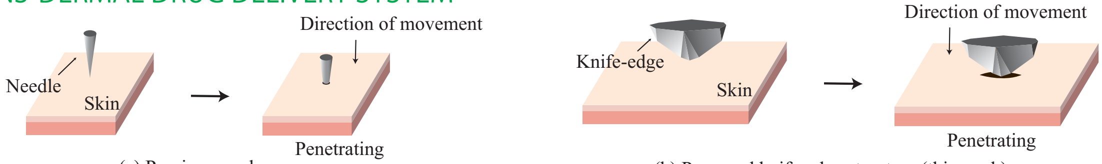

(a) Previous works

(b) Proposed knife-edge structure (this work)

FABRICATION

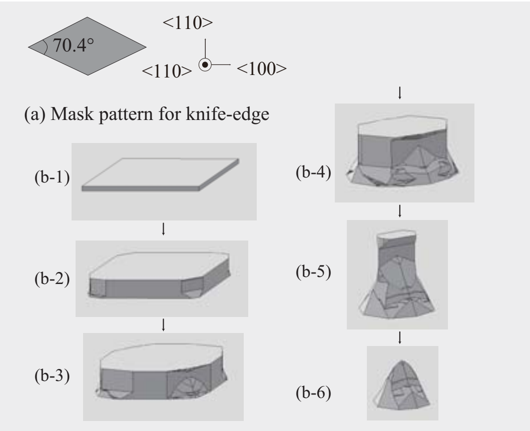

(a) Mask pattern for knife-edge

(b) Simulated shape change during TMAH etching

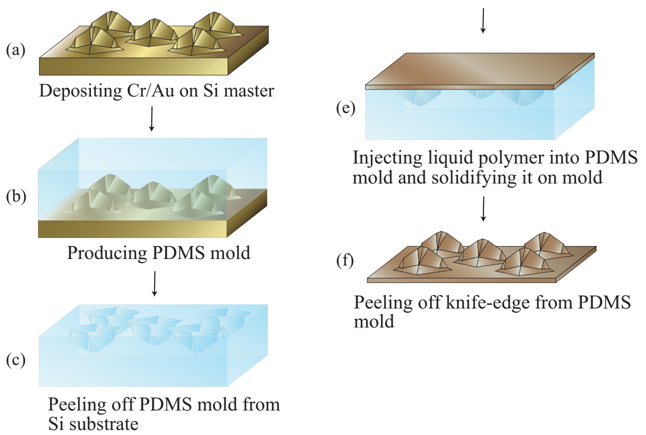

Fabrication of biodegradable knife-edge by molding

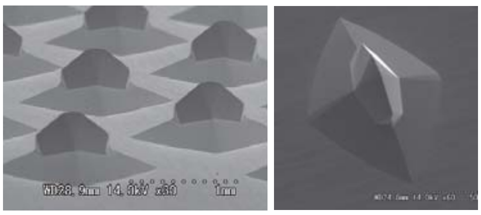

Fabricated Si knife-edge structures by etching

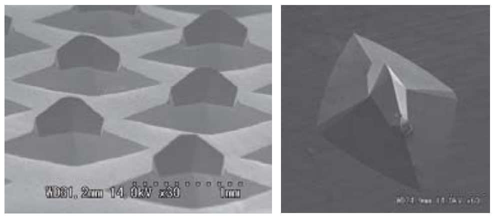

Fabricated biodegradable knife-edge structures by molding

PENETRATION TEST

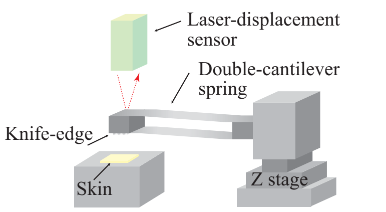

(a) Schematic view

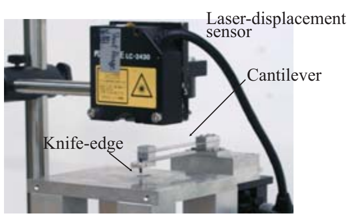

(b) Photograph

Experimental setup

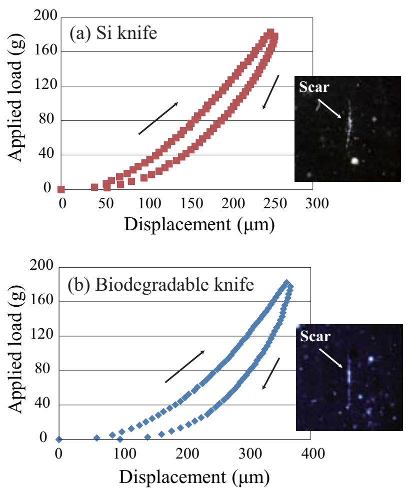

Penetration of single knife-edge into silicone rubber sheet

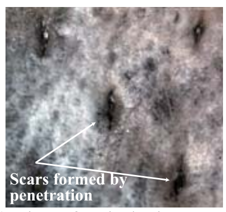

(a) View of optical microscope.

(b) View of SEM.

Penetration of arrayed bio-degradable knife into mouse skin

Scheduling Sports Tournaments Using Local Search Heuristics

Akira TSUZUKI， Nagoya University

1. Introduction

Sports scheduling problems are important for their economical value. National sport leagues, mainly in the US and Western Europe, represent a big business whose profits also depend on the quality of schedules.

AIM

To find a schedule with the minimum sum of the cost of every team satisfying constraints.
A cost of a team as the total distance that it has to travel starting from its home, playing the scheduled games, and returning back home.

2. Problem Description

○ Input

- A positive integer n
- $n \times n$ symmetric matrix D, such that d_{ij} represents the distance between the homes of teams T_i and T_j.

○ Output

A double round robin tournament on n teams satisfying following constrains.

- NoRepeat : Any pair of teams cannot play in consecutive days.
- AtMost : A team cannot play more than 3 consecutive games at home or away.

Double round robin tournament is a schedule in which each team plays with each other twice, once in each team's home.

Example

Inputting the left distance matrix, we get the right schedule. (and this is the optimal solution)

	ATL	NYM	PHI	MON
ATL	0	745	665	929
NYM	745	0	80	337
PHI	665	80	0	380
MON	929	337	380	0

team＼day	1	2	3	4	5	6
ATL	PHI	NYM	MON	@PHI	@NYM	@MON
NYM	@MON	@ATL	@PHI	MON	ATL	PHI
PHI	@ATL	MON	NYM	ATL	@MON	@NYM
MON	NYM	@PHI	@ATL	@NYM	PHI	ATL

3. Local Search Heuristics

TTP is NP-hard problem.
It is Difficult to solve by means of **exact methods**.
The most successful approaches have been based on **local search heuristics**.

Outline

1. Generate a feasible starting solution S;
2. Define neighborhoods $N(S)$;
3. While S is not locally optimal **do**
   Choose $S' \in N(S)$ such that $Distance(S') < Distance(S)$;
   $S \leftarrow S'$;
4. Output S.

We use…

Initial solution using a Traveling Salesman Problem's solution

Large neighborhood of size $O(n^3)$

1. Get a better starting solution S.
2. Explore large area on neighbor search.

4. Proposed Method

As for constraint optimization problems, good solutions exist near the infeasible region.
But it is difficult to move to a better solution by exploring only feasible region.
Our proposed method explores both feasible and infeasible regions. And we introduce a new evaluation function to balance the exploration of the feasible and infeasible regions.
The function includes advanced technique "strategic oscillation".

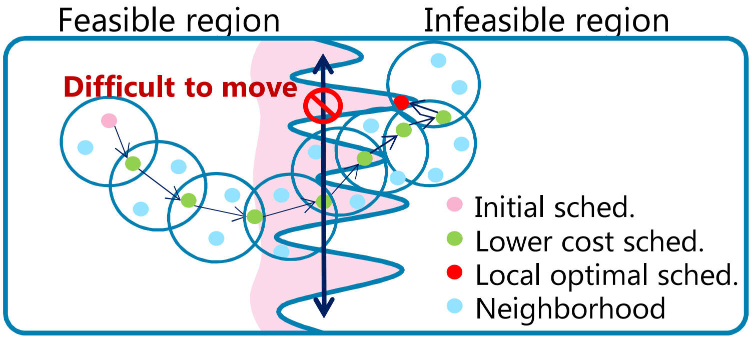

Proposed evaluation function

$$Cost(S) = \sqrt{Distance(S)^2 + [Weight \cdot Violation(S)]^2}$$

The key idea is to vary the parameter "Weight" during the search.
Weight is updated according to the frequencies of feasible and infeasible configurations in the last iterations.
This operation makes it possible to do the followings,

1. To explore widely keeping violations within certain ranges.
2. To force the solution to move to a feasible solution at the end.

5. Numerical Experiment

We experimented our algorithm on various instances.
The NFL-x family is based on real data of the US National Football Leagues.

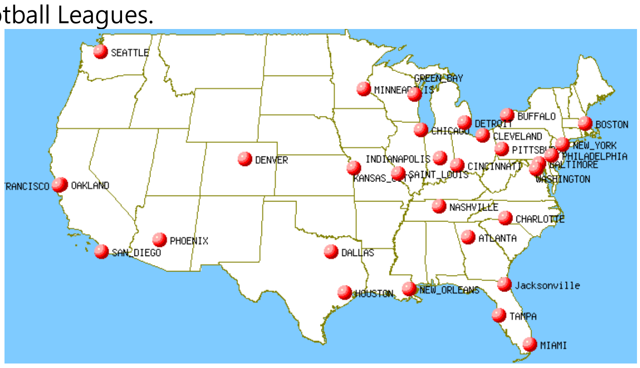

Ex. Original cities of NFL32

Instance	Feasible region search		Proposal method	
	Total Distance	Computation Time[sec.]	Total Distance	Computation Time[sec.]
NFL20	391698	26.3	386735	63.1
NFL26	587597	70.1	581061	238
NFL32	989161	159	983178	745

Max 1.2% reduction !

Fabrication and Manipulation of 3D Hybrid Nanorobot for Single Cell Puncture

Takayuki Hasegawa, Takeshi Hayakawa, Fumihito Arai

Department of Micro-Nano Systems Engineering, Nagoya university

NAGOYA UNIVERSITY

Biorobotics LAB

Puncture Single Cell with CNT Integrated Nanorobot!!

Background

Conventional Single Cell Puncture

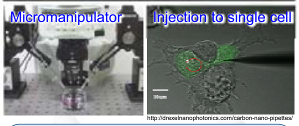

Optically Driven On-Chip Robot

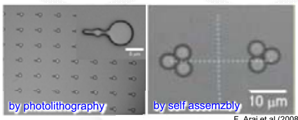

F. Arai et al (2008)

Conventional Problem
- Open space (Contamination)
- Low throughput
- Low repeatability

Advantage
- Noncontact manipulation
- High positioning accuracy
- High repeatability

Problem
- ✓ Difficulty of Functionalization
- ✓ Low manipulation force

Experimental system

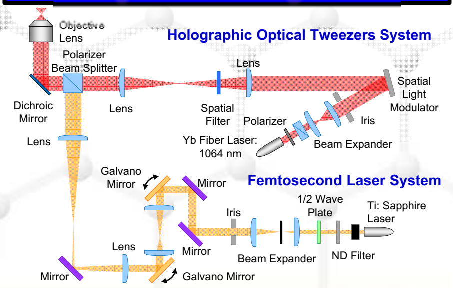

Carbon nanotube (CNT)
- High photothermal efficiency
- High thermal conductance

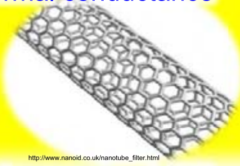

http://www.nanoid.co.uk/nanotube_filter.html

Single Cell Puncture

CNT Integrated 3D Hybrid Nanorobot

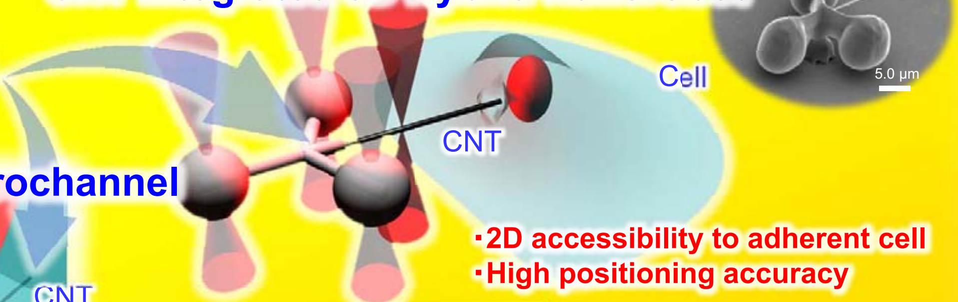

- 2D accessibility to adherent cell
- High positioning accuracy

CNT Integrated Microchannel

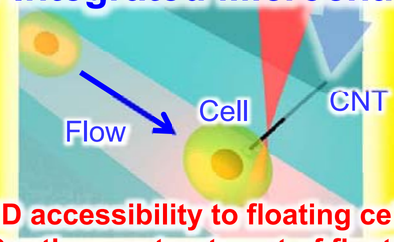

- 1D accessibility to floating cell
- Continuous treatment of floating cell

Purpose
1. Fabrication of 3D hybrid nanorobot integrating CNT.
2. Optical manipulation of fabricated hybrid nanorobot.
3. Single cell puncture with hybrid nanorobot.

Fabrication

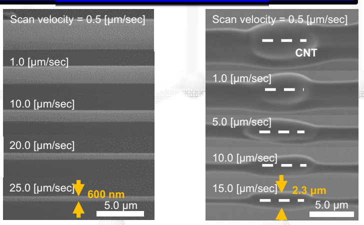

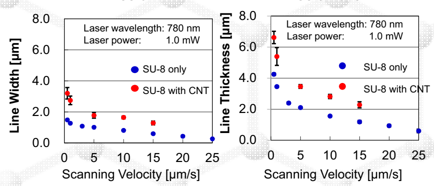

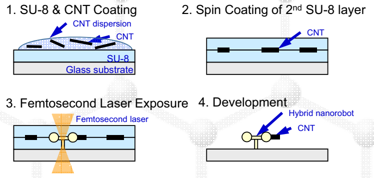

Manipulation

Position Measurement

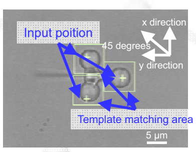

Frequency Response

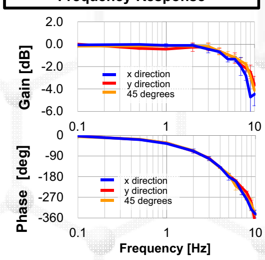

Step Response / Ramp Response

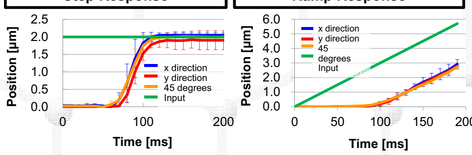

Cell Puncture

Nanobeads injection Experiment

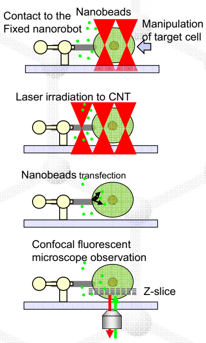

- MDCK cell dispersion
- Life technologies Cell Mask for membrane stain
- 100nm for each z slice interval

Irradiated laser energy

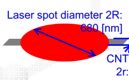

P: Laser Power $= 3.55 \times 10^{10}\ [W/m^2]$

A: Irradiated Area $= 2R \times 2r = 1.02 \times 10^{-13} [m^2]$

$P \times A = 3.62 [mW]$

Control Cell Image without nanobeads

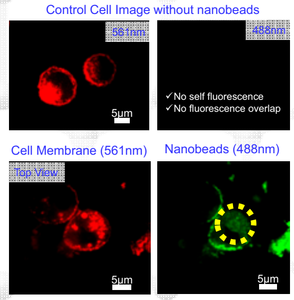

100nm beads was injected into target cell

Conclusion
1. We succeeded in fabrication of hybrid nanorobot integrating CNT.
2. We succeeded in optical manipulation of the hybrid nanorobot.
3. We succeeded in single cell puncture with the hybrid nanorobot by irradiating IR laser on CNT.

Contact Person: Takayuki Hasegawa
E-mail: hasegawa@biorobotics.mech.nagoya-u.ac.jp
http://www.biorobotics.mech.nagoya-u.ac.jp/

Arai Laboratory,
Department of Micro-Nano Systems Engineering, Nagoya University
Furo-cho, Chikusa-ku, Nagoya-City, Aichi-Pref., 464-8603, Japan
TEL: +81-52-789-5220, FAX : +81-52-789-5027,

Acknowledgements : This work was financially supported by Core Research for Evolutional Science and Technology (CREST), Nagoya University Global COE program for Education and Research of Micro-Nano Mechatronics, and Japan Society for the Promotion of Science (JSPS) Fellows.

The Effect of Plasma-on time on the hardness of DLC film deposited with microwave-assisted plasma CVD

Yoshihiko Hagiyama, Hiroyuki Kousaka, Noritsugu Umehara, Takayuki Tokoroyama
Nagoya University

Background

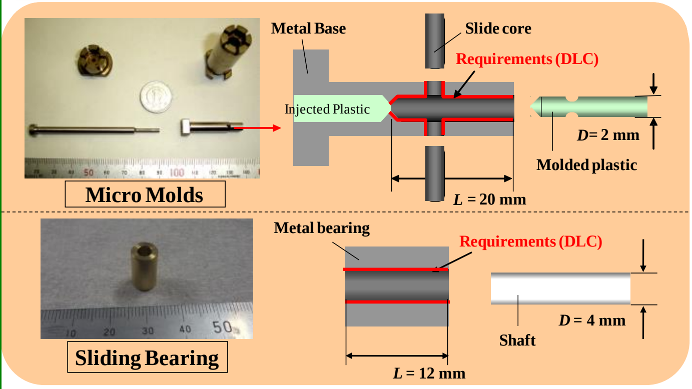

For saving the energy, it is required to coat the inner surface of narrow tube with DLC (Diamond-Like Carbon), which is a hard carbon film with great mechanical properties, such as low friction coefficient, wear resistance and corrosion resistance. Generally we form DLC films by plasma CVD method. Though it is difficult to generate plasma in the narrow tube, by using the MVP (Microwave-sheath Voltage combination Plasma) method we can generate plasma even in the narrow tube and coat the inner surface.

MVP (Microwave-sheath Voltage combination Plasma)

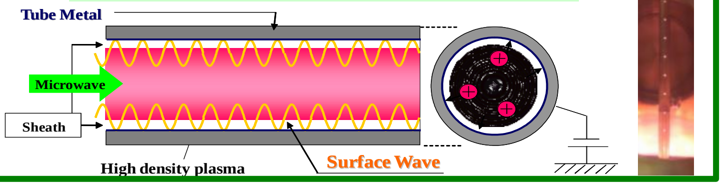

Problem and purpose

Hardness of DLC films coated on inner surface of narrow tube is not sufficient (15GPa).

Suggest the guidelines to form the hard DLC film on inner surface of narrow tube.

Experimental setup

Gas flow, sccm	Ar	9.0
	CH_4	2.0
	TMS	0.2
Microwave	Frequency, GHz	2.45
	Pulse frequency f_{mw}, Hz	10
	Duty ratio D_{mw}, %	0.85, 1.25, 1.65, 2.05
	Peak power, kW	0.8, 1.0, 1.7
Substarate bias	Pulse frequency f_{dc}, Hz	10
	Duty ratio D_{dc}, %	0.80, 1.20, 1.60, 2.00
	Voltage, V	-200
Plasma-on time T_{on}, ms		0.80, 1.20, 1.60, 2.00
Pressure, Pa		80
Deposition time, min		120

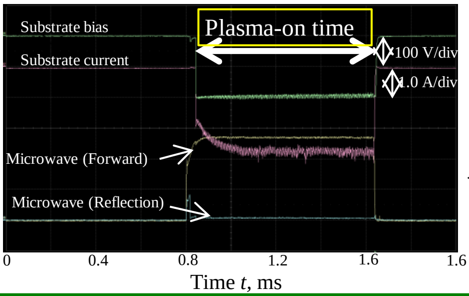

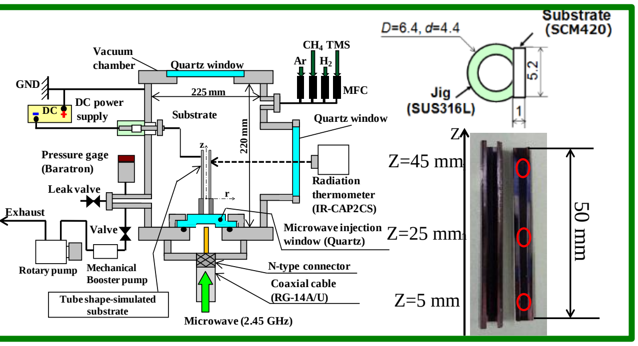

The effect of Plasma-on time

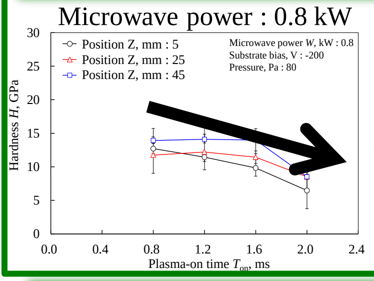

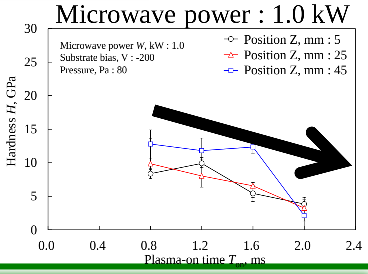

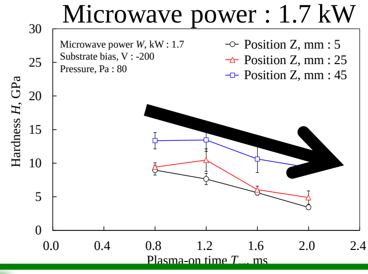

S. S. Tzeng informed that DLC filmes became softer by conducting the processing of Ar sputtering[1]. We consider that our inside coating had the same effect because we flow Ar into chamber. Thus increasing the plasma-on time resulted in the increase in Ar sputtering time and decrease in hardness of DLC film.

The effect of ion flux per film thickness

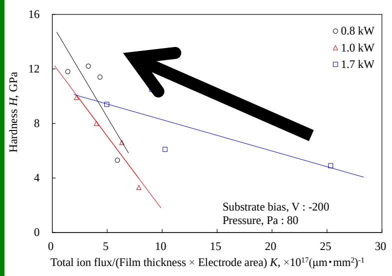

$$K = \frac{\int_0^{t_{dep}} I(t)dt \cdot 1/e}{d_{DLC} \cdot S}$$

d_{DLC} : Film thickness [μm]
S : Substrate surface area [mm^2]
$I(t)$: substrate current [A]
D_{DC} : Duty ratio [%]
t_{dep} : Deposition time [s]
e : Elementary electrical charge [C]

Decrease in K ➡ High hardness

Under the condition of short plasma-on time, DLC films are likely to be hard.

Slope: $\alpha_{0.8} > \alpha_{1.0} > \alpha_{1.7}$
Under the condition of microwave power 0.8 kW, DLC films are likely to be hard.

Conclusion

(1) Hardness of DLC film decreased with increasing the Plasma-on time.
(2) Hardness of DLC film decreased with increasing the K-value.

References
[1] S. S. Tzeng, Y. J.Wu, J. S. Hsu, Vacuum, 83 (2009) 618-621.
[2] H. Kousaka, Y. Takaoka, T. Okamoto, N. Umehara, Tribology conference proceedings, B12

March 2014

Discussion of super low friction mechanism of CNx coating against CNx under oil

K. Ichimura, N. Umehara, T. Tokoroyama and H. Kousaka Nagoya University

Background and Purpose

The Carbon Nitride (CNx) coating exhibit lower friction coefficient than other DLCs under lubrication. However, low friction mechanism has not been clarified.

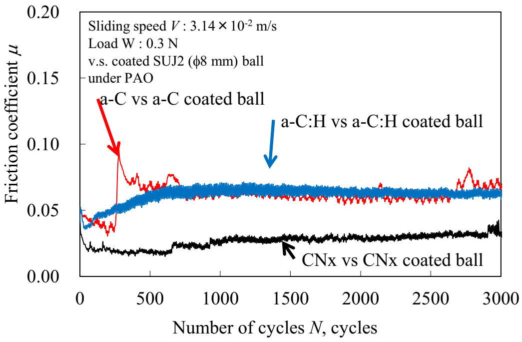

Fig.1 Result of friction test

⇒I want to know the reason why CNx show low friction coefficient.

EXPERIMENT

Pendulum Style Friction test

This tester can measure friction coefficient under boundary lubrication.

Friction coefficient under boundary lubrication does not depend on viscosity and speed but oiliness.

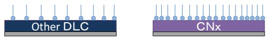

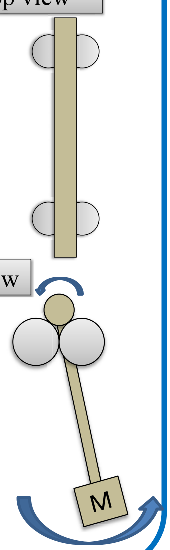

Experimental conditions

Specimen	CNx on SUJ2 pin vs. CNx on SUJ2 ball a-C on SUJ2 pin vs. a-C on SUJ2 ball a-C:H on vs. a-C:H on SUJ2 ball
Normal load	:0.46 [N]
Temperature	: 25, 80, 120, 160 ℃
Lubricant	: PAO
Max angle	: 0.5rad

RESULT and DISCUSSION

Low speed cause low friction

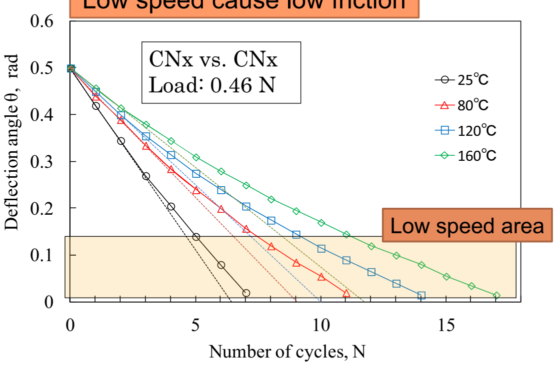

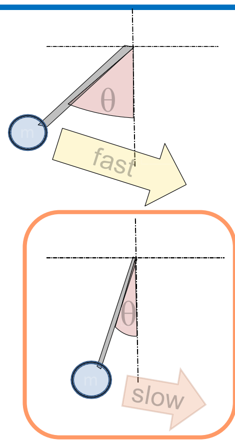

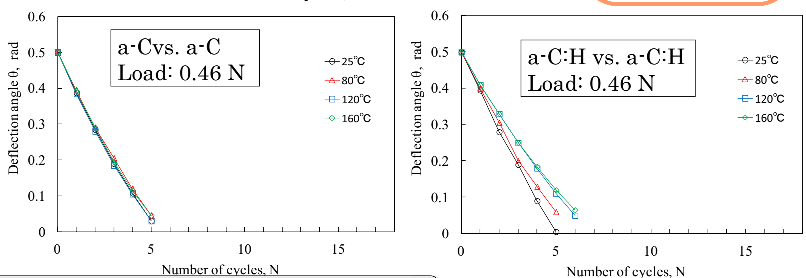

High temperature cause low friction

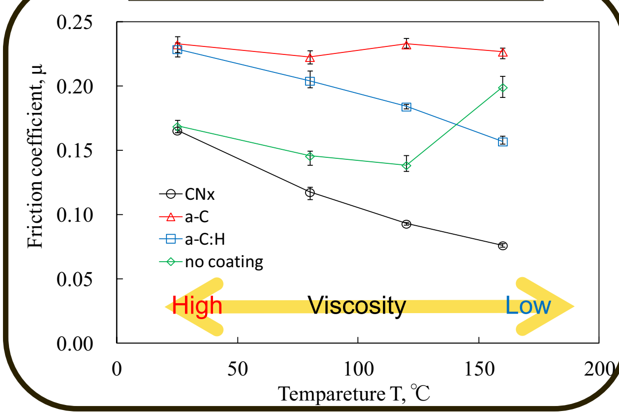

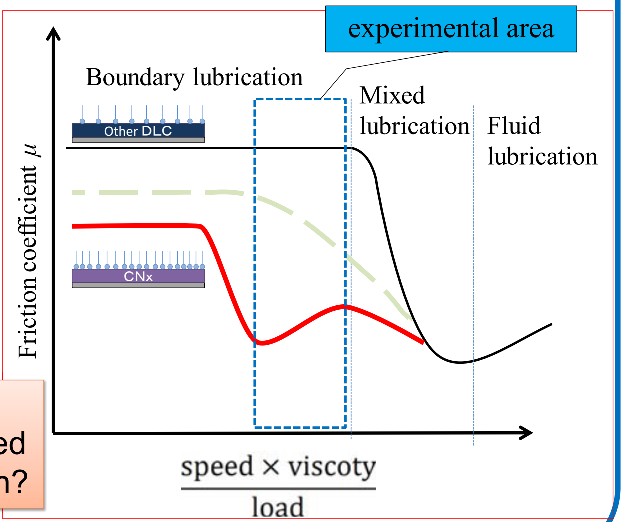

Measuring dangling bond density

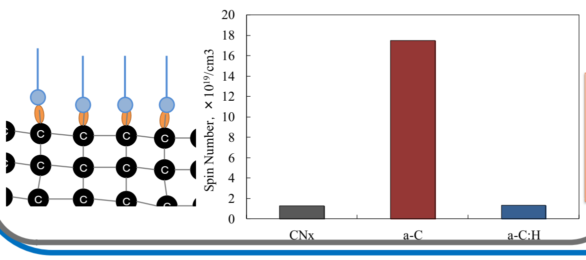

Decrease of Viscosity or speed cause low friction?

CONCLUSION

CNx shows unusual behavior under the boundary lubrication.
Friction coefficient does not depend on dangling bond density.

Development of lubricating sheet in drilling materials for aircraft

NEW LUBRICATION

Takayuki Kawasaki, Noritsugu Umehara, Hiroyuki Kousaka and Takayuki Tokoroyama Nagoya University March, 2014

WHAT is LUBRICATING SHEET

Lubricating sheet is made by aluminum sheet, lubricating layer and bonding layer. Lubricating layer is solid lubricant, mainly made from polyethylene glycol, polyethylene oxide and epoxy resin. Lubricating layer is water soluble and melting point of lubricating layer is 55~60 ℃.

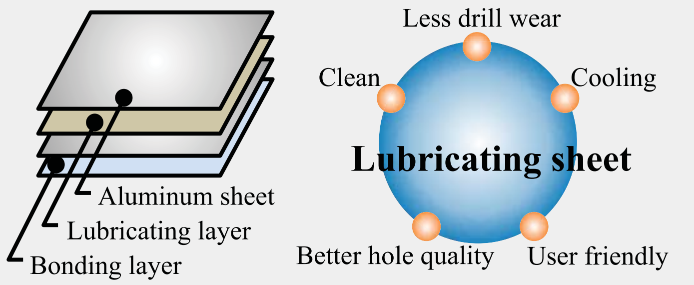

Background

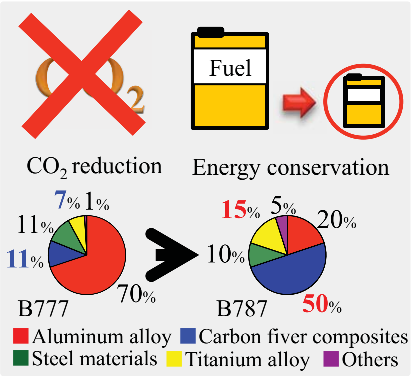

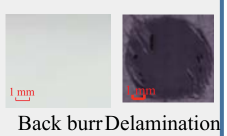

In this research, we suggest the guide line to develop lubricating sheet in drilling materials for aircrafts such as CFRP and titanium alloy.

EXPERIMENTAL

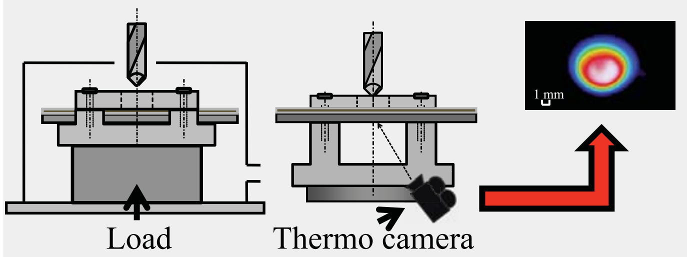

Workpiece cell	Titanium alloy (3mm)
Workpiece temperature, ℃	-197 25 200
Drill material	WC
Drill diameter, mm	6
Drill rotation speed, rpm	380 500 720 980 1330 1800
Table feed speed, mm/min	6 25 100
Lubrication	Dry Lubricating sheet

RESULTS

It turned out that burr formation is classified into two types by 350~400℃. Top of the back burr was flat in Type1 and sawlike in Type2.

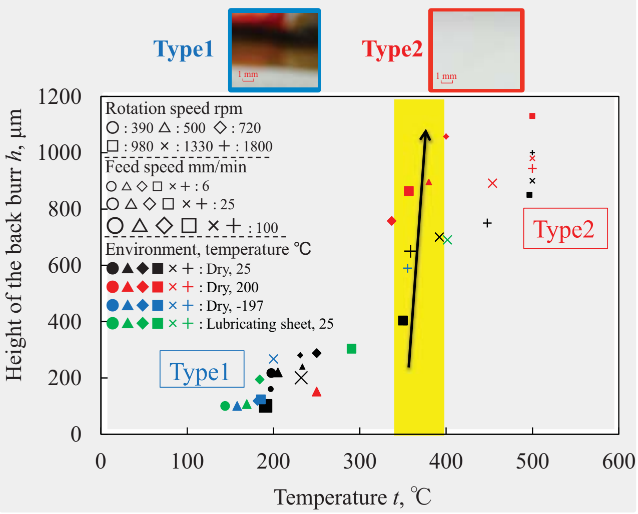

It turned out that height of back burr decreased with increasing lubricant layer. Lubricating layer was needed more than 0.04 g in this working condition.

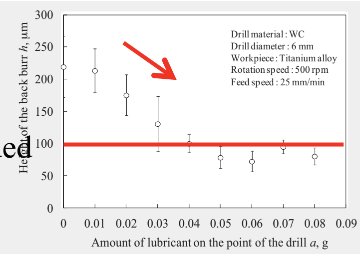

It turned out that Lubricating sheet could decrease height of back burr and drill wear.

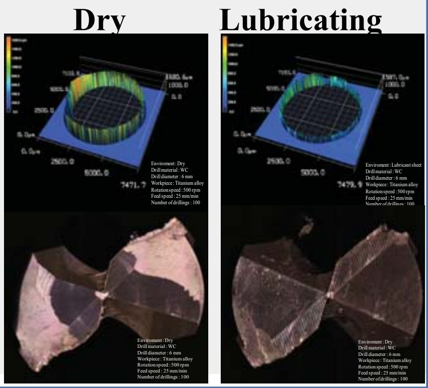

CONCLUSION

It turned out that burr formation was classified into two types by 350~400 ℃. Lubricating layer is needed 0.04 g on the point of drill in this working condition. Lubricating sheet can decrease height of back burr and drill wear. Lubricating sheet must have cooling effect which males burr generation area less than 350~400 ℃ and cover the point of drill.

Effect of substrate temperature on deposition of carbon film keeping molecular structure of adamantane

E. Nakatani N. Umehara H. Kousaka T. Tokoroyama Nagoya University March 2014

BACKGROUND

To make transparent films from carbon materials

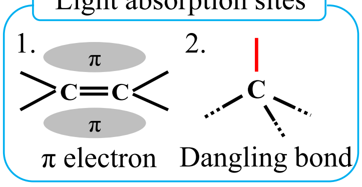

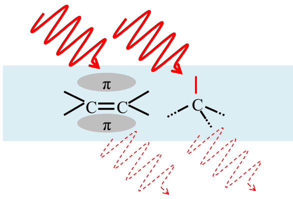

Light absorption is strengthened with number of these light absorption sites.

Need to decrease light absorption sites

Adopt Adamantane as source gas in this research

What is Adamantane?

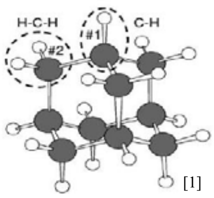

Adamantane

Name	Adamantane
Chemical formula	$C_{10}H_{16}$
Chemical weight	136.23
Melting point	269℃
Feature	**sp^3 carbon only** Sublimability

By utilizing molecular structure of adamantane, it is possible to minimize light absorption factors.

[1] Shirafuji, T. "Plasma-enhanced chemical vapor deposition of carbon films using dibromoadamantane" Thin Solid Films, vol. 518 (2009) pp. 993-1000

EXPERIMENTAL

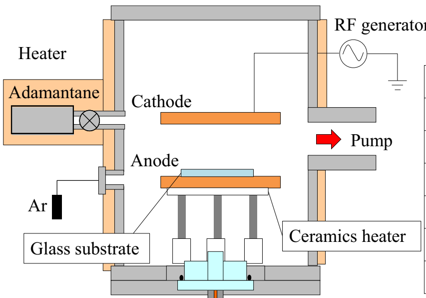

Experimental conditions

Adamantane, Pa	5
Ar, sccm	50
Pressure, Pa	47
$T_{adamantane}$, ℃	75
$T_{chamber}$, ℃	80
RF power, W	50
$T_{substrate}$, ℃	50, 150, 250, 400

1. Deposit adamantane film on the glass substrate by RF plasma CVD method.
2. Examine relation between wavelength and transparency (Ex.1), relation between wavelength and extinction coefficient (Ex.2) and infrared spectrum (Ex.3).

SPECIMENS

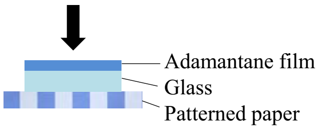

Photographing method

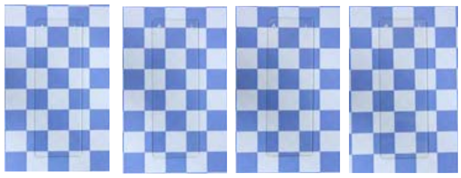

Glass | T_{sub}=50℃ d=360 nm | T_{sub}=250℃ d=646 nm | T_{sub}=400℃ d=497 nm

RESULTS & DISCUSSION

Ex.1 Relation between wavelength and transparency

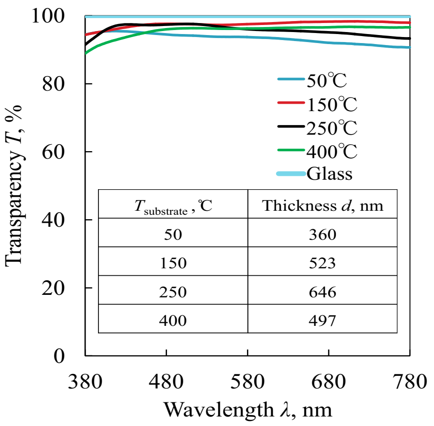

Ex.2 Relation between wavelength and extinction coefficient

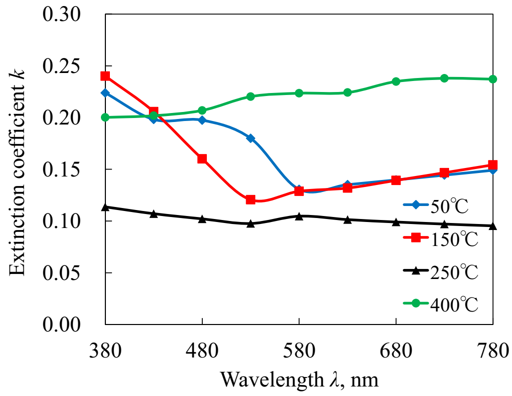

Ex.3 Infrared spectrum

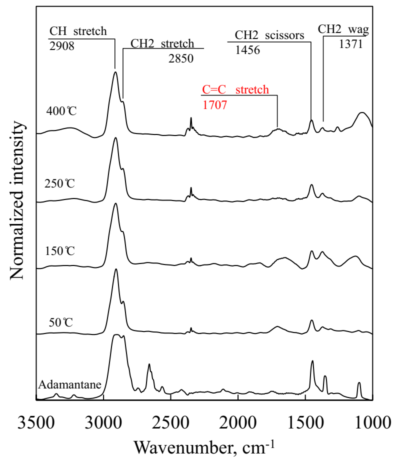

Ex.1: Adamantane films in this research had high transparency.
Ex.2: The adamantane film of T_{sub}=250℃ had the least extinction coefficient.
Ex.3: The adamantane film of T_{sub}=250℃ had no peak at 1700 cm^{-1} (C=C).

It is considered that the adamantane film of T_{sub}=250℃ has the least π electrons and dangling bonds.

CONCLUSION & FUTURE PLAN

We obtained the result that extinction coefficient of the adamantane film became low by heating substrate at 250℃. It was expected that the number of π electrons and dangling bonds became the least by heating substrate at 250℃. So, we are going to measure the number of π electrons and dangling bonds in the adamantane films by using XPS (X-ray Photoelectron Spectroscopy) and ESR (Electron Spin Resonance).

Study of basic friction properties of Ta-CNx film

Fuminori Nakayasu, Noritsugu Umehara, Hiroyuki Kousaka and Takayuki Tokoroyama
Development of Mechanical Engineering, Nagoya University, Japan

March, 2014

Back ground

Needs : Solid lubricants

- Energy and environment issues
- The domain that cannot use lubricate oil (Clean room, High load, In vacuum, etc…)

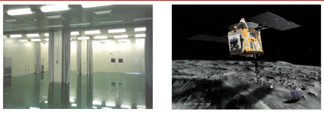

Improvement of the friction properties without lubricant oil

Previous Research : Ultra-low friction ($\mu < 0.01$) in the atmosphere

Ta-DLC (Tantalum-DLC) Low friction in the atmosphere + CNx (Carbon Nitride) Ultra-low friction in N_2

Ta-CNx
Ultra-low friction in the atmosphere

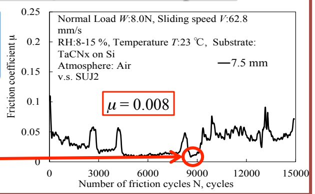

Problem

Ta-CNx : a new material
→ **Much unknown friction properties**
→ No clarification of the mechanism of ultra-low friction in the atmosphere in TaCNx film
→ No industrial design guide

Purpose

Obtaining knowledge of Ta-CNx fiction properties

Focus

1 : Elements contained in film — **Nitrogen, Oxygen**
Oxygen : A suggestion of contribution to ultra-low friction by a previous research
Nitrogen : The contribution to ultra-low friction in CNx friction

2 : The atmosphere gas — **Argon, Dry air, Nitrogen**
CNx friction properties depending on the Atmosphere gas

Experimental

The Control experiment — 3 disk specimens and 3 atmosphere gases

- Friction tests with a tribometer
- Observations of transfer layers and wear tracks with an optical microscope
- AES surface analyses before and after friction test
  (AES : Auger electron spectroscopy)

		Disk specimen		
		Ta-C	Ta-CNx	Ta-CNx:O
Atmosphere gas	N_2		N	O
	Dry air			
	Ar			

Friction test — Ball on Disk Tribometer

Changing the atmosphere gas by blowing different gases (N_2, Dry air, Ar)

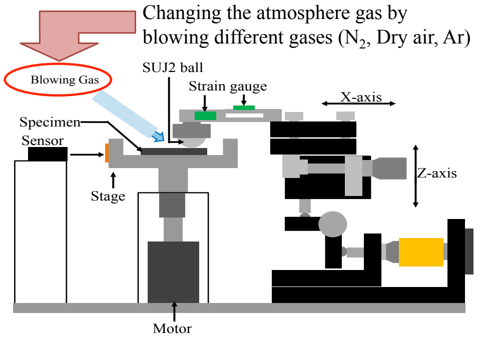

Fig.1 The Schematic of tribometer

Deposition system — ECR Ion Beam Sputtering System

The Deposition method : Ion Beam Sputtering Deposition

Changing elements contained in film by changing the Ionization gas

Target
Carbon
Tantalum

+

Ionization gas
- Ar
- Ar, Nitrogen
- Ar, Dry air

Reactive Sputtering

Film
- Ta-C Ta-CNx containing no Nitrogen
- Ta-CNx Regular Ta-CNx
- Ta-CNx:O Ta-CNx containing Oxygen

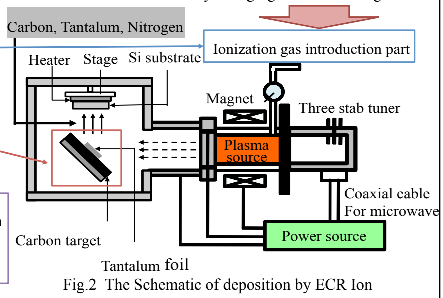

Fig.2 The Schematic of deposition by ECR Ion Beam Sputtering System

Result

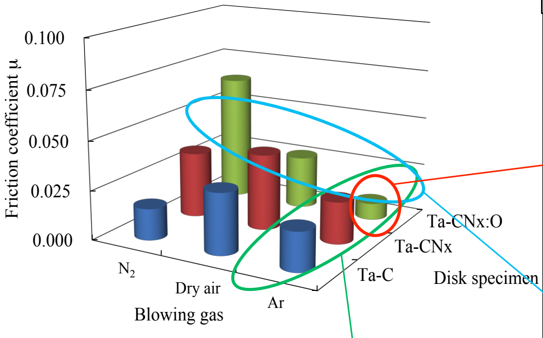

Fig.3 The relation between the minimum friction coefficient, disk specimens, and atmosphere gas

AES analysis

- Decreasing of Oxygen and Nitrogen in all friction tests
- Contribution of Oxygen contained in film to ultra-low friction in Ta-CNx:O friction

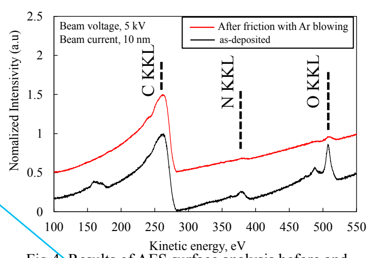

Fig.4 Results of AES surface analysis before and after friction test of Ta-CNx:O in Argon

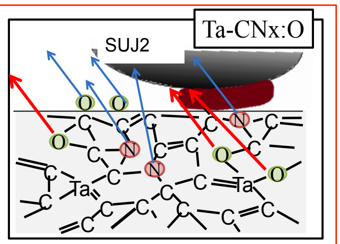

Fig.5 The mechanism of decreasing of Nitrogen and Oxygen in friction of Ta-CNx:O

Observations of Transfer layers

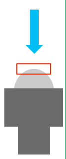

- Formations of a transfer layer regardless of contained elements

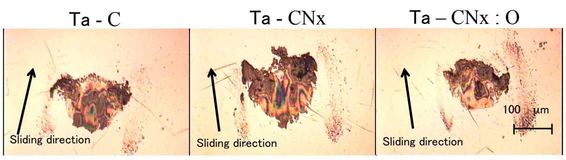

Fig.6 Transfer layers formed in friction test of different disk specimens in Argon

- Clear differences of transfer layers depending on atmosphere gases

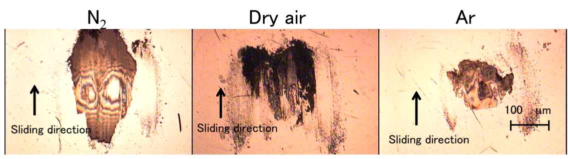

Fig.7 Transfer layers formed in friction test of Ta-CNx:O in different atmosphere gases

Conclusion

- Relations between number of cycles and friction coefficients
- Formations of the transfer layer regardless of elements contained in Ta-CNx
- Clear differences in formation of transfer layers depending on atmosphere gases
- Decreasing of Oxygen and Nitrogen induced by friction
- Contribution of Oxygen contained in film to ultra-low friction in Ta-CNx:O friction

Study of soot separation method from diesel engine oil by applying electric field

H. Shibasawa, N. Umehara, T. Tokoroyama, H. Kousaka   Nagoya University March, 2014

Background

Diesel engine oil become dirty in using by soot

Soot cause oxidative decomposition of ZnDTP which is antiwear agent

Soot : Very small (20-100 nm)

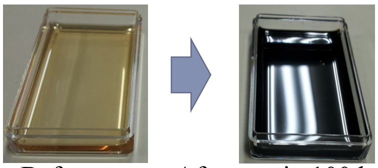

Before use   After use in 100 hour

Purpose

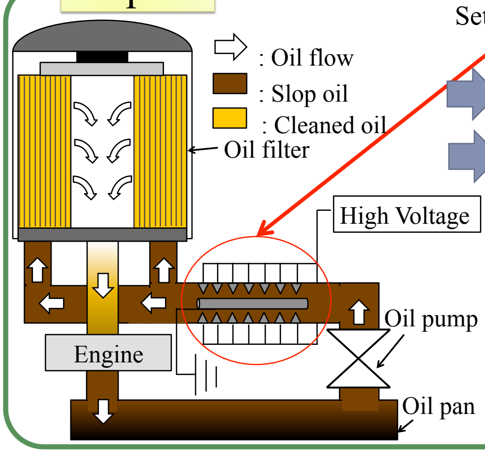

Set coagulation part which is made by many needles

- Coagulate soot at needle tip by electric field
- Remove coagulated soot by oil filter

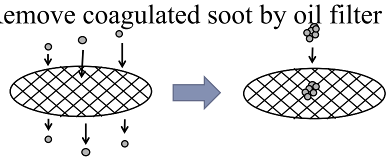

1. Evaluate soot coagulation to needle tip by electric field
2. Study the possibility of collecting the soot filter coagulation

Experimental

1. Study the effect of voltage, frequency time of voltage application

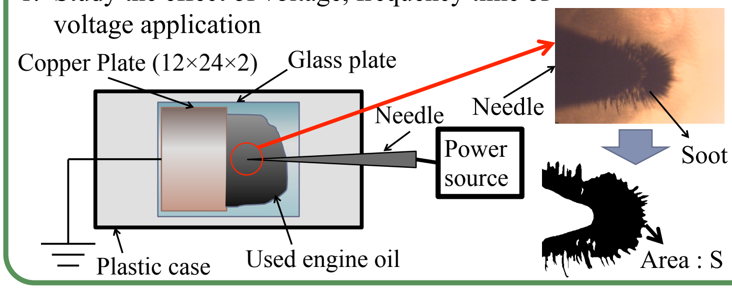

2. Study the possibility of collecting the coagulated soot on filter

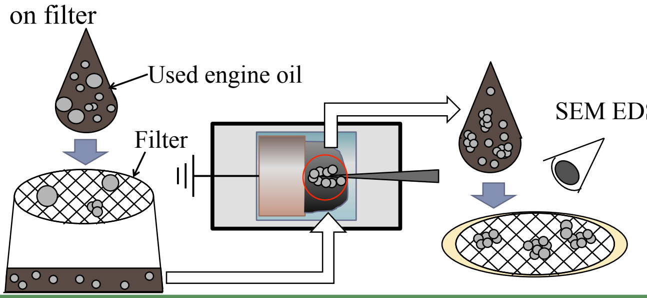

Results

Experimental 1

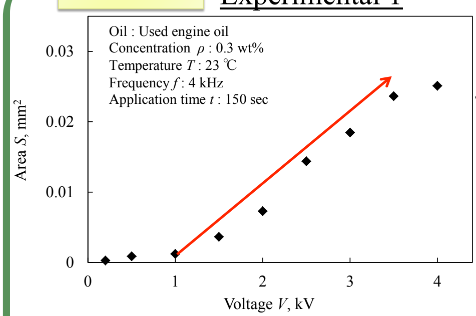

Coagulated area increases with the increase of the applied voltage

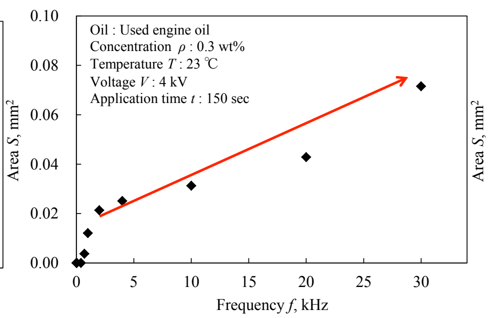

Coagulated area increases with the increase of the frequency

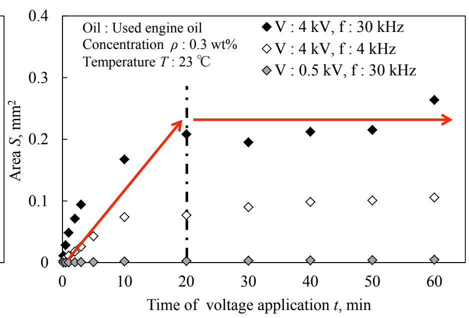

Coagulated area increases up to 20 minutes. With the increase of the time of voltage application, After 20 minutes, area becomes constant.

Experimental 2

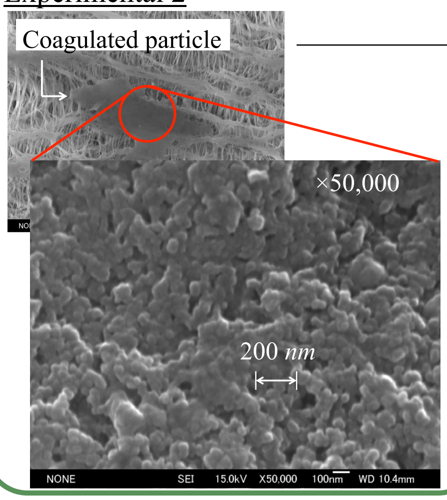

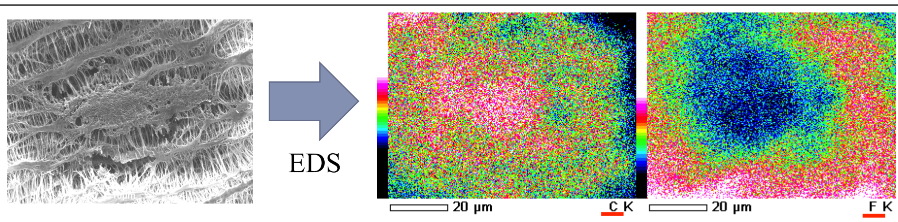

This coagulated particle is soot and coagulated soot can be captured by filter

Conclusion

We suggested soot coagulate filter system. And We evaluated the effects of voltage, frequency, time of voltage application to coagulation area and studied the possibility of collecting coagulated soot with filter.

The Tribological Characteristics of DLC Film under High Temperature Vapor Environment

TAKUYA YAMANOUCHI, NORITSUGU UMEHARA, HIROYUKI KOUSAKA and TAKAYUKI TOKOROYAMA
DEPARTMENT OF MECHANICAL AND AEROSPACE ENGINEERING, NAGOYA UNIVERSITY

Mechanical seals

Mechanical seal for water pump is used in high temperature vapor environment. It used by the combination of sintering Carbon and SiC. But the sintering carbon has problems. It is not a high hardness material. So, it is appreciably worn down.

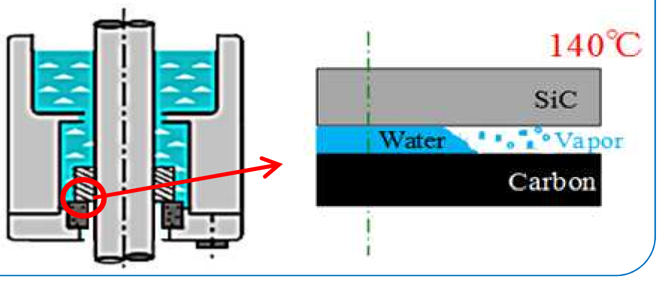

DLC

Today, the application of DLC (Diamond-Like Carbon) to the sliding surfaces of mechanical parts is gradually gaining popularity. It saves energy by reducing friction and extends the life of parts by reducing wear and tear.

Purpose

This study's purpose is revealing the effect of

- in air: (1)Type of DLC, (2)Substrate temperature
- in vapor: (3)Type of DLC

to tribological characteristics.

Experimental

Composition of DLC

	Hardness ,GPa	Film thickness, μm
ta-C	50	1
a-C:H	19	1
CNx	10	0.5
Si-DLC	13	1

ball-on-disk friction test

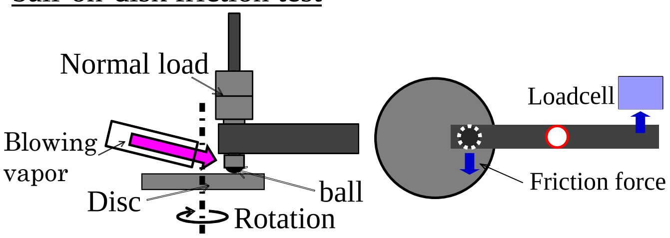

Specific wear rate

$$w = V / W \cdot L$$

V : wear volume (mm³)
W: Normal load (N)
L : Sliding distance (m)

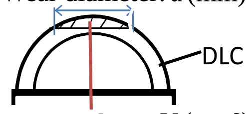

Wear volume: *V* (mm³) > $V = \pi\int_{\sqrt{4-(d/2)^2}}^{4}(4-x^2)dx$

Result

Sintering Carbon pin vs. SiC disk in substrate temperature 140℃
In air: Specific wear rate *w*: 190×10^{-8} mm³/Nm, Friction coefficient μ: 0.1
In vapor: Specific wear rate *w*: 3400×10^{-8} mm³/Nm, Friction coefficient μ: 0.13

Specimen		ta-C		a-C:H		CNx		Si-DLC	
		w	μ	w	μ	w	μ	w	μ
Substrate temperature ℃	23	0.8	0.13	1.9	0.13	4.2	0.22	270	0.12
	80	26	0.05	4.2	0.02	1	0.05	4.2	0.07
	140	39	0.04	8.3	0.02	2.4	0.05	11	0.078
	140 v	23	0.07	5.3	0.09	14	0.08	67	0.08

Specific wear rate w: 10^{-8} mm³/Nm, Friction coefficient : μ, opposite material SiC
Normal load N: 0.53 N, Sliding speed V: 0.0565 m/s

Conclusion

- Specific wear rate of ta-C is the lowest among DLC in substrate temperature 23℃ in air.
- Specific wear rate of CNx is the lowest among DLC in substrate temperature 80℃,140℃ in air.
- Specific wear rate of a-C:H is the lowest among DLC in substrate temperature 140℃ in vapor

Analytical prediction of chatter stability in ball end milling

A. Saito, E. Shamoto
Graduate School of Engineering, Nagoya University, Japan, saito@upr.mech.nagoya-u.ac.jp

1. Introduction

The ball end milling is an important precision machining process, which is used in production of dies, molds, impellers, screw propellers and parts with free-form surfaces. But if the slender ball end mills are flexible, the self- excited chatter vibration often occurs and causes severe problems such as short tool life and deterioration of surface quality.

- ✓ Altintas et al. developed the analytical model to predict the stability limits in ball end milling.
- ✓ Shamoto and Akazawa extended the analytical model to predict the stability limits in ball end milling with consideration of the tool inclination.

⇨ *Machining conditions will be optimized by applying the analytical model of ball end milling process with the chatter vibration.*

□ Analytical model
→ A new model will be developed for ball end milling of various workpieces with arbitrary shapes.

□ Experimental validation of chatter stability
→ The ball end milling experiments will be conducted to verify the analytical model and the optimization.

2. Analytical model to predict chatter stability in ball end milling

Self-excited chatter mechanisms
- Regeneration of previous vibration left on cut surface
- Coupling of multi-directional vibrations

Simple plunge turning process is introduced first, in which only the regenerative effect caused the chatter vibration.

□ Plunge turning process with regenerative chatter

Apply to ball end milling !

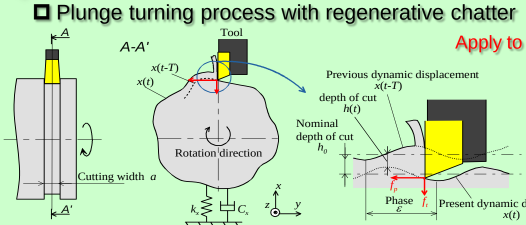

[Schematic of plunge turning process with regenerative chatter]

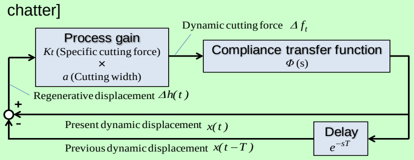

[Block diagram of plunge turning process with regenerative chatter]

$$g_m = \frac{-1}{2aK_f\,G(i\omega_c)}$$

$$n = \frac{60\omega_c}{2k\pi + \varepsilon},\quad n = \frac{60}{T}$$

$$\varepsilon = 3\pi + 2\tan^{-1}\left(\frac{H(j\omega_c)}{G(j\omega_c)}\right)$$

$G(i\omega_c)$:Real part of $\Phi(s)$
$H(i\omega_c)$:Imaginary part of $\Phi(s)$
ω_c:Chatter frequency
ε :The phase shift between the present and previous vibration waves

→ If this gain margin g_m is more than one, the system is unstable and generates the self-excited chatter vibration.

□ Ball end milling process with chatter vibrations

- ✓ Not only regenerative chatter, but also mode-coupling chatter can mix.
  → Vibrations in three directions are considered.
- ✓ Directions and magnitudes of cutting forces vary with position of cutting edge.
  → Cutting edge is discretized into elemental cutting edges.

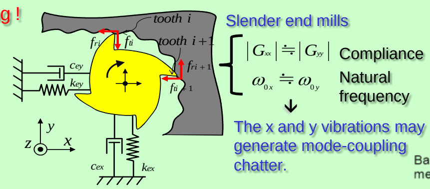

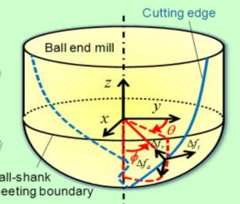

[Schematic of milling process with mode-coupling chatter] [Cutting forces acting on cutting edge]

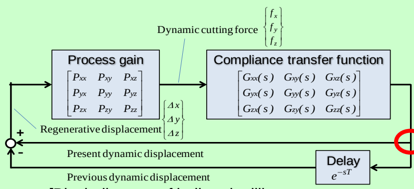

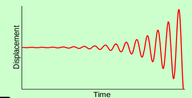

Mode-coupling chatter is caused by only present dynamic displacement !

[Block diagram of ball end milling process with regenerative chatter and mode-coupling chatter]

g_m, n and ε can be obtained by solving the above block diagram in a similar way to the plunge turning process.

3. Analytical and experimental results

The machining experiments were conducted with a slender ball end mill without inclination, utilizing a vertical machining center (Millac 415V, Okuma Corp.). The cutting force was measured with a dynamometer fixed between the workpiece and the feed table. The vibration was measured at the tool shank with the gap sensors, and the chatter vibration was detected by excluding its spindle speed harmonics, and forced vibrations. The compliance transfer function matrix was measured by the impulse response method at various tool rotational angles. The averaged matrix was utilized directly in the stability analysis. Oblique cutting tests were conducted by using the cutting edge in the shank region and the dynamometer, and the specific cutting forces in the shank region were identified, excluding the edge force components. Then, the specific cutting forces at different inclination angles were simulated, and used to calculate the process gain.

[Experimental conditions]

Tool	Diameter mm	R3×6
	Number of flutes	2
	Projecting length mm	60
Workpiece	SKD61(Hardened steel)	
Cutting conditions	Radial depth of cut mm	0.5
	Feed rate mm/tooth	0.025
	Atmosphere	Soluble
	Feed direction	Y

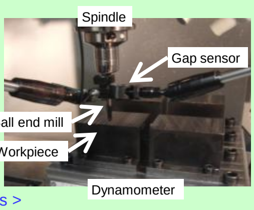

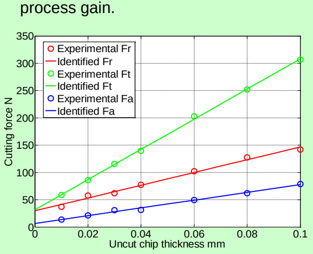

[Specific cutting forces identified experimentally]

[Identified material properties]
Shear strength, τ = 747 MPa
Friction angle, β = 28.0 deg

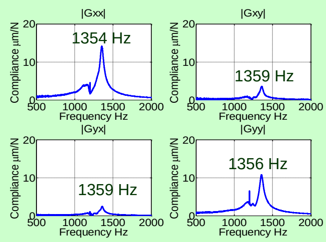

[Compliance transfer function]

Because the dynamic stiffness in the z direction is much higher than in the x and y directions, the other elements of transfer function matrix are assumed to be zero.

< Experiment >
Black marks: Experimental results
Chatter vibrations were classified as follows:
- ○ (No chatter) ≦ 0.5 μm
- 0.5 μm < △ (Slight chatter) ≦ 1 μm
- 1 μm < × (Chatter)

< Analysis >
Black line : Chatter stability limits
- Unstable above the line
- Stable below the line

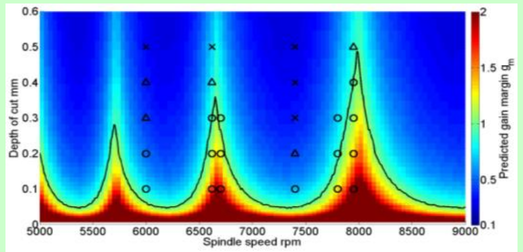

[Predicted gain margins and chatter stability limits, and experimental results]

→The predicted chatter stability agreed well with the experimental results !

4. Conclusion

The analytical model of the ball end milling process with the self-excited chatter vibration was developed, and it was applied to predict the chatter stability of various workpieces with arbitrary shapes at varied spindle speed in the present research. The machining Experiments of the basic machining conditions were conducted, and the analytical and experimental results are in a good agreement. It is expected that the present analytical model will be applied to optimization of machining conditions.

MEMS and Micromachining Laboratory, Department of Micro-Nano Systems Engineering,
Graduate School of Engineering, Nagoya University

High throughput evaluation of multi cell array for searching electrode materials of lithium-ion battery

M. Miyamoto S. Hata

Abstract In this study, as a first step to develop the high throughput evaluation of new electrode materials in lithium-ion batteries, evaliation device with an array of 9 cells is fabricated. The device has multiple counter electrodes, and its attachment to the library forms 3×3 electrochemical cells. To evaluate this 9 cells in the array, we measured charge-discharge curves of each cell. We ensured validity of this evaluation method using the array was conformed. This method is efficient for the exploration of new electrode materials.

1. Purpose

(1) Proposition of the evaluation device with an array of 9 cells for high throughput evaluation
(2) Construction of the evaluation program for performing cell evaluation
(3) Verification of the validity of the evaluation method using the device

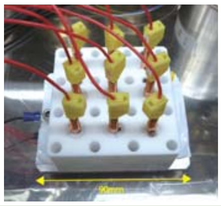

Fig.1 Evaluation device

2. Evaluation device

We fabricated the evaluation device with 9 cell array (Fig.1)

- It has 9 current collectors and common under plate
- Current collector hold down anode, separator×2 and cathode (Fig.2)

3. Cell materials

In this study, we fabricated the 9 cell using the same materials (Table1).

Table1 Information about the cell materials

Role	Material	Size
Anode	Li	Dia 12.5mm*0.3μm
Cathode	$LiCoO_2$ (Al foil)	Dia 10mm*15μm
Separator	PP/PE/PP	90mm×60mm
Electrolyte	$LiPF_6$ /$C_3H_4O_3$/$C_5H_{10}O_3$	0.1cc

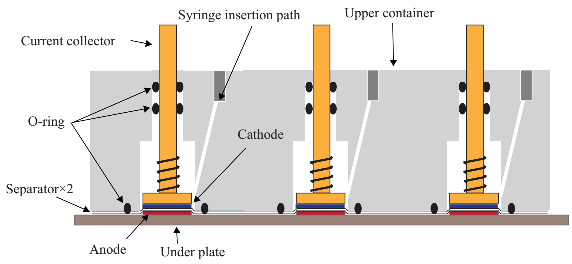

Fig.2 Cross-section diagram of the device

4. Experimental setup

Electonic circuit configuration (Fig.3)

- DC power source (GS200, Yokogawa Meters & Instruments)
- Digital Multi-Meter (PXI-4071 DMM, National Instruments)
- Swiches (PXI-2527, National Instruments, USA)

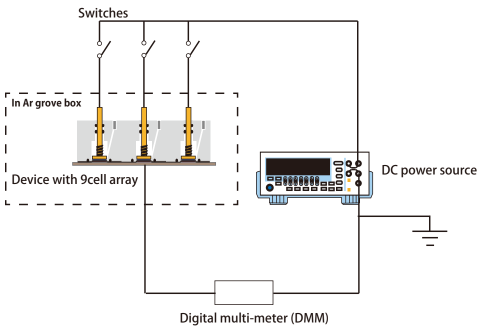

Fig.3 Schematic diagram of the electronic circuit

5. Charge-discharge test

Method

We defined these processes as 1 cycle (Fig.4).
We researched charge-discharge characteristics of 2 cycles in this study.

Result

9 curves are similar curves (Fig.5)

The device is verified the validity of the evaluation

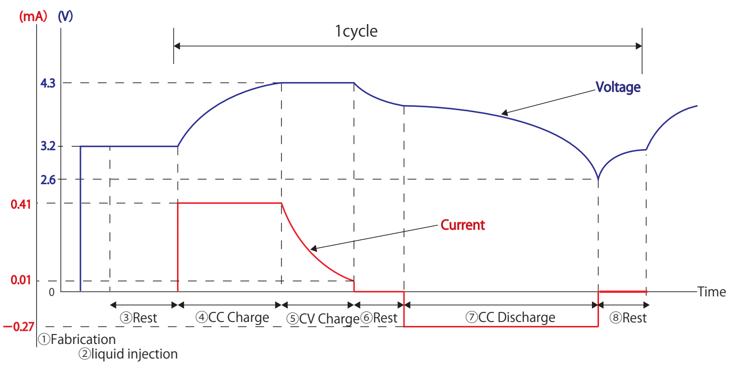

Fig.4 Charge-discharge cycle

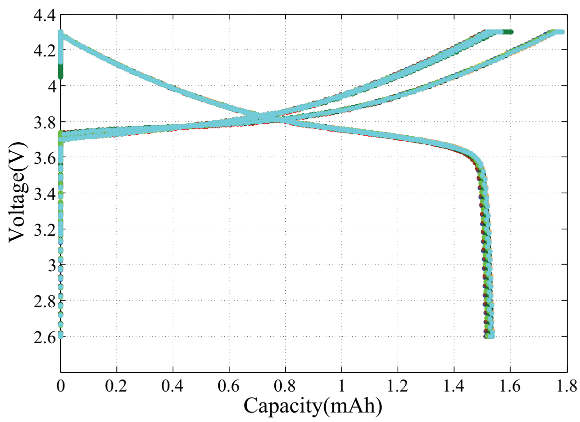

Fig.5 Superposition of 9 charge-discharge curves

http://www.mnp.mech.nagoya-u.ac.jp
E-Mail : hata@mech.nagoya-u.ac.jp TEL : 052-789-5223

Experimental Study of Heat Transfer Enhancement in Heat Pipe by Changing the Wetting Condition on the Wall.

Masaru Ogasawara (Nagoya University, Japan)

Introduction

Thermal performance of Heat pipe

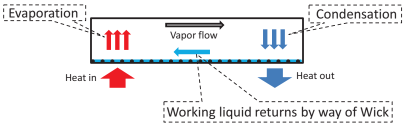

Fig.1 Heat pipe working principle

Important factors

Working liquid
Wick materials
Inner shape ...

Experimental parameters

Focus on inner wall wettability of HP

Objective of present study

Effect of the wetting condition of heated region on thermal performance of Heat pipe is studied with the aid of visualization.

Heat Pipe in this work

Material・・・Aluminum

Distribution ratio

1 : 4 : 1

Heated region | Adiabatic region | Cooled region

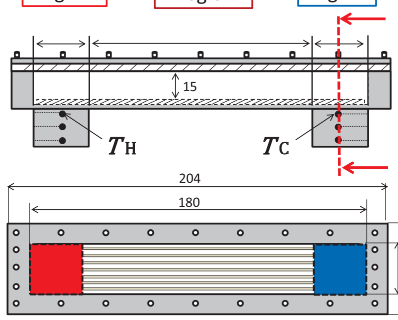

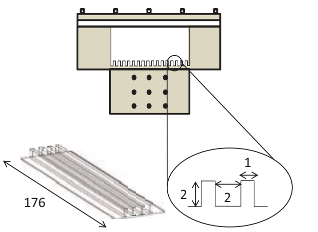

A groove(2.0mm × 2.0mm × 176mm) is made on a surface of Aluminum plate.

Fig.2 Schematics of experimental facility (top:cross section, down:front view)

- The heated and cooled areas are 9.0 cm^2 .
- Purified water is employed as the working liquid.
- To observe fluid behavior, top face is composed of polycarbonate which is transparent and thermoplasticity.
- Temperature is measured at several points by small thermistor as indicated by symbols ●.

Experiment

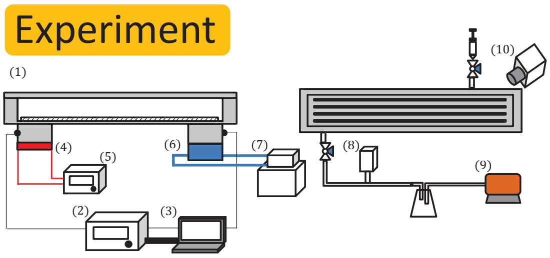

(1)Heat pipe
(2)Data logger(thermistor)
(3)Personal computer
(4)Heater
(5)Power source
(6)Water-cooling vessel
(7)Chiller
(8)Vacuum gauges
(9)Vacuum pumps
(10)CCD camera

Fig.3 Schematic diagram of experimental setup

Experimental Conditions

- Liquid charge amount V=0, 7,10ml
- Thermal input Q= 6〜30W
- Temperature of cooling water T_w = 10〜30℃
- Degree of vacuum P= 4.5×10^3 Pa

Thermal resistance evaluation

- The thermal performance of Heat pipe can be usually defined by thermal resistance.
- Thermal resistance between the heated region and the cooled region is calculated by using Eqs.(1) and (2).

Thermal resistance [K/W]

$$R = \frac{T_H - T_C}{Q} \quad (1)$$

T_H : Temperature of the heated region
T_L : Temperature of the cooled region
Q : Input heat load

Heat load [W]

$$Q = -k\frac{dT}{dx}\times A \quad (2)$$

A: Heated area[m^2]
k: Aluminum thermal conductivity(236[W/m・K])

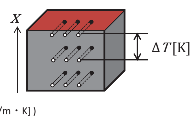

Results and discussions

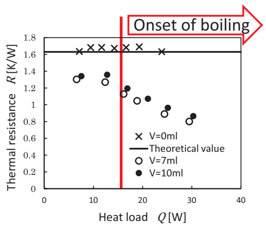

Fig. 4 Thermal resistance of Heat pipe

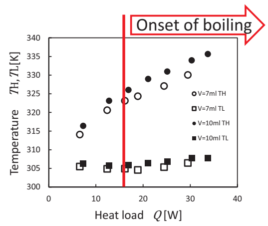

Fig. 5 Temperature of heated and cooled region

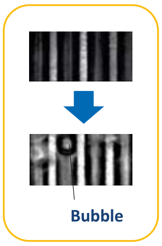

Effect of heat conduction in Aluminum plate is included in R.

Effective thermal conductivity λ_{eff}

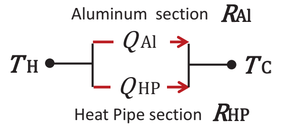

Fig. 6 Thermal resistance model of Heat pipe

$$Q = Q_{HP} + Q_{Al} = \left(\frac{1}{R_{HP}} + \frac{1}{R_{Al}}\right)(T_H - T_C) \quad (3)$$

R_{HP} : Thermal resistance in Heat pipe section
R_{Al} : Thermal resistance in Aluminum plate section

$$\lambda_{eff} = \frac{L}{R_{HP}\times A} \quad (4)$$

A: Cross-sectional area of Heat pipe
L: Length of Heat pipe

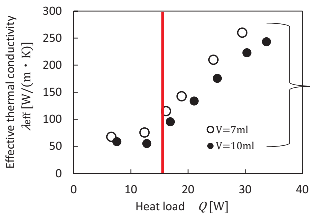

Fig. 6 Effective thermal conductivity of Heat pipe

$60 \leqq \lambda_{eff} \leqq 260$ at $6 \leqq Q \leqq 30$

Heat transfer coefficient

Boiling > Evaporation

- Thermal performance under different inner surface treatment (V=7ml)

Table. 1 Contact angle

Non treatment	Hydrophilic
81°	11°

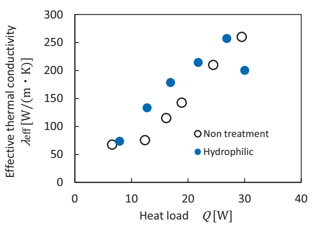

Fig. 7 Effective thermal conductivity of Heat pipe

Change of the route of working liquid

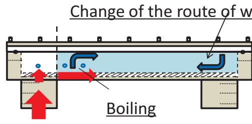

Boiling

Heat conduction along the Aluminum plate

Heat transfer coefficient decreases due to hydrophilic treatment over the heated region.

Conclusions

Summary

- The thermal performance of Heat pipe was confirmed to be improved by boiling occurring in the heated region.
- Hydrophilic treatment over the heated region does not increase the effective heat conductivity. This may be because the working liquid is not supplied to the heated region.

Future works

- Redesign of the structure of heat pipe
- Observation of the working fluid behavior in the partially wetting conditions over the heated region

Partially wetting conditions

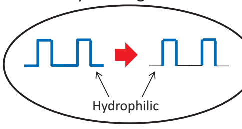

Experimental study on axisymmetric jet controlled by vortex generators

Mamoru TAKAHASHI, Kensuke MIURA, Kouji NAGATA, Yasuhiko SAKAI, Osamu TERASHIMA, and Yasumasa ITO
Dept. of Mechanical and Aerospace Engineering, Nagoya University

Introduction

Turbulent jet mixing is seen in wide variety of situations in industry. From an engineering point of view, it is of great importance to control the jet and increase mixing efficiency. In this study, small vortex generators (VGs) are inserted into the exit of axisymmetric jet and their effects are experimentally investigated.

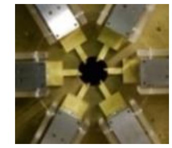

Experimental

VG patterns

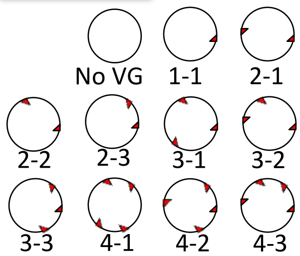

Measurement equipment

Hot-wire probe
for streamwise velocity

Cold-wire probe
for temperature

Coordinate system

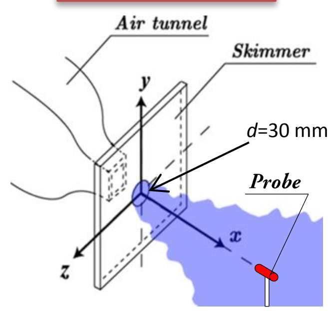

Measurement locations	x/d= 2.0,6.0
Initial velocity	U_J≅9.6 m/s
Temperature gap	Θ_J-Θ_a=7.5 K
Re=$U_J d/\nu$	20,000
Sampling frequency	20 kHz
Sampling time	13 s

Results

Mean velocity

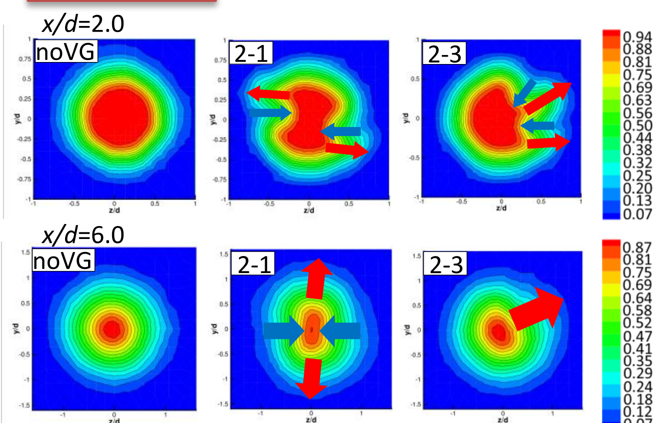

Entrained Fluid Volume ζ

$$\zeta = \frac{Q - Q_J}{Q_J} = \frac{\iint_S UdS}{U_J \frac{\pi d^2}{4}} - 1$$

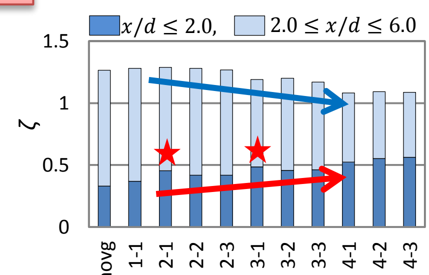

x/d=2.0:
The VGs work effectively when they are widely spaced.(2-1,3-1)

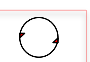

Widely-spaced

At x/d=2.0:
Increase with the number of VGs.

At x/d=6.0:
Decrease with the number of VGs

Mean temperature

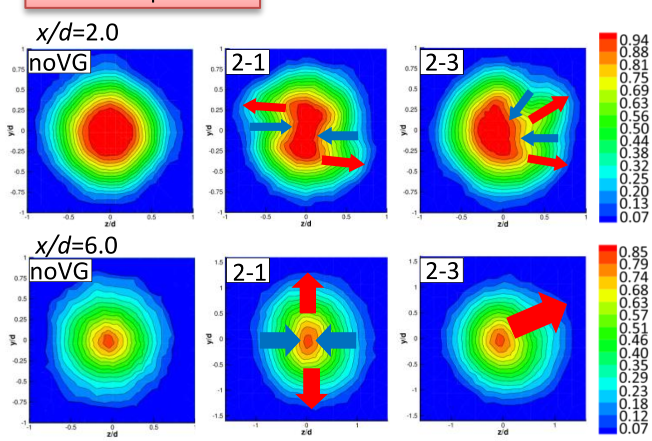

Thermal Diffusion η

$$\eta = \frac{\iint_{S_1}(\theta - \theta_a)dS}{\iint_{S_1 \cup S_2}(\theta - \theta_a)dS}$$

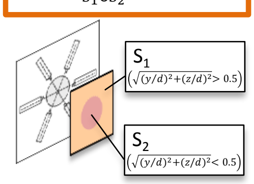

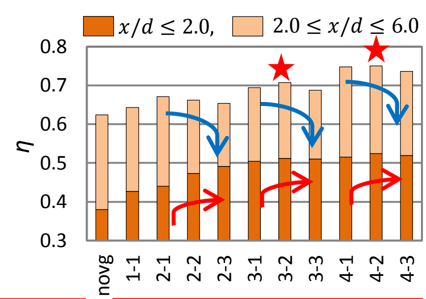

Both x/d=2.0 and 6.0:
The VGs work more effectively when closely- and widely-spaced VGs are combined.(3-2,4-2)

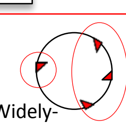

Widely-spaced Closely-spaced

At x/d=2.0:
The VGs work effectively when they are widely spaced.

Closely-spaced

At x/d=6.0:
The VGs work effectively when they are closely spaced.

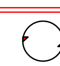

Widely-spaced

Summary

- The VGs increases fluid entrainment in the upstream region but becomes ineffective in the downstream region.
- The VGs promote thermal diffusion and the effect increases with the number of VGs.
- It is possible to control jet diffusion by arranging the locations of VGs.

Scale-up of a Test Apparatus for Precise Measurement of Liquid Axisymmetric Jet

M.Yokoi, T.Takeichi, Y.Sakai, O.Terashima, K.Nagata, Y. Ito

(Department of Mechanical and Aerospace Engineering, Nagoya University)

1, The Background of The Research

・Our Past Study on the Liquid Axisymmetric Jet

Taylor's microscale λ is given by $\lambda = \sqrt{\dfrac{\overline{u_1'^2}}{\overline{\left(\frac{\partial u_1}{\partial x_1}\right)^2}}}$

(u; the axial fluctuating velocity, x; Axial distance)

We could not measure λ, one of the representative turbulence scales, precisely. It is known that Taylor's microscale is along with The Friehe et al's empirical relation given by

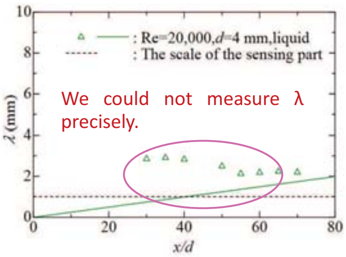

$$\frac{\lambda}{d} = 0.88\,\mathrm{Re}_d^{-\frac{1}{2}}\,\frac{x}{d} \Longleftrightarrow \lambda = 0.88\frac{\sqrt{\nu d}}{\sqrt{U_0}}\frac{x}{d}$$

(λ; Taylor's microscale, d; The outlet diameters of the nozzles Re; The Reynolds number, x; Axial distance)

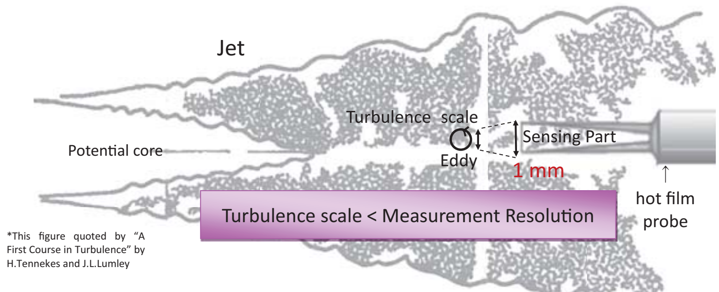

[Relationship between the Sensor and Turbulence]

・This study

To improve the measurement accuracy, there are 3 possible ways.

1, Increase the resolution of the sensor → Impossible
2, Decrease the Reynolds number → Turbulence becomes too weak
3, Increase the outlet diameter of the nozzle → Present Work

Because the jet becomes larger, we need a larger water tank.

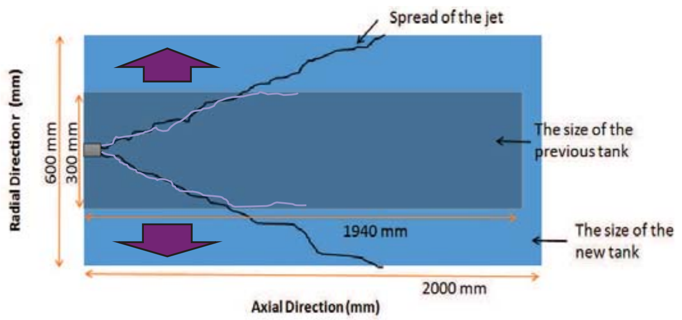

3, The Design of The Water Tank and Nozzles

	OLD	NEW
The size of the water tank	W=300 mm H=300 mm L=1940 mm	W=600 mm H=600 mm L=2000 mm
The diameters of the nozzle	4 mm	6,8,12 mm
Reynolds number	～20,000	～60,000
Measurement Position *x/d*	30～100	20～150

4, The New Apparatus

[Water Tank]

[Visualized Jet]

5, Jet Characteristics

Velocity Fields

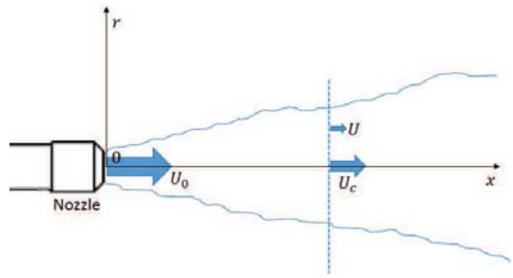

・Axial Mean Velocity (*d*=6mm, Re=20,000)

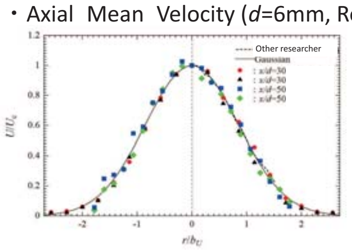

Radial distribution

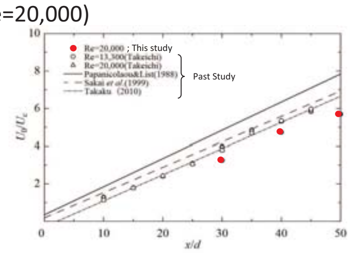

Streamwise distribution

The results are reasonable and close to the past studies.

We've confirmed that the new system forms jets properly.

・Taylor's microscale

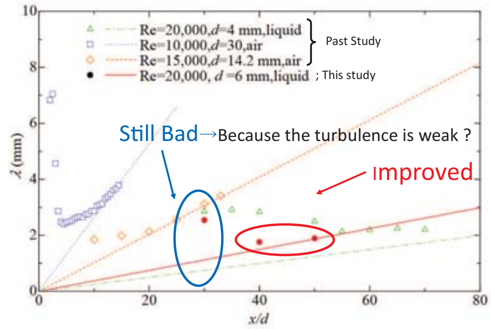

Future works

For better results, we'll measure on the condition that the outlet diameter of the nozzle or the Reynolds number is much larger than those of past.

<4> Appendix

a) Travel schedule

b) Photo album

c) Summary of questionnaire
(in Japanese, excerpts)

a) Travel Schedule ...March 9-17, 2014

Date	Event #	Time	Event
Mar 9		12:30	DL630 NGO --> DTW
		11:20	Arrival at the Detroit Airport
		13:30	Check in at Ann Arbor Regent Hotel
University of Michigan			
Mar 10		8:45	Arrival at the North Campus, UM
	1	9:00-9:30	Introduction of UM
	2	10:00-11:00	Campus tour starting at Pierpont Commons reception desk
	3	11:00-11:50	Poster setup and lunch for Nagoya students at Duderstad Hallway.
	4	11:50-14:00	Poster presentation by Nagoya students at Duderstad Hallway (Lunch)
	5	14:30-15:00	Introduction of the College of Engineering
	6	15:00-15:30	Talks by the Japanese students studying at UM
	7	15:30-16:00	Briefing session for UM students coming to Nagoya
	8	18:00-20:00	Casual meet-up at Johnson Rooms A,B,C (Dinner)
Mar 11	9	9:00-9:45	3D tour at UM 3D Lab
	10	10:30-11:30	Wilson Student Team Project Center tour
	11	13:00-15:00	Lab visits
Mar 12		15:20	DL019 DTW --> LAX
		17:24	Arrival at Los Angeles Airport
		19:00	Check in at Claremont Hotel
UCLA			
Mar 13		9:00	Arrival at UCLA
	12	9:30-10:30	Introduction
	13	10:30-11:30	Special lectures by Prof. Tsao, Mechanical Engineering and Dr. Keller, Director of Industrial Relations
	14	12:00-14:00	Poster presentation by Nagoya students at CNSI (Lunch)
	15	14:00-16:00	CNSI tour
	16	16:00-17:00	Briefing session for UCLA students
	17	18:00-20:00	Casual meet-up at UCLA Faculty Center (Dinner)
Mar 14	18	9:00-11:00	Campus tour starting at UCLA Sculpture Garden
	19	11:00-12:00	Lab tour (Dept. Mechanical Engineering and Dept. Materials Science)
	20	13:30-16:00	Individual lab visits
Mar 15	21		Free lab visits
Mar 16		10:00	Departure from Hotel
		13:20	DL283 LAX --> NRT
Mar 17		17:05	Arrival at Narita Airport
		18:48	Narita --> Shinagawa --> Nagoya by train

b) Photo album

Workshop at University of Michigan
Mar. 10 & 11

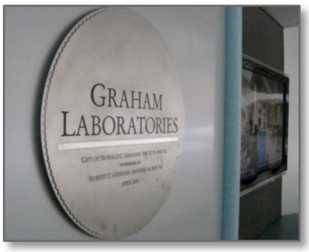

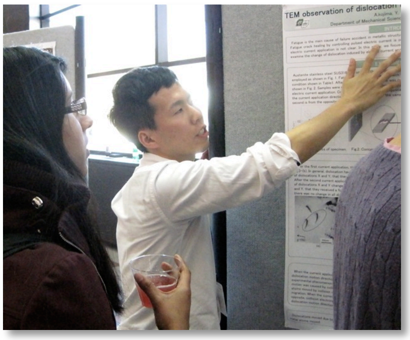
TEM observation of dislocation

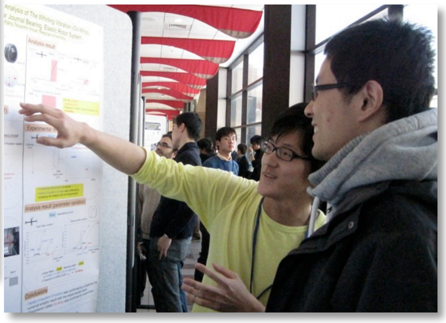

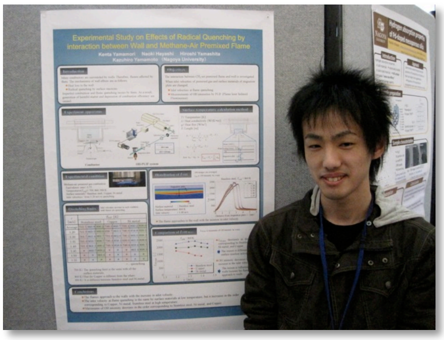
Experimental Study on Effects of Radical Quenching by Interaction between Wall and Methane-Air Premixed Flame

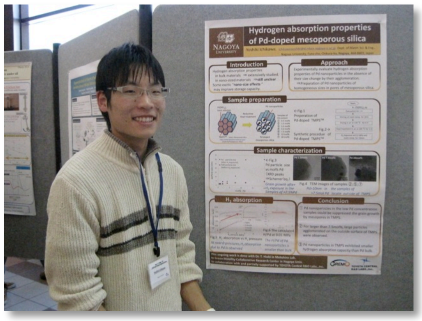
Hydrogen absorption properties
of Pd-doped mesoporous silica
Introduction
Approach
Sample preparation
Sample characterization
Conclusion

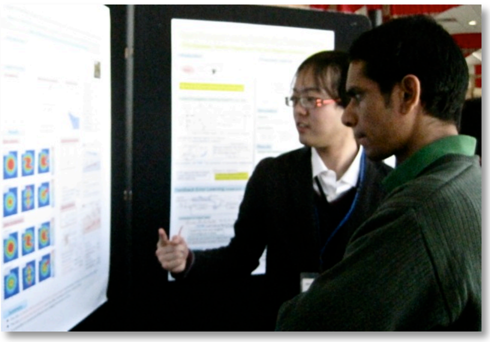

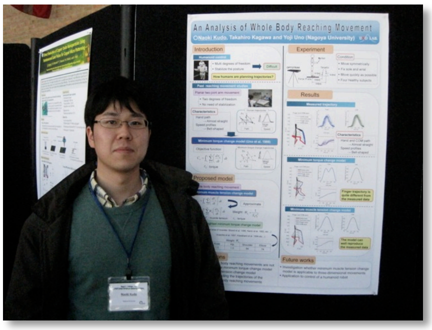
An Analysis of Whole Body Reaching Movement
Introduction
Experiment
Results
Future works

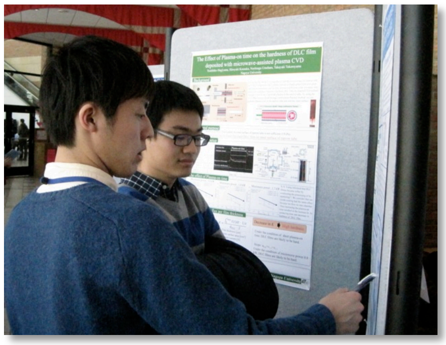

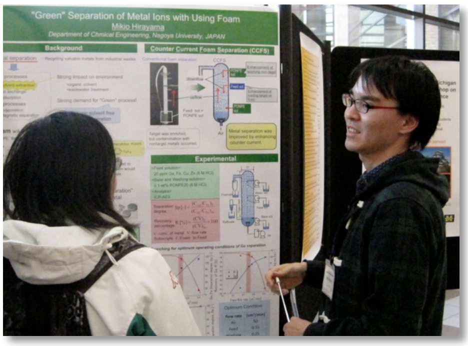
"Green" Separation of Metal Ions with Using Foam
Mikio Hirayama
Department of Chemical Engineering, Nagoya University, JAPAN
Background
Counter Current Foam Separation (CCFS)
Experimental


DTE Energy

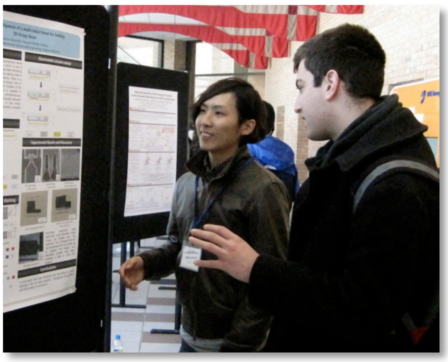

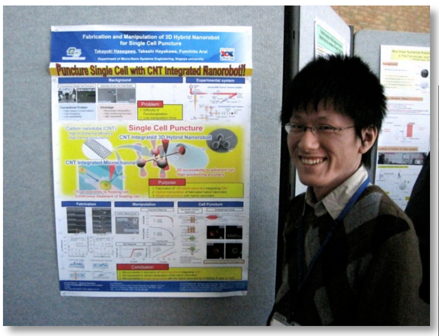
Fabrication and Manipulation of 3D Hybrid Nanorobot
for Single Cell Puncture
Puncture Single Cell with CNT Integrated Nanorobot!
Single Cell Puncture

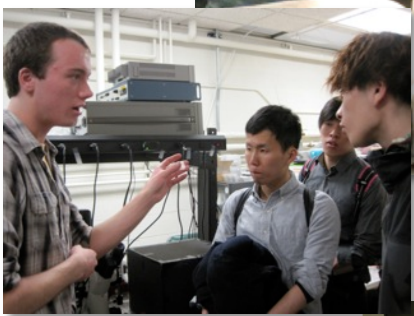


GAP

Workshop at UCLA
Mar. 13 & 14

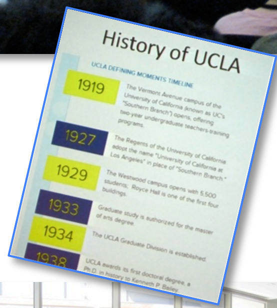

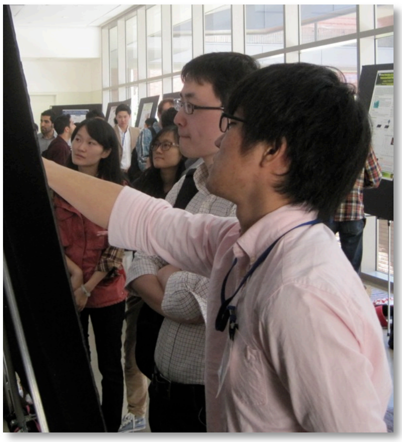

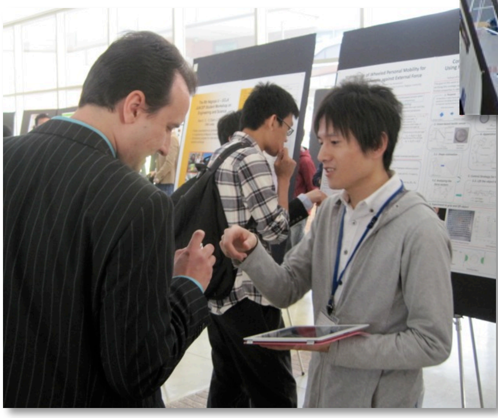

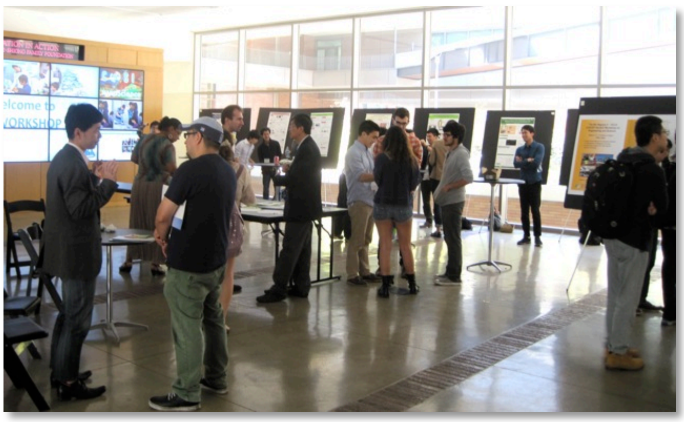

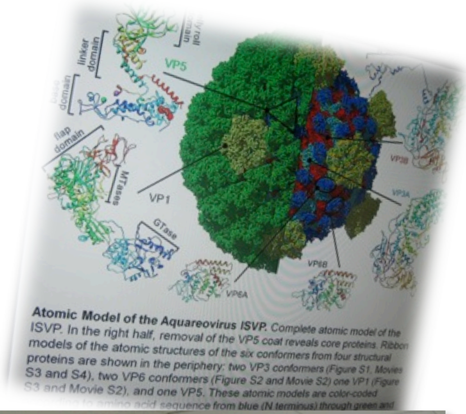
VP5
VP1
GTase
VP6A
VP6B
VP3A
Atomic Model of the Aquareovirus ISVP. Complete atomic model of the ISVP. In the right half, removal of the VP5 coat reveals core proteins. Ribbon models of the atomic structures of the six conformers from four structural proteins are shown in the periphery: two VP3 conformers (Figure S1, Movies S3 and S4), two VP6 conformers (Figure S2 and Movie S2) one VP1 (Figure S3 and Movie S2), and one VP5. These atomic models are color-coded


DPhPC


EXPRESS


A.P.C.


3ON3
2012

c) Summary of questionnaire

ワークショップ実施アンケート 概要

The 8th JUACEP Workshop at University of Michigan and UCLA アンケート概要

1. 米国の大学についての感想

【ミシガン大学】

- 研究設備が素晴らしく、大学の雰囲気も良かった。
- 教授や学生が温かく迎えてくれた。設備はとても充実していて圧倒された。
- 学生は昼休み中にもかかわらず熱心にポスターを見る人が多く勉強熱心だと思った。また気さくで優しい人が多い。
- 建物そのものや研究室が広く規模の大きさを感じた。忙しい中、熱心にポスター発表を聞いてくれる学生が多くレベルも意識も高さを感じた。
- クリーンルームが大きくきれい。なじみやすい雰囲気。
- 実際に自動車エンジンを用いて研究しているところがあり、実用に近いところで研究ができていると感じた。
- 学生はミシガン大が大好きなようで、大学のロゴが入った服を着ている人がたくさん居て、地元愛に溢れていた。学生の研究に取り組む姿勢はとても真摯で見習うべきだと感じた。
- 自然豊かで施設も立派。
- 名大の工学部と違い、実践的だと思った。
- 学生が有志で作成しているフォーミュラやサブマリン等が印象的。
- 雰囲気がとても良いが、留学するとなると周りに何もないので不便だと思った。
- 学生主体のプロジェクトの多さが印象的。
- 国際的。
- 建物内に窓が少なく閉塞的に感じた。

【UCLA】

- 人が多く，広い，きれい。
- 気候や大都市であることから明るい雰囲気。
- 複合施設が中心部にあっていいと思った。研究室のスケールも大きいし、大学内は学生にとって最適。しかし街からの誘惑が多そう。
- ミシガン大学と同様に建物の広さや研究設備の規模の大きさを感じた。研究室見学では教授方がご多忙のなか丁寧に説明してくださったのが印象的。試験前ということもあり、図書館で仮眠をとる学生も多くて勉強量の多さが感じられた。
- 日本が好きな学生がいてうれしかった。日本の漫画を知っていた。研究室では説明している時間以外は研究をしており、忙しそうな雰囲気だった。
- ミシガンに比べ活気があった。学生はミシガン同様意識が高く、丁寧に研究室を紹介してくれた。
- 設備に関してはミシガン同様よい環境であると感じた。
- 研究室でさかんにディスカッションしていて良い雰囲気。
- UCLA は大学内とは思えないくらいおしゃれな建物が並んでいる。学生はいきいきと研究に没頭して大学生活を楽しんでいるように感じられた。ミシガン同様勉強に対する意識が非常に高く、見習うべきだと痛感した。
- 街と同化していて、日本の大学とは違う雰囲気。
- Tsao 先生の研究室の内容に興味をひかれた。
- 学生ベンチャーに対する支援が充実している。
- 研究室ごとの計算機等の設備は日本のものと似ているが、研究で関わる機関・企業の数がとても多いことに驚いた。それゆえ一つの研究室でも多様な研究が行えるのだと納得した。

2. 自分の英語についてどう思ったか？

- 語学留学していた時よりかなりできなくなっていた。
- 想像していたより意思疎通ができた。聞き取ることはできても自分で文章を考えて発言することができなかった。
- 外国人相手に英語で話した経験があまりないので不安は大きかったが、ポスター発表や研究室見学を通して、知っている単語や身振り手振りを通しある程度伝わったので安心した。自分の実力が分かったのが一番良かった。また相手の質問の意図が分からないことが多々あり、リスニングの上達の必要性も感じた。
- 自身の研究内容と簡単な日常会話なら意外になんとかなることが分かった。アイコンタクトが必要と言われる意味も分かった。総じて必要なのは英語を聞き取ることだと思った。
- 専門用語の知識、スピーキング能力が欠けていると思った。
- 早口で言われると聞き取れない部分を改善したい。
- 自分の英語能力の低さに心が折れそうになった。リーディング・ライティングができても日常生活では役に立つことが少なく、リスニング・スピーキング能力の不可欠さを痛感した。
- 研究の話ならわかるが、日常生活に関して英語力がない。
- 研究についての会話がとても難しい。専門用語に対する英語力などが劣っていると感じた。
- ポスター発表は準備ができることや日頃から学んでいることもあり、出発前に心配していたよりはスムーズに会話できた。一般的な英会話については、海外を訪れるごとに少しずつ上達しているとは感じるが、今回はゆっくりと行われる会話で何とか意思疎通が出来るという程度だった。しかし「自分の英語力はこの程度だ」と思うことで、英語力を気にせずに情報を伝えることに集中できるようになったという点で、成長できた。

3. 参加してよかった or 有益ではなかった？

- 日本とアメリカの大学の相違点を自分の目で確認できただけでも有益だったが、グローバルに活躍するために必要なスキルが何かを身を持って感じることができたことが収穫したものの中で一番大きい。
- 自身の英語力の低さを感じ、悔しい思いをした。また米国学生のレベルの高さに多くの刺激を受けた。有益であった。
- JUACEP 留学を望むアメリカの学生とポスターやディナーで話せたのは楽しかった。
- 研究室訪問のアポを自分で取れたこと、個人行動が多かったことは良かった。一人で研究室を訪問したり観光したりしたが、おかげで自信がついた。ポスター発表もよかった。
- 3D ラボツアーが個人的に面白かった。
- 見学できる研究室を豊富に確保されていたため、夏からのプログラム参加につながる内容だった。
- 大学訪問ということでミシガン大学・UCLA の施設・研究室を紹介してもらう受け身なイベントは非常に有益だったが、ポスター発表という自発的なイベントがあることはより自分を成長させるために貴重な体験になると感じた。
- 研究に関する話題を英語で行うという経験は貴重。
- アメリカの大学の雰囲気に触れられたこと。
- UCLA でのポスター発表がミシガンと違って部屋で行ったことで、人が捕まりやすかったため話しやすく良かった。
- 主に食事は自分でとることになっていたので自分でオーダーし、色々なジャンルの料理を食べることが出来て良かった。また自由時間が多く、キャンパス内を自由に見て回ることが出来て良かった。
- ミシガン大での JUACEP 留学生の説明がよかった。
- 旅費をすべて負担してもらったこと。

4. 改善点、要望

- UM, UCLA ともにむこうの教授が JUACEP の制度を知らず、直接言われたわけではないが、何をしに来たのかと思われている感じがした。同時にむこうの教授や学生たちも対応に苦慮している様子だった。メールでの説明では伝わりきらない部分もあるため，事前に説明をしておくとスムーズな訪問ができたと思う。
- 研究室訪問の時間にもっと余裕を持たせてほしい。移動時間も考慮してほしい。
- ポスター発表で、カテゴリを作ると面白いと思う。環境、レアメタル、マテリアル…など。聞く側も関心があるところに行きやすいし、日本人側も話しかけ易いと思う。
- 施設ツアーのとき、もっと少ない人数でたくさんグループを作れると、日本人側は質問しやすいし説明もよく聞けると思う。
- 自分の認識不足もあったが、夏の留学先の教授のアポ取りに直接的に重要であることを応募段階からプッシュしてほしかった。そうすれば簡易的なレジュメも準備できたかと思う。
- 教授へのコンタクトのスムーズなやり方。(UCLA)
- 内容的に重複するような時間帯があったこと。
- ミシガンでのポスター発表を通路でなく部屋でやってほしかった。
- 研究室訪問のアポ取りを学生に任せるのか JUACEP が調整するのかがあいまいで混乱した。
- マイクロ・ナノや材料系だけでなく他分野（制御系など）の研究室を増やして欲しい。自分の分野とあまり関係のない研究室を訪問してもよく分からない。出発直前や出国後まで研究室訪問のアレンジをさせるのはできればやめて欲しかった。初心者が研究室訪問のアポイントを取るのは、余裕のある時でないと難しい。実際 Soatto 先生には研究室訪問の意図が全く伝わっておらず、office での数分の会話で終了した（あまり相手にされておらず，いい加減にあしらわれて追い返されたという印象であった)。
- 夏季留学先の受入教授を決定するための大事な機会であることの説明をもう少し強くアナウンスしてほしかった。
- 帰りの飛行機の到着地をセントレアにしてほしかった。
- プログラム日程の面で工学部の全専攻から参加しやすいようなプログラムになればより良い。
- 研究室訪問のアポのメールや参加学生間の連絡がうまく回っていなかった。出発前に参加学生＋事務局でメーリングリストの登録などをされては？そのほうが訪問リーダーから各学生への連絡がしやいと思う。

5. 名古屋大学で実施してほしい授業、プログラム、設備などの要望

- こちらに来た留学生と触れ合う機会
- 留学に関するセミナー
- Chemical Engineering 主体の今回参加させていただいたようなプログラム
- 多くの学生が今回のような体験をできるチャンス
- 実際の外国人と会話できる授業
- クリーンルーム設備を増やしてほしい。
- アメリカの学生のポスターセッションも同時に行う。
- 英語でプレゼンテーションを行う機会をより多く設けてほしい。
- アメリカの大学と違い、自発性が考慮された授業が日本の大学には少ないと感じるので、自分で考えて行い創造力を培える授業が必要。
- アメリカのように実際に製品を作ったり，グループ単位で行い最後にはものが残るようなプロジェクト形式の授業。

- 英語を使った工学系の授業を実施してほしい。
- グループ単位でプロジェクトを達成するような授業。基礎セミナーがあるが，本をパワポでまとめるなど個人で出来てしまうことが多いので、もっとグループでの協力が必要とされる授業があると良い。
- 自動研磨装置などがほしい。
- 留学生とペアになって学生実験。
- JUACEP のようなプログラムをより大きく、より広い範囲で実施して、多くの学生が関われるようになれば良いと思う。

6. ワークショップ申込時に、その後の短期/長期留学に興味があったか？

- あった/少しはあった： 25
- なかった/あまりなかった： 9

7. ワークショップ申込時に、今後のアメリカの大学への正規留学（たとえば博士課程からアメリカの大学に進学）に興味があったか？

- あった/少しはあった： 6
- なかった： 28

8. ワークショップ参加によって、今後の短期留学/正規留学への思いはどのように変化したか？

- 短期では、研究あるいは語学への興味が湧く段階で終わると思った。
- 国内でもっと実力をつけてからでなければ留学したとしても英語能力は身についても、エンジニアとしての能力は身に付かないのではないかと感じた。
- 行きたいという気持ちが強くなった。
- アメリカで生活・勉強するのは自分には厳しく、無理だと感じた。
- 短期留学をしてみたいという興味・願望が芽生えた。
- 短期留学を考えていたが、今回のワークショップで自身の英語力を認識し、2 か月では多くの成長は望めないと考え、申込みを見送った。
- 短期は、受入教員方も留学する学生としてもやれることが限られてしまうと思うので，留学するならば半年以上の期間でやる方が良いのではないかと思った。
- 現地の人柄に馴染めるか不安だったが，優しく接して下さったので，皆さんの助けがあれば留学できそうだと感じた。
- 自分の英語力をもっと究め、研究能力を向上させたいと思うようになった。
- 以前は留学について前向きだったが、様々な研究室を見学すると留学してまで取り組みたい研究内容はなく，研究目的での留学に対する意欲はなくなった。
- 「研究」留学という意味では、先生とディスカッションする時間や薬品・装置などの購入のしやすさを勘定すると、今の研究室の方が充実していると感じた。
- 今までは考えたこともなかったが、ミシガン大学で実際にした人の話を聞いて少し身近に考えるようになった。
- まったく考えてなかったが、こういう選択肢もありなんだと思うようになった。
- 海外での Ph.D 取得を少し意識するようになった。
- 研究室や学生の雰囲気は日本より良かったが､実験の設備としては日本の研究室の方が良いと思う。実験を進める上では日本の方が良さそうだった。
- やや興味は増した。少し留学について調べる気がわいた。

- 日本とは異なり、Ph.D が重宝される雰囲気ということで、本格的に研究者としての進路を選択した場合には大変好都合だろうと感じた。
- 留学前にそれなりの英語力を備えていなければ話にならないのではないかと思っていたが、留学中の学生からの話を聴いて、現地に行ってから語学も同時に鍛えていくというやり方でも通用していると知った。

9. その他の感想

- 私は一度も海外を訪れたことがなかったため，とても大きな経験となりました。アメリカの学生や現在留学している学生と話したことで、自身の視野をかなり広げることができたと感じています。ありがとうございました。
- ワークショップを通して留学の必要性を感じましたが、経済的にも自分の英語の実力からも厳しいとも思いました。しかし、アメリカの学生の意欲、態度から多く刺激を受け、今後の大学院生活を頑張っていきたいと強く感じました。
- アメリカの大学の良い面と悪い面を知ることが出来たし、街でもいろいろなモノを見て感じることが出来ました。自分の中の価値観が大きく変わり、予想以上に充実した１週間を過ごせました。本当にありがとうございました。
- 化学・生物工の参加でしたが、機械工学のことも知れて、また終始先導していただいた教授、JUACEP 職員の方々のおかげで存分に楽しむことができました。ありがとうございました。
- 今回のワークショップに参加したことにより、今後の研究・勉強に対する意欲が湧きました。留学に関しては現段階では興味･願望を持つようになった程度で､実際に留学をする自信がありません。しかし非常に良い経験をさせていただいたので、今後の自分に生かしていきたいと思います。本当にありがとうございました。
- アメリカについてから体調が芳しくなく滞在中ずっと風邪のような体調だったので結構辛かったです。折角の機会だったのでワークショップに参加させてもらいましたが，言葉の壁や食の違いなど自分には精神的なストレスがあったようです。
- 海外の研究の有り方を見学できて非常に有意義だった。しかしやはり留学の際のシステムが難しいと思う。実際に行けるかわからないのに受け入れ許可を頂くことはなかなかできないと思う。
- ワークショップ申し込み時は，留学に興味はなかったが，参加してみて初めて経済的余裕があるなら留学したいと思うようになった．留学申込み締切が，アメリカから帰ってきてすぐだったので，留学に興味を持った人が申込みにくいのではないかなと思った。
- 海外の、世界最高レベルの研究者や研究機関と交流する機会を得られたことは大変幸いで有益でした。敷居が低いことがこのプログラムの最大の魅力と感じるので、今後とも続くようであれば後輩にも勧めます。
- 現在，修士１年(4 月から２年)であり就職活動を行っているため，大変残念ですが留学するタイミングを逃してしまったなあと感じています。